UNIVERSIDADE DE LISBOA

FACULDADE DE MEDICINA DA UNIVERSIDADE DE LISBOA

U LISBOA | UNIVERSIDADE DE LISBOA

Establishment of pancreatic cancer zebrafish xenografts for personalized medicine in oncology practice

Mariana Isabel Tavares Barroso

Orientador: Rita Fior, PhD

Coorientador: Sandra Casimiro, PhD

Dissertação especialmente elaborada para obtenção do grau de Mestre em Oncobiologia

Lisboa, Novembro 2020

UNIVERSIDADE DE LISBOA

FACULDADE DE MEDICINA DA UNIVERSIDADE DE LISBOA

U LISBOA | UNIVERSIDADE DE LISBOA

Establishment of pancreatic cancer zebrafish xenografts for personalized medicine in oncology practice

Mariana Isabel Tavares Barroso

Orientador: Rita Fior, PhD

Coorientador: Sandra Casimiro, PhD

Dissertação especialmente elaborada para obtenção do grau de Mestre em Oncobiologia

Lisboa, Novembro 2020

"A impressão desta dissertação foi aprovada pelo Conselho Científico da Faculdade de Medicina de Lisboa em reunião a: 23 de Fevereiro de 2021."

Acknowledgments

My Zebrafish Team is better than yours ♥

E agora, uma das minhas partes preferidas e que nunca me canso de o fazer: agradecer a todas as pessoas que, da sua forma única e especial, me ajudaram e acompanharam durante este ano incrível e *full of emotions*.

A começar com a minha orientadora e grande *leader* deste laboratório, Rita Fior. Nunca vou conseguir agradecer o suficiente pela oportunidade de fazer Ciência consigo e com uma equipa fantástica. Foi um ano muito importante para mim, a todos os níveis. Obrigada Rita, do fundo do coração, por todo o ensinamento, pelo apoio incondicional e constante desafio.

Um obrigada gigante à minha Cati, uma das pessoas mais trabalhadoras que conheço e com um coração do tamanho do mundo. Obrigada por toda a ajuda, conselhos, paciência, companhia e abracinhos. Uma amiga que fica comigo para sempre.

Bruna, obrigada por me receberes de braços abertos desde o primeiro dia desta grande aventura. Adorei trabalhar ao teu lado. Transmites muita calma e confiança. Acho que o yoga está a surtir efeito!

Para a Ana Logrado, um obrigada muito quentinho. És uma pessoa incrível e extremamente inteligente, pena não gostares de cor-de-rosa. Obrigada por toda a tua ajuda, foste muito importante para mim durante este percurso.

Obrigada Vanda pela tua ajuda e energia contagiante, principalmente nesta reta final. Contigo é impossível não aprender algo ou não dar boas gargalhadas.

Para as recentes mamãs da equipa, Marta e Raquel, um muito obrigada pelo vosso apoio, disponibilidade e espírito maternal.

Luís Milk, homem do tiramisú e meu *partner* de tese, também mereces um grande obrigado pelas tuas boas energias. Conseguiste transformar muito dos meu stresses em *relax*.

Thank you Mayra for your support, encouragement and for understanding my injection frustrations. Good luck with your future experiments! You can do it!

Márcia, um beijinho de boa sorte nesta tua nova etapa. Dá o teu melhor e agarra esta oportunidade com todas as tuas forças!

Ao *staff* da *Fish Facility*, muito obrigada pelo vosso excelente trabalho, dedicação e ajuda.

Obrigada à Unidade de Histopatologia da Champalimaud, principalmente à Tânia Carvalho. Uma força da natureza, sempre com uma boa disposição e recetiva para ajudar a qualquer segundo.

Um grande obrigada à minha turma de mestrado! Foi um ano de muitas partilhas, aprendizagens e boas amizades.

Para o meu pequeno mas que vale infinitos grupo de amigas – Madalena, Marta, Catarina, Lina, Inês e Beatriz - muito obrigada pela vossa amizade, *boost* de ânimo, força, e momentos de riso incontrolável.

Claro que não poderia deixar de agradecer aos meus mais que tudo: a minha Família. Ao meu pai que nunca me deixa desistir, à minha mãe com as palavras certas

no momento certo, e ao meu maninho que já me pega ao colo e é o meu maior orgulho.

E para terminar, para a pessoa que entrou na minha vida e tornou-a ainda mais brilhante, um obrigada ao meu namorado, Rodrigo, que teve a paciência de um anjo, os abraços de um peluche gigante e um coração de um verdadeiro príncipe encantado.
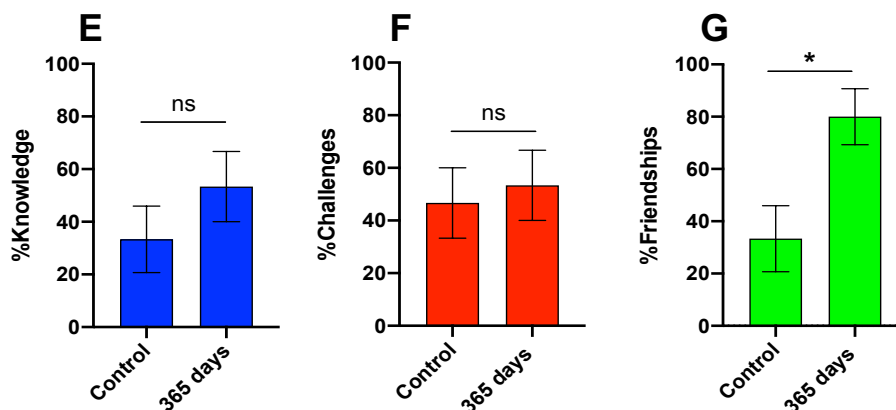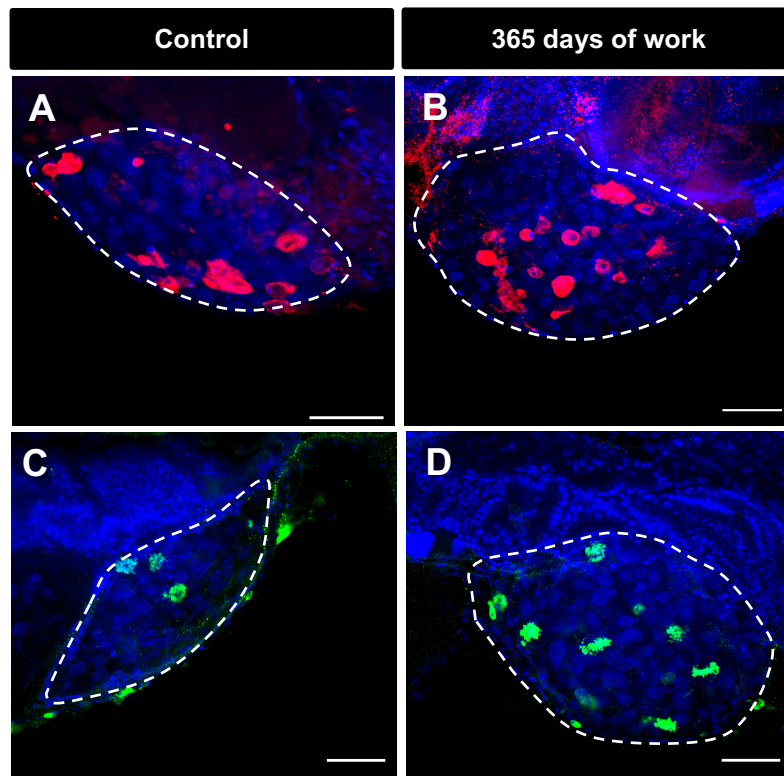
MB zebrafish xenografts responded to one year of work in Fior's Lab. 2dpf zebrafish larvae were injected with fluorescently labelled MB cells in the PVS (not shown). Successfully implanted xenografts were divided into two groups: non-challenged xenografts (**A, C**), and xenografts challenged to 365 days of work in Fior's Lab (**B, D**). After a whole year of work in Fior's Lab, zebrafish xenografts were sacrificed and fixed, and imaged by confocal microscopy. Knowledge (size of the tumor), challenges (in red) and friendships (in green) were analyzed and quantified (**E-G**, respectively).

After 365 days of work, knowledge increased, with big tumors full of new ideas and skills, although not significant because knowledge is infinite and there is no end of learning.

Throughout the year, new challenges were always emerging, on the way to extraordinary discoveries.

Last but not least, life-changing friendships appeared, which made this year significantly more memorable in all possible ways.

Resumo

O cancro do pâncreas é das malignidades mais agressivas e mortais. Esta doença raramente é diagnosticada num estadio em que a resseção cirúrgica é viável. A maioria dos doentes, a quando do diagnóstico, encontram-se num estadio avançado onde as opções terapêuticas são limitadas. Para além disso, as características peculiares do microambiente tumoral do cancro do pâncreas, com um estroma fibrótico extremamente denso, compromete a distribuição eficaz dos fármacos anticancerígenos. A quimioterapia sistémica é a única opção terapêutica para doentes com cancro do pâncreas avançado – FOLFIRINOX ou gemcitabina+nab-paclitaxel. No entanto, ainda não existe na clínica marcadores eficazes com valor preditivo que permitem identificar qual a melhor terapêutica para cada doente. Consequentemente, os doentes são submetidos a múltiplas rondas de tratamento e toxicidades desnecessárias, até encontrar a terapia que seja mais eficaz.

A imunoterapia também tem sido explorada como terapia complementar para o tratamento do cancro do pâncreas, incluindo inibidores de checkpoint imunológicos. Contudo, o microambiente tumoral rico em fibroblastos e células imunes com atividade imunossupressora, constitui um obstáculo significativo. Além disso, muitos dos doentes não são elegíveis para este tipo de terapia e portanto estratégias mais personalizadas estão a ser a investigadas em ensaios clínicos.

Desta forma, um teste capaz de prever as respostas de cada doente antes do tratamento, seria de grande valor para o tratamento personalizado do cancro do pâncreas.

O principal objetivo deste projeto de investigação foi testar as principais opções terapêuticas para o cancro do pâncreas em estadio avançado - FOLFIRINOX e gemcitabina+nab-paclitaxel - utilizando o modelo xenógrafo de peixe-zebra. Com este objetivo, xenógrafos de peixe-zebra foram gerados utilizando linhas celulares humanas de cancro do pâncreas (Panc-1 e MIA PaCa-2), e várias características tumorais foram analisadas por microscopia confocal, incluindo dinâmica tumoral – proliferação e morte celular – e composição do microambiente tumoral. Os efeitos citotóxicos do nivolumab em monoterapia e em combinação com gemcitabina+nab-paclitaxel (ensaio clínico a decorrer) também foram avaliados.

Os resultados demonstraram que as linhas celulares de cancro do pâncreas apresentam diferentes capacidades de implantação no modelo de xenógrafos de peixe-zebra.

Relativamente às terapias anticancerígenas, os nossos resultados demonstraram que os xenógrafos de peixe-zebra são capazes de revelar respostas tumorais ao FOLFIRINOX e gemcitabina+nab-paclitaxel, incluindo comprometimento da proliferação celular e indução da apoptose.

Neste projeto, testámos também a imunoterapia com o anticorpo anti-PD-1-nivolumab. Surpreendentemente os xenógrafos de peixe-zebra submetidos ao nivolumab em monoterapia e em combinação com gemcitabina+nab-paclitaxel também revelaram sensibilidade celular, com indução significativa da apoptose e redução do tamanho tumoral. De seguida, decidimos caracterizar o microambiente tumoral em particular o infiltrado de neutrófilos e macrófagos. Aos 4 dias pós-injeção,

a percentagem de neutrófilos aumentou em relação ao primeiro dia, e os macrófagos do tipo M2 (atividade pró-tumoral) passaram a dominar o microambiente tumoral. Para estudar o papel destes infiltrados na tumorigénese, gerámos xenógrafos em mutantes hipomórficos. A redução de neutrófilos, levou a um aumento do tamanho tumoral, enquanto que a redução de macrófagos, levou a um efeito contrário – diminuição do tamanho tumoral. Estes dados sugerem que os neutrófilos e macrófagos têm um papel antagónico, os neutrófilos com um papel anti-tumoral e os macrófagos pró-tumoral.

Sumariamente, os nossos resultados realçam a viabilidade de usar xenógrafos de peixe-zebra como um modelo in vivo para o screening de respostas tumorais às opções terapêuticas do cancro do pâncreas, e para o estudo da complexidade do microambiente tumoral.

Abstract

In the modern era of cancer research, pancreatic cancer has proven to be one of the most aggressive and lethal malignancies. Pancreatic cancer is rarely diagnosed at a time when surgical resection is feasible. Therefore, most of the patients present with an advanced disease, at the time of diagnosis, in which treatment options are limited. In addition, the pancreatic cancer microenvironment has peculiar characteristics with a thick layer of stroma, which builds up around the tumor and compromises an efficient drug delivery. Systemic chemotherapy remains the only treatment option for patients with advanced pancreatic cancer – FOLFIRINOX or gemcitabine+nab-paclitaxel. However, effective biomarkers to help predict treatment responses for each patient are still lacking. Consequently, patients go through several trial-and-error approaches and subjected to unnecessary side effects, until the best therapy is found.

Immunotherapy has also been explored as a complementary therapy for the treatment of pancreatic cancer, including immune checkpoint inhibitors. But, the tumor microenvironment enriched in fibroblasts and immune cells with immunosuppressive activity poses a major obstacle. Besides, many patients are not eligible for this type of treatment, and therefore more personalized regimens are being investigated in clinical trials.

In this way, a test able to predict individual responses before treatment would be of great value for personalized pancreatic cancer treatment.

The ultimate goal of this research project was to screen the major therapeutic options for PC treatment, FOLFINIROX and gemcitabine+nab-paclitaxel, using the zebrafish xenograft model. Additionally, the cytotoxic effects of nivolumab as a monotherapy, and in combination with gemcitabine+nab-paclitaxel (clinical trial ongoing) were also evaluated. To address this, zebrafish xenografts were generated with established human pancreatic cancer cell lines (Panc-1 and MIA PaCa-2), and several cancer hallmarks were analyzed through confocal microscopy, including tumoral dynamics – proliferation and cell death – and composition of the tumor microenvironment.

Data revealed that pancreatic cancer cell lines have different capacities to engraft in the zebrafish xenograft model.

Regarding anticancer therapies, results showed that zebrafish xenografts are able to reveal anti-tumor responses to both FOLFIRINOX and gemcitabine+nab-paclitaxel regimens, leading to impaired cell proliferation and induction of apoptosis.

In this project, we also tested anti-PD-1-nivolumab immunotherapy. Surprisingly, zebrafish xenografts subjected to nivolumab and nivolumab in combination with gemcitabine-nab-paclitaxel also revealed cellular sensitivity, with significant induction of apoptosis and tumor size shrinkage.

Next, we decided to characterize the tumor microenvironment, in particular neutrophil and macrophage populations. At 4 days post-injection, the percentage of neutrophils increased in comparison with the first day, and M2-like macrophages (pro-tumoral activity) started to dominate the tumor microenvironment. To study the role of both populations in tumorigenesis, zebrafish xenografts were generated using

hippomorphic mutants as hosts. Reduction of neutrophils induced an increase in the tumor size, while reduction of macrophages induced an opposite effect – decrease of the tumor size. These results suggest that neutrophils and macrophages are playing opposing roles, neutrophils as anti-tumoral and macrophages as pro-tumoral.

Altogether, and most importantly, our results highlight the feasibility of using the zebrafish xenograft model as an *in vivo* screening platform for pancreatic cancer therapy, and to study the complexity of the tumor microenvironment.

Table of Contents

Contents of Figures

Contents of Tables

List of Abbreviations

5-FU	5-Fluorouracil
ADM	Acinar-to-Ductal Metaplasia
ALL	Acute Lymphoblastic Leukemia
ATRA	All Trans Retinoic Acid
CA 19-9	Carbohydrate Antigen 19-9
CAFs	Cancer-Associated Fibroblasts
CAR	Chimeric Antigen Receptor
CTLA-4	Cytotoxic T Lymphocyte Antigen-4
DAPI	4',6-diamidino-2-phenylindole
DCs	Dendritic Cells
DMEM	Dulbecco's Modified Eagle Medium
DMSO	Dimethyl Sulfoxide
DPBS	Dulbecco's Phosphate-Buffered Saline
dpf	Days post fertilization
dpi	Days post injection
ECM	Extracellular Matrix
EMT	Epithelial-Mesenchymal Transition
ESMO	European Society for Medical Oncology
FA	Formaldehyde
FBS	Fetal Bovine Serum
FGF2	Fibroblast Growth Factor-2
GFP	Green Fluorescent Protein
GM-CSF	Granulocyte-Macrophage Colony-Stimulating Factor
GnP	Gemcitabine plus nab-paclitaxel
H&E	Hematoxylin and Eosin
HA	Hyaluronan
hpf	Hours post fertilization
hpi	Hours post injection
ICIs	Immune Checkpoint Inhibitors
MDSCs	Myeloid-Derived Suppressor Cells
MIF	Macrophage Migration-Inhibitory Factor
MMPs	Matrix Metalloproteinases
MPCs	Multipotent Cells
mPDXs	Mouse Patient-Derived Xenografts
MPO	Myeloperoxidase
MTC	Maximum Tolerated Concentration
n	Number of Samples
NCCN	National Comprehensive Cancer Network
Ngn3	Neurogenin 3
ns	Not significant (statistically)
ORR	Overall Response Rate
OS	Overall Survival
P	P-value

P/S	Penicillin-Streptomycin
PanIN	Pancreatic Intra-Epithelial Neoplasia
PC	Pancreatic Cancer
PD-1	Programmed Cell Death-1
PDAC	Pancreatic Ductal Adenocarcinoma
PDOs	Patient-Derived Organoids
Pdx1	Pancreatic and duodenal homeobox 1
PDXs	Patient-Derived Xenografts
PSCs	Pancreatic Stellate Cells
Ptf1a	Pancreas-specific transcription factor 1a
PVS	Perivitelline Space
RB	Retinoblastoma *gene*
RT	Room Temperature
SEM	Standard Error of the Mean
Shh	Sonic hedgehog
T-Regs	Regulatory T cells
TAAs	Tumor-Associated Antigens
TAMs	Tumor-Associated Macrophages
TGF-β	Transforming Growth Factor Beta
TME	Tumor Microenvironment
TNF-α	Tumor Necrosis Factor Alpha
WHO	World Health Organization
zPDXs	Zebrafish Patient-Derived Xenografts
NETs	Pancreatic Neuroendocrine Tumors
nivo	nivolumab

1. Introduction

1.1. *Cancer – when cells break the rules*

The human body is a complex and organized biological system composed of a society of interacting cells with specialized functions[1]. The behavior of each cell must be carefully regulated for the correct functioning of the whole organism[1,2]. To ensure appropriate coordination of cell activity, cells communicate with each other, mainly by extracellular signal molecules that serve as "social controls"[1,2].

However, multiple external factors combined with internal genetic changes can disrupt these "social controls" and promote the gain of malignant properties in normal cells that will, eventually, generate cancer[1,2]. Cancer is among the leading causes of death worldwide and is characterized by the development of abnormal cells that divide without stopping and have the ability to invade and destroy adjacent and healthy tissues[1,2].

In 2000 and then in 2011, Douglas Hanahan and Robert Weinberg proposed that cancers share common traits – hallmarks – essential for tumor growth and metastatic dissemination[3]. The hallmarks of cancer are:

- Sustaining proliferative signaling – Cancer cells can maintain constant growth even in the absence of external stimuli;
- Evading growth suppressors – Cancer cells can avoid the action of tumor suppressor genes that negatively regulate cell proliferation, such as the TP53 and retinoblastoma (RB) *genes*;
- Resisting cell death – Cancer cells can escape apoptosis. The most common strategy is the loss of TP53 tumor suppressor function;
- Enabling replicative immortality – Cancer cells have unlimited replicative potential. Telomere length and structure can be maintained by overexpressing of telomerase;
- Inducing angiogenesis – Cancer cells may induce pro-angiogenic factors to sustain tumor growth;
- Activation of invasion and metastasis - Cancer cells acquire migratory and invasive properties by undergoing epithelial-mesenchymal transition (EMT);
- Deregulating cellular energetics - Cancer cells have an aberrant glucose metabolism – Warburg effect - to sustain uncontrolled growth;
- Avoiding immune destruction – Cancer cells develop mechanisms to escape the immune system and may generate an immunosuppressive environment avoiding detection and destruction by the immune system[3].

1.2. *Clonal Evolution of Cancer – from one single cell*

Throughout a person's lifetime, healthy cells are constantly subjected to somatic mutations[1,4]. Mutations arise from replication errors or from DNA damage, but, luckily, most of them are repaired and do not have a negative effect on cell fitness[1,4]. However, some mutations may alter a key gene and confer a selective advantage to one cell, allowing it to proliferate more than its neighbors and escape cell death[1,4]. One end product of these phenotypic alterations is cancer.

In 1976, Peter Nowell proposed cancer as a dynamic and microevolutionary process, driven by several rounds of somatic cell mutations followed by natural selection[5]. According to this process, tumor initiation occurs when a single cell undergoes a mutation that confers a selective advantage to proliferate quicker among its neighbors, "so that its progeny become the dominant clone in the tumor"[2,5]. Throughout repeated cycles of somatic mutations and natural selection, different subclones with different mutations may arise, generating, at the end, an invasive heterogenous tumoral mass (**Figure 1.1**)[2,5].
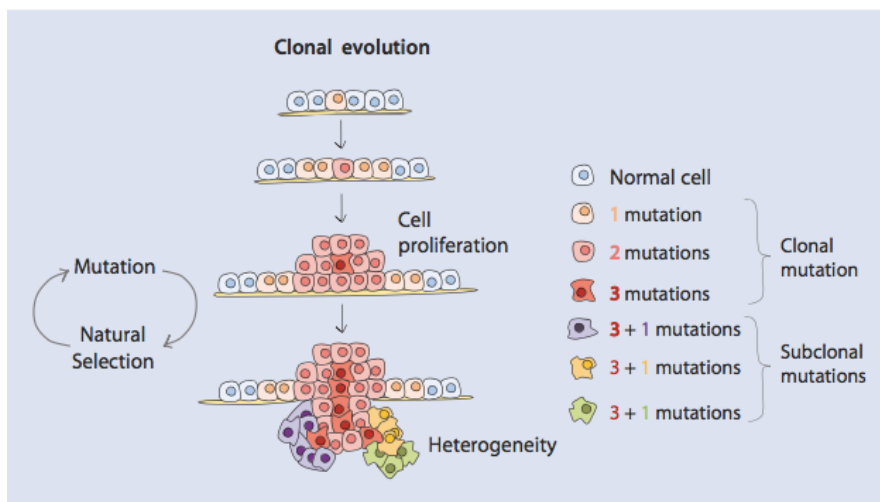
Figure 1. 1- Clonal Evolution of Cancer. According to Peter Nowell's theory, cancer is driven by repeated cycles of somatic cell mutations and natural selection, ending up with a heterogeneous tumoral mass composed of different subclonal populations. Adapted from [1].

1.3. *Tumor Heterogeneity – each tumor is unique*

Due to several rounds of somatic mutations and natural selection, a heterogeneous tumoral mass may arise[1]. This heterogeneity can be influenced by several genetic factors, such as germline genetic variations and somatic mutations, but also non-genetic factors, including epigenetic differences and tumor microenvironment (TME)[6,7].

Tumor heterogeneity can be divided into intertumoral and intratumoral heterogeneity, and they are closely related. Intertumoral heterogeneity refers to variability between patients harboring tumors of the same histological type[6]. Intratumoral heterogeneity refers to the presence of distinct subpopulations of cancer cells within the same tumor[6]. As a consequence, these distinct cancer cells can have differential dominances over cell population, that is reflected in different drug profiles

(sensitivity or resistance to)[8] (**Figure 1.2**). This diversity represents one of the major challenges for the design and selection of more-effective and personalized therapies[1,6].
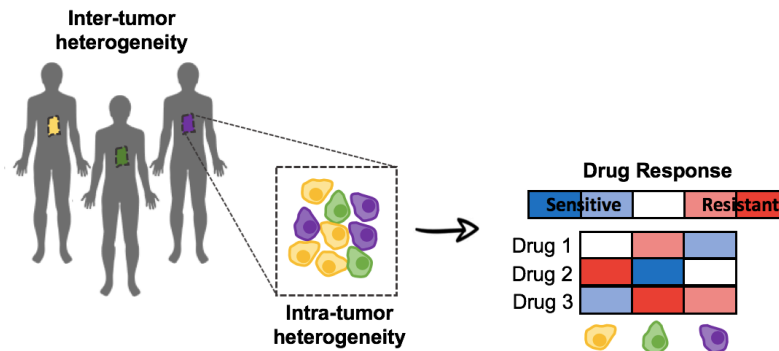
Figure 1. 4 - Tumor heterogeneity: a challenge in cancer therapy. Tumors are a heterogeneous mass composed by a variety of cancer cells with different phenotypes and distinct responses to therapy. This heterogeneity fuels drug resistance and represents one of the major challenges to drug development and precision medicine. Partially adapted from [8].

1.4. *Pancreatic Cancer (PC) – a stubborn malignancy*

Among all malignancies, PC is one of the most lethal solid organ tumors, with a five-year survival rate of only 7% for all stages of the disease[9]. The incidence and mortality rates of PC are closely related which reflects the fatal nature of this disease[10].

Based on GLOBOCAN 2018 estimates, PC is the seventh most frequent cause of cancer death in industrialized countries, being the highest incidences reported for Europe and North America[11]. However, within a decade, it is expected to rise to the second leading cause of cancer-related mortality, only surpassed by lung cancer[12].

Pancreatic ductal adenocarcinoma (PDAC) is an epithelial neoplasm originating from the pancreatic ducts, that are part of the exocrine portion of the organ. This type of PC is the most common malignancy of the pancreas, representing 85-90% of all PC cases[13]. The remaining cases, 10-15%, display tumors in the endocrine portion of the organ, called pancreatic neuroendocrine tumors (NETs)[13].

PC extremely poor prognosis and lethality are mainly due to:
(1) it is frequently diagnosed at advanced stages, which is often due to lack of symptoms in the early stages of the disease (only 10% of PC patients are diagnosed at an early stage);
(2) lack of prognostic and predictive biomarkers for early diagnosis, and of precision treatments;
(3) PC metastasizes microscopically early in the disease course, with high perineural invasion;
(4) drug resistance as a result of the commonly dense and fibrotic tumor microenvironment, and heterogeneity of the disease[9,14].

The risk factors for PC that have been identified so far are ageing (>65 years old), smoking (the strongest environmental factor), abuse in alcohol, obesity, diabetes, chronic inflammation of the pancreas (pancreatitis), and family history of PC[15].

PC symptoms do not occur until the disease is advanced and may at first appear to be associated with other less serious and more common conditions[16]. Jaundice can

occur in 50-70% of PC patients, and it is characterized by blockage of the liver's bile duct by the tumor, which impairs liver function[16,17]. Signs include yellow skin and eyes, dark-colored urine, light-colored stools, and unintended weight loss[17]. Fatigue, abdominal pain, and new-onset diabetes are also common symptoms of PC[16,17].

1.4.1. Pancreas Anatomy and Physiology – a two-in-one organ

The biology of the pancreas has been intensively studied with the hope to deeply understand its pathology, and to find efficient therapies for pancreatic disease, namely cancer.

In humans, the pancreas is an elongated organ located behind the stomach in the upper abdomen[18]. It is adjacent to other organs - small intestine (duodenum), liver and spleen - and several major blood vessels that supply blood not only to the pancreas but also other abdominal organs[18]. Anatomically, the pancreas is divided into four main portions:

- head (widest part);
- the neck (central section);
- the body (central section);
- the tail (thin end part)[18] (**Figure 1.3**).

In terms of cancer, the tumors' anatomical location has been suggested to predict the survival of PC patients[19].

Approximately 65% of PC tumors are localized in the head of the pancreas, 15% occur in the body and tail, and the remaining lesions are located in the endocrine compartment of the pancreas or are unspecified[20]. Although tumors in the head of the pancreas have a poor prognosis, tumors in the body and tail have an even worse prognosis[19,20]. Unlike tumors in the head, which are generally associated with jaundice as a signal, tumors in the body and tail are insidious, with vague abdominal discomfort and pain for several months, accompanied by unexplained weight loss[19,20].
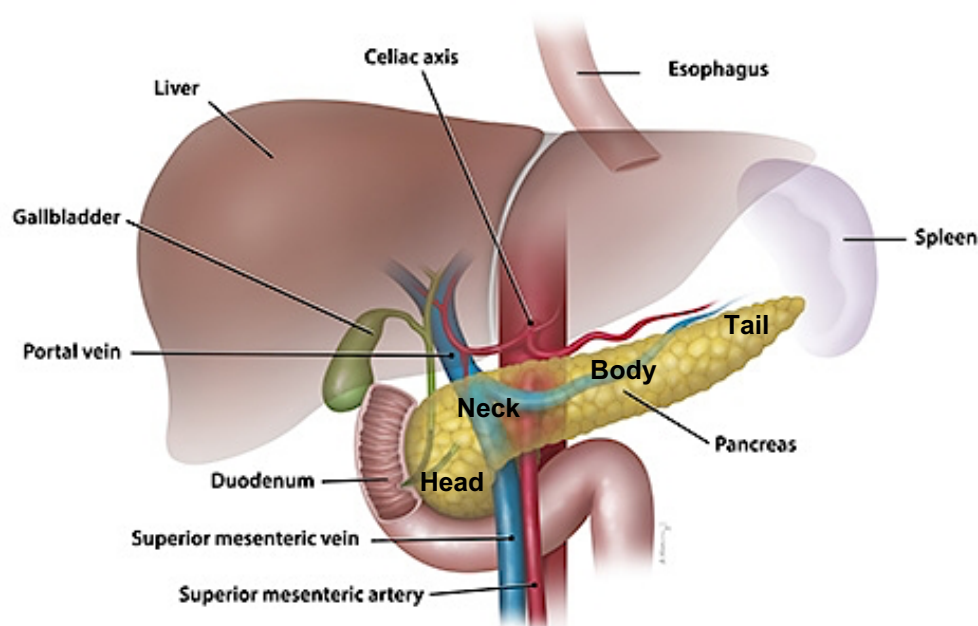
Figure 1. 7 - Overview of adult pancreas localization and anatomy. Pancreas is located in the upper abdomen between the duodenum, the liver, and the spleen and is surrounded by several major vessels - the superior mesenteric artery, the superior mesenteric vein, the portal vein and the celiac axis. The anatomical structure of the pancreas consists of four main regions: the head, the neck, the body and the tail. Adapted from [18].

The pancreas is often described as a two-in-one organ, due to the distinct functions and organization of its endocrine and exocrine compartments[21] (**Figure 1.4**). The exocrine compartment comprises up to 85% of the pancreatic mass, and it is composed by[13,22]:

- Acinar cells, representing the bulk of the pancreatic tissue, responsible for secreting digestive enzymes, including amylase, lipase, and protease;
- Ductal epithelium that neutralizes these enzymes, by secreting bicarbonate, and transports them into the duodenum to help with food digestion.

The pancreas' endocrine compartment makes up 5% of the pancreas mass and comprises the so-called Islets of Langerhans, first described in 1969 by their namesake Paul Langerhans[23]. These islets are typically composed of five main cell types - α, β, δ, PP, and ϵ cells - that produce and secrete hormones directly into the bloodstream to regulate nutrient metabolism and blood glucose homeostasis[24,25]. The β-cells are the most prominent (50-80% of the total), and α-cells are the next most-common cell type (15-20% of the total)[24,25]. These two cell types are responsible for secreting the hormones insulin and glucagon, respectively[24,25]. The balance and coordination between these two hormones is essential for glucose homeostasis[24,25]. The remaining islet cells, δ, PP and ϵ cells, comprise a small minority of the total, and secrete the hormones somatostatin, pancreatic polypeptide, and ghrelin, respectively[24,25]. Somatostatin regulates glucagon and insulin release in a paracrine manner to prevent hormonal overproduction[26]. Pancreatic polypeptide is released rapidly into circulation following nutrient ingestion[27]. Although its functions are uncertain, it is thought to control appetite as a satiety hormone[27]. Ghrelin became famously recognized as the "hunger hormone", because it stimulates food intake and fat storage[28].

The cellular composition and architecture of these pancreatic islets, differ between species and within species, according to the functional and metabolic needs[29]. For example, in obese humans, β-cells increase in number to compensate for increased insulin demand[30]. In contrast, humans with type 1 diabetes have an abrupt reduction of β-cells, and 50-70% of the islet is composed of α-cells[31]. Together, this diversity highlights the high plasticity and fast adaptation of these pancreatic islets in response to metabolic alterations[29].
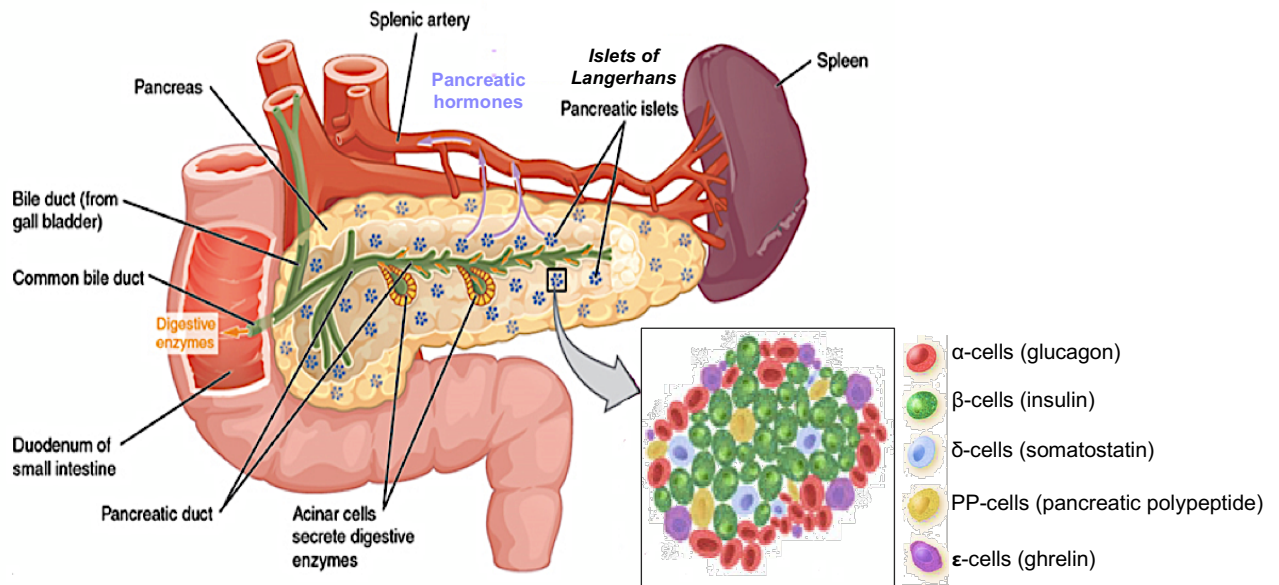
Figure 1. 11 - Physiology of the exocrine and endocrine pancreas. Pancreas consists of an exocrine and an endocrine compartment. The exocrine compartment is composed by acinar cells responsible for secreting digestive enzymes via the pancreatic duct system to the duodenum. The endocrine compartment is composed by aggregates of cells called the Islets of Langerhans. The islets comprise α, β, δ, PP and ε-cells, that secrete specific hormones into the bloodstream to regulate glucose homeostasis and nutrient metabolism. Adapted from [25].

1.4.2. Pancreas Embryonic Development

The formation of the pancreas' mature architecture depends on a series of embryologic events carefully orchestrated. During the development of an embryo, the blastula (produced by the first few cellular divisions of a fertilized egg) gives rise to three germ layers – ectoderm, mesoderm, and endoderm – through the process of gastrulation[32]. The endoderm is the innermost germ layer and generates the epithelial lining of the digestive and respiratory system and associated organs such as the liver and the pancreas[32,33].

The human pancreas originates from a pool of multipotent cells (MPCs) in the gut endoderm after receiving inductive and permissive signals from the notochord. The notochord secrets signals, including Activin-β and fibroblast growth factor-2 (FGF2), that inhibit sonic hedgehog (Shh) signaling in the endoderm and permit pancreas embryonic development to initiate[34].

Pancreas development becomes first evident with the emergence of epithelial buds on opposing sides of the gut endoderm: dorsal and ventral pancreatic bud (**Figure 1.5 A**)[21,35,36]. These buds are formed by MPCs co-expressing pancreatic and duodenal homeobox 1 (Pdx1) and pancreas-specific transcription factor 1a (Ptf1a), both crucial for further pancreas development[21,35]. The two pancreatic buds subsequently elongate alongside the presumptive duodenum and stomach and eventually fuse into a single organ[36,37]. This early phase of pancreas development is called the primary transition,

6

and is characterized by an undifferentiated pancreatic epithelium surrounded by mesenchymal cells[21,35–37].

The transition of noncommitted MPCs into a mature organ with different cell types is known as the secondary transition[21,35–37]. The first step of this new transition is the segregation of a tip and trunk domain (**Figure 1.5 B**)[34,36,37]. During this time, the pancreatic epithelium undergoes dynamic structural changes, resulting in multiple protrusions that grow from the edges[36,37]. The outer cells represent the tip domain and are fated to produce acinar cells, while the inner cells represent the trunk domain and organize into rosette-like structures of newly polarized cells that will produce ductal and endocrine cells[34,36,37]. After the tip and trunk domains have separated, cells in the trunk domain undergo extensive morphogenetic changes to form a 3-D network of tubules lined by a single layer of polarized epithelial cells, resembling a tree-like structure[36,37]. This process is called branched morphogenesis and is driven by dynamic cell rearrangements and controlled cell proliferation[21,34–37]. This tubules network is referred to as the primitive ducts or progenitor cords (**Figure 1.5 C**)[36], in which a subset of cells initiates expression of the transcription factor Neurogenin3 (Ngn3), responsible for the beginning of endocrine cell differentiation[34,36,37]. Trunk epithelial cells that do not express Ngn3 eventually contribute to the ductal tree[34–37]. Therefore, the endocrine and ductal cell fate is regulated by the controlled expression of Ngn3 transcription factor. Cells that express Ngn3 generate, as a whole, five different endocrine cell types: glucagon-producing α-cells, insulin-producing βcells, somatostatin-producing δ-cells, pancreatic polypeptide–producing PP-cells, and ghrelin producing ε-cells[34–37].

By the end of the secondary transition, the pancreas has mostly acquired the architecture and organization of the mature organ, with clusters of acinar cells lined up around the ends of the ductal network and endocrine cell aggregates – islets of Langerhan- distributed throughout the organ (**Figure 1.5 D**)[34–37].
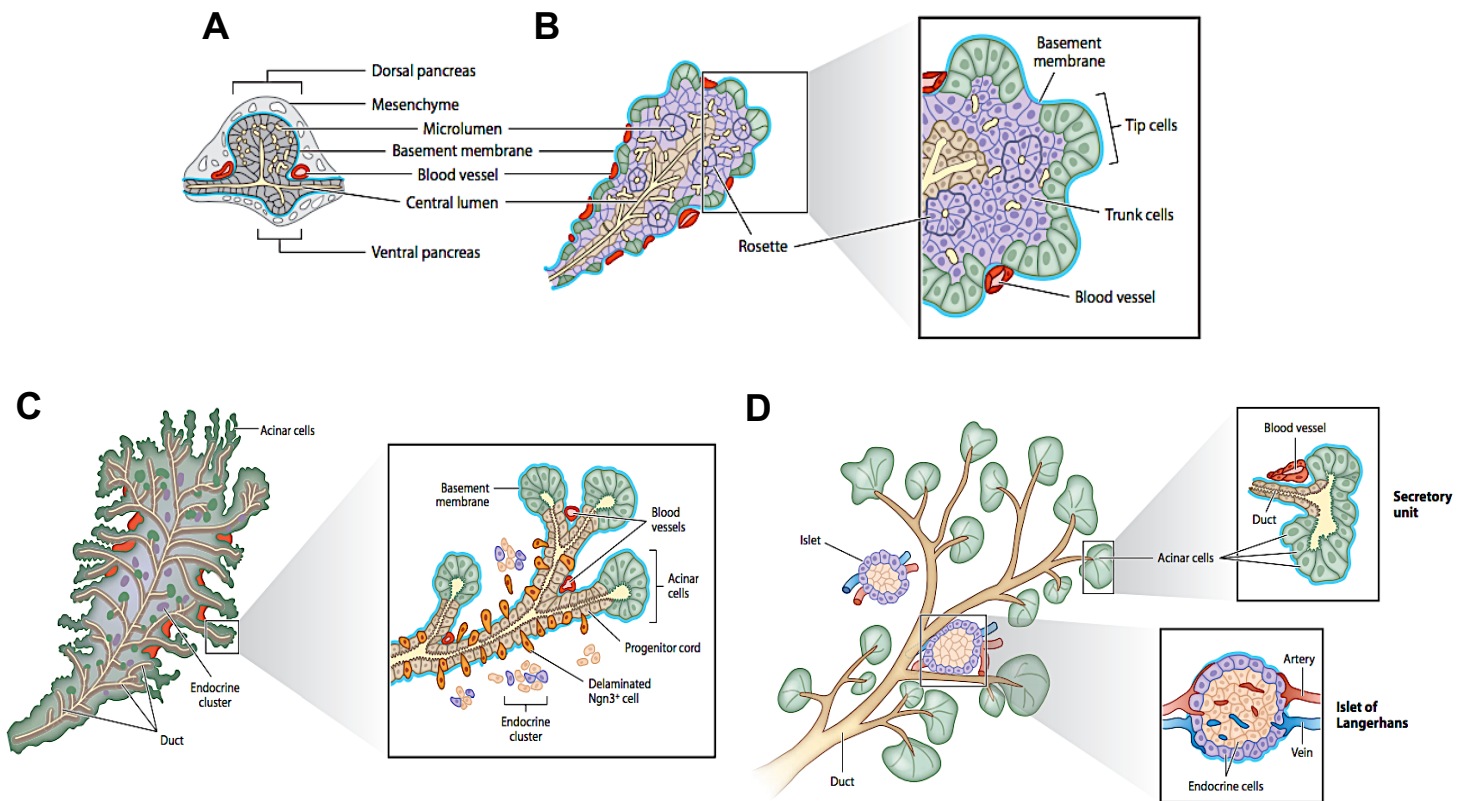
Figure 1. 13 - **Overview of pancreas embryonic development. (A)** Evagination of the gut endoderm to form two epithelial buds encased in mesenchyme: dorsal and ventral pancreatic bud. At this stage the pancreatic epithelium is formed by a multilayer of non-differentiated cells. **(B)** The outer layer or tip domain (*in green*) branches into multiple protrusions and produces acinar cells. The inner layer or trunk domain (*in purple*) organizes into rosette-like structures and produces ductal and endocrine cells. **(C)** Trunk cells progressively remodels into a 3-D network consisting of highly branched primate ducts (or progenitor cords) lined by differentiated acinar cells. Ngn3 expressing cells (*in orange*) generate, as whole, endocrine clusters composed by five different cell types. **(D)** Pancreas acquires the organized architecture of the mature organ, with acinar cells covering the ends of terminal ducts and endocrine cells clustered in so-called Islets of Langerhans. Adapted from [36].

1.4.3. *Genetic evolution of PC – accumulation of genetic alterations*

As mentioned previously, the pancreas has its exocrine portion, composed of epithelial cells (acinar and ductal cells), and its endocrine portion[38]. Acinar cells show high plasticity and are crucial for pancreas homeostasis and regeneration[38,39]. Under stress and inflammatory conditions, acinar cells can undergo a process called acinar-to-ductal metaplasia (ADM), where they differentiate to a more ductal phenotype[38,39]. These metaplastic cells are capable of proliferating and regenerate the damaged organ[38,39]. However, with sustained environmental stress and/or oncogenic genetic insults, ADM may lead to pancreatic intra-epithelial neoplasias (PanINs)[38,39], which is thought to be the cancer precursor[13,38]. Histologically, PanINs are classified into three stages of increasingly dysplastic growth: PanIN-1 and -2 (low-grade PanIN) and

PanIN-3 (high-grade PanIN)[40–42] – detailed info about histological characteristics of an adult normal pancreas versus PanINs progression in **Figure 1.6**.
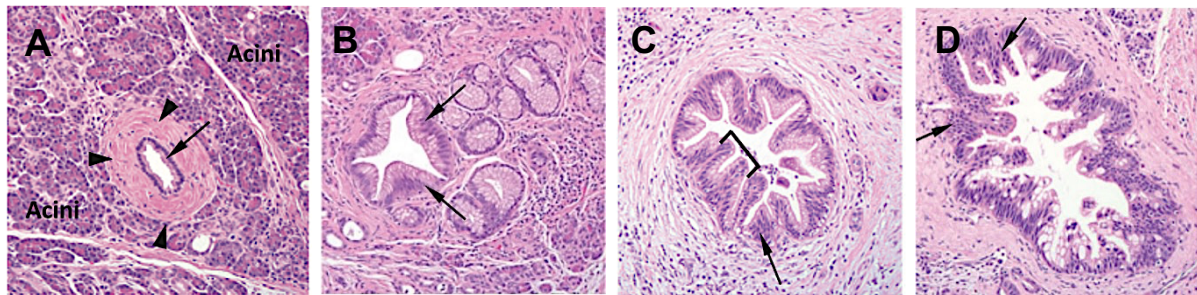
Figure 1. 16 - Histological changes of PanIN progression. **(A)** Representative microphotograph of the normal histology of a pancreatic duct. A mature ductal epithelium is characterized by a low epithelium of cube-like cells (arrow) surrounded by a thick dense collagenous wall (arrowheads) and a vast acinar component. **(B)** PanIN-1 lesions can be flat (PanIN-1A) or papillary (PanIN-1B), and are characterized by mucinous hyperplasia of the duct cells (arrows), with basally oriented round nuclei and without cytologic atypia. **(C)** PanIN-2 lesions typically have papillary architecture of the epithelium (bracket) with mild-to-moderate cytologic atypia, including hypercromasia (nucleus darker than usual), nuclear crowding (touching nuclei, arrow), increase nuclear size and pseudostratification (nuclei appearing at varying levels causing the appearance of stratified epithelium). **(D)** PanIN-3 lesions have many features of invasive carcinoma, including papillary growth of the neoplastic epithelium with cribriform architecture (small holes in between the cells), complete loss of nuclear polarity (arrows), and marked cytological atypia in association with frequent mitotic figures (occasionally abnormal) and macro-nucleoli. Adapted from [41].

Each stage of PanINs is also associated with specific mutational profiles, acquired in a temporal sequence[13,38] (**Figure 1.7**). The first genetic changes detected in the progression series are activating KRAS mutations and telomere shortening[43]. KRAS mutations are found in approximately 90% of pancreatic adenocarcinomas and not only initiates the disease but it is also necessary for rapid stromal remodeling and tumor progression[13,38,43]. Higher-grade PanIN lesions are commonly associated with genetic alterations mainly in three tumor suppressor genes: CDKN2A, TP53, and SMAD4[13,38,43]. CDKN2A is a tumor suppressor gene important for cell cycle regulation, and its inactivation is found in over 90% of PC cases[13,38,43]. Loss of function of this gene is induced by promoter hypermethylation, mutation or deletion and normally arises in moderately advanced lesions[13,38,43]. TP53 tumor suppressor gene is inactivated, generally, by missense mutations of the DNA-binding domain in near 70% of PC cases[13,38,43]. TP53 mutations arise in later stage PanINs with significant features of dysplasia and promote genetic instability[13,38,43]. SMAD4 gene is inactivated in approximately 50% of PC cases. Alterations in SMAD4 leads to aberrant cell cycle regulation, which is associated with a more aggressive phenotype [13,38,43]. Genetic alteration in SMAD4 occurs typically during late PanIN-3 lesions, however, it has been shown that SMAD4 deletion alone does not initiate PC[38].

Epigenetic dysregulation, such as DNA methylation, histone acetylation or interactive regulative microRNAs, is also largely linked to different morphological and genetic changes during pancreatic carcinogenesis[38,44].
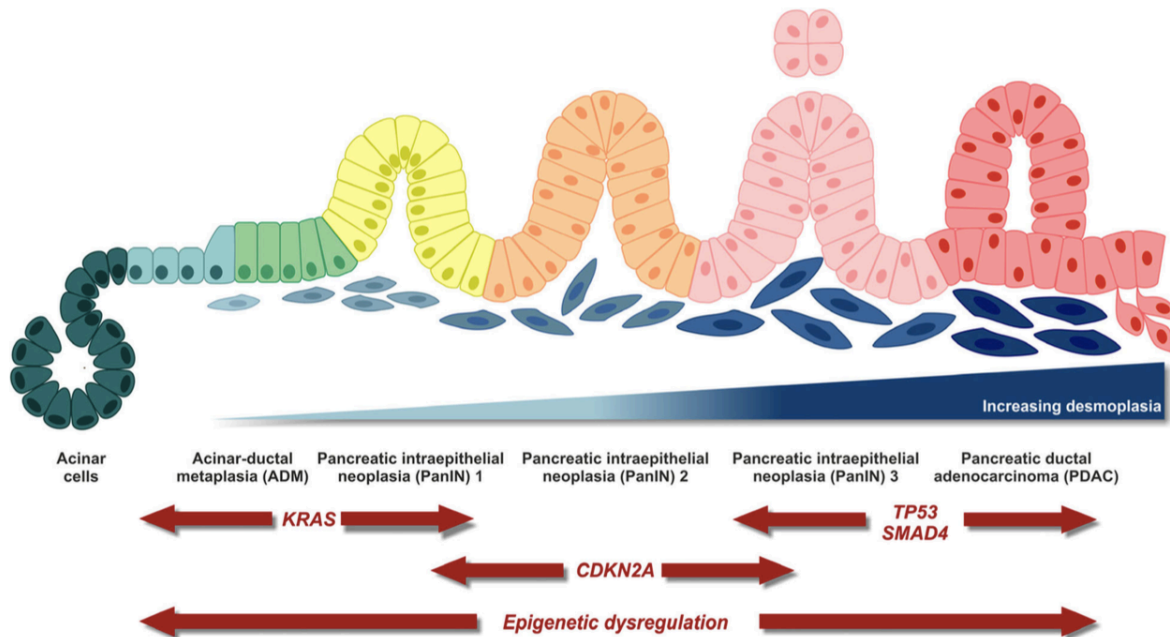
Figure 1. 19 - Multi-step pancreatic carcinogenesis. Under sustained stress conditions or oncogenic mutations, acinal-ductal metaplasia (ADM) may lead to pancreatic intra-epithelial neoplasias (PanINs). PanINs are considered the initial step of PC development followed by sequential progression associated with genetic alterations in several tumor suppressor genes. Adapted from [38].

Although PC carcinogenesis is mainly a result of sporadic genetic and environmental changes, 5-10% of PC cases have a familial basis[45]. Familial PC is defined as an inherited predisposition in families in which there are at least two first degree relatives with PC[45].

PC also occurs in the setting of cancer susceptibility syndromes, where an identifiable germline mutation may lead to the development of the disease[46]. To date, five hereditary syndromes have been described to increase the risk of developing PC[46]:

- Hereditary Breast-Ovarian Cancer Syndrome (mutations in the BRCA1 or BRCA2 genes);
- Familial Atypical Multiple Melanoma Syndrome (mutations in the CDKN2A gene);
- Peutz-Jeghers Syndrome (mutations in the STK11 gene);
- Hereditary pancreatitis (mutations in the PRSS1 gene);
- Lynch Syndrome (mutations in mismatch repair genes – MLH1, MSH2, MSH6, and PMS2).

1.4.4. PC Microenvironment – "partners in crime"

Cancer is not a solo performance. Cancer cells play "the leading villains", but they actively recruit other cell types to reshape the TME in favor of the promotion of tumor growth and invasion[47].

PC microenvironment carries unique features that have made it particularly challenging to treat. It is characterized by a dense desmoplastic stroma and extensive immunosuppression, both essential for tumor promotion and progression (**Figure 1.8**).[14]

Among other solid tumors, PC is reported to have the highest amount of stroma, which may constitute up to 90% of the tumor volume. This dense and fibrotic stroma results from the abnormal proliferation of stromal cells along with aberrant extracellular matrix (ECM) dynamics, which is termed desmoplasia reaction – pathophysiological hallmark of PC[14,48,49]. As a result, a dense mechanical barrier is created around tumor cells leading to low immune cell infiltration, preventing proper vascularization, and limiting the delivery of therapeutics[48,49]. Pancreatic stellate cells (PSCs), a subset of cancer-associated fibroblasts (CAFs), are the main responsible for desmoplasia[49,50]. In health, PSCs are in a quiescent state and produce matrix metalloproteinases (MMPs) and their inhibitors to regulate ECM turnover. During PC, quiescent PSCs are transformed into an activated myofibroblast-like phenotype by pro-inflammatory cytokines, such as IL-1, IL-6, IL-8 and tumor necrosis factor-alfa (TNF-α), and growth factors secreted by PC cells[49,50]. Activated PSCs undergo functional changes, including increased proliferation and migration and aberrant secretion of ECM proteins, primarily collagen and hyaluronan acid (HA), leading to pancreatic fibrosis[49,50].

In addition to the prominent desmoplastic reaction, PC is also described as a poorly immunogenic tumor[14,51]. Cancer cells have developed several strategies to suppress immune cells involved in tumor rejection (CD4^{+}/CD8^{+} T lymphocytes and natural killer cells), and to hijack the immune system by recruiting immunosuppressive cells to help tumor escape and progression[1,51]. The immunosuppressive microenvironment of PC is mainly composed by:

- Regulatory T cells (T-Regs) play a critical role in immunosuppression during PC progression and are associated with a poor prognosis in PC patients. T-Regs can prevent the development of anti-tumor immunity through several pathways, such as secretion of suppressive cytokines, including transforming growth factor-β (TGF-β) and IL-10, and expression and release of granzyme B which directly kill T cells. Besides, T-Regs can competitively bind to IL-2 to starve effector T cells and block the maturation or function of dendritic cells (DCs), suppressing tumor-specific immune responses [1,14,52].
- Myeloid-derived suppressor cells (MDSCs) can migrate from the bone marrow to the PC TME in response to granulocyte macrophage colony-stimulating factor (GM-CSF) secreted by PC cells. Once in the TME, MDSCs can suppress effector T cell functions through direct contact or indirect mediators, such as secretion of immunosuppressive cytokines such as TGF-

β and IL-10, release of reactive oxygen species, and induction of T-Reg cells [1,14,52].

- Tumor-associated macrophages (TAMs) are a major component of the TME that can either adopt an anti (M1-like) or pro-tumoral phenotype (M2-like), which can be modulated by tumor-specific signals. In PC, TAMs are involved in both desmoplasia, by upregulating PSCs functions and stimulating ECM secretion, and immunosuppression. The immunosuppressive activity of TAMs includes: secretion of immunosuppressive cytokines and chemokines, recruitment of T-Regs and induction of T cells apoptosis by expressing PD-L1 on their surface [1,14,52].
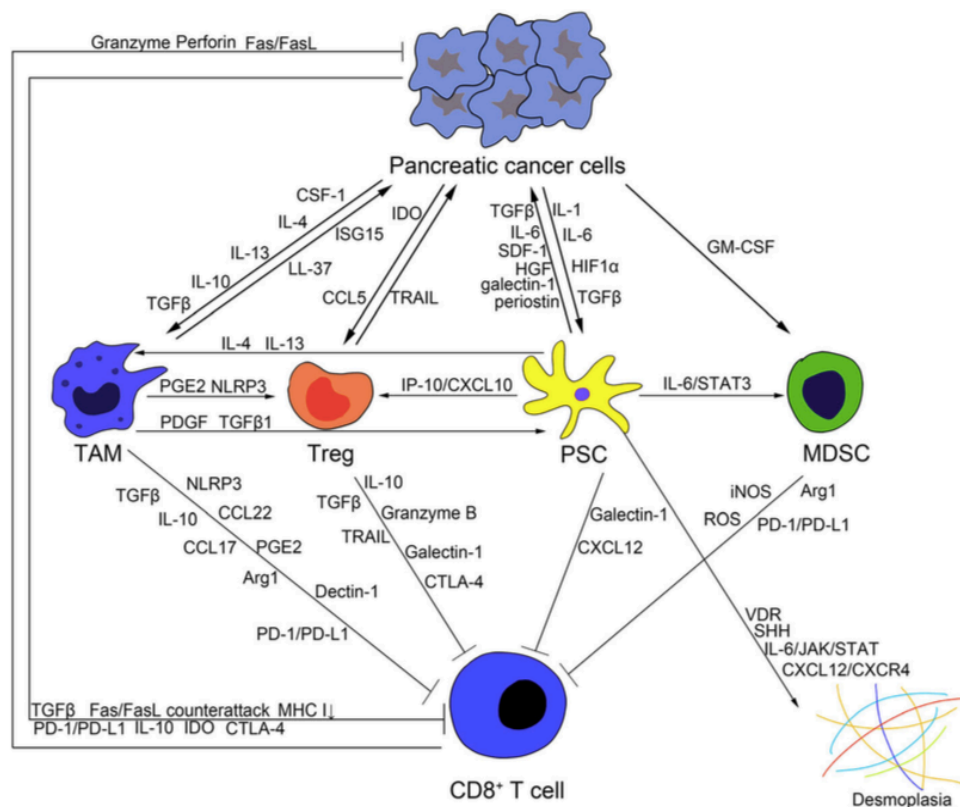
Figure 1. 22 - Pancreatic Cancer Microenvironment. PC is characterized by a desmoplastic and immunosuppressive microenvironment. PC cells recruit PSCs, T-Regs, MDSCs and TAMs for desmoplasia and immunosuppression. PSCs are the main responsible of desmoplasia by abnormal secretion of ECM proteins. These cells are also able to suppress T cell activity to overcome the immune surveillance an help PC cancer development. Adapted from [14].

The complexity of PC microenvironment constitutes a cellular dense milieu, rich in inflammatory cytokines that support tumor growth and progression, and immune evasion[53]. Cytokines are small, low-molecular-weight proteins secreted by tumor cells and surrounding cells of the TME, responsible for modulating biological processes, including cell growth and differentiation, immunity, inflammation, and metabolism[53,54]. Both anti and pro-inflammatory cytokines have been found to be overexpressed in PC, supporting tumor progression by acting directly on tumor cells and modulating the TME[53,54]. Additionally, cytokines overexpression is also correlated with clinical features in PC patients, such as cachexia – a complex metabolic syndrome that

causes loss of weight and loss of adipose and skeletal tissue - poor performance status, and negative clinical outcomes[55].

Among several cytokines, IL-6, IL-8, TNF-α, macrophage migration-inhibitory factor (MIF), and IL-1β are the main pro-inflammatory cytokines found overexpressed in PC patients and have been associated with the prevalence of cachexia[53,55]. IL-6 and IL-8 can both regulate the expression of VEGF in PC cells, therefore promoting angiogenesis and invasion[53,54]. TNF-α has pleiotropic functions in normal conditions and cancer-related inflammation. Although several studies revealed that high doses of TNF-α has toxic effects on tumor cells, it has been demonstrated that TNF-α can promote cancer cell proliferation by upregulating EGF receptor in PC microenvironment[56]. MIF and IL-1β are also implicated in tumor growth and metastasis by increasing the migratory potential of PC cells[53,54].

Several studies have evaluated the expression profile of many cytokines in the plasma of PC, and revealed that cytokine expression patterns differ from patient to patient, and are associated with different survival probabilities[57]. Nevertheless, the exact role of most cytokines in the progression of PC remains unclear[57].

1.4.5. Pancreatic Cancer Therapy

1.4.5.1. <u>Current treatment strategies – best available options</u>

Over the last few decades, cancer patients' average survival has significantly increased due to advances in treatment strategies together with an earlier diagnosis. Nevertheless, some malignancies, such as PC, have shown very little improvement because there is still no adequate therapy, and there are no specific and sensitive predictive biomarkers for the current treatments used.

Surgical resection remains the only potential cure for PC patients[58,59]. However, only 10% are diagnosed with tumors that can undergo surgical resection, while 60% present with non-resectable and metastatic disease[58,60]. The remaining 30% of patients have locally advanced tumors and are generally treated as having advanced disease[60]. But, surgery alone is not enough, as > 90% of PC patients relapse and/or die without additional therapy[58–60]. Thus, after surgery, adjuvant treatment strategies offer the only hope for long-term survival for PC patients with resectable disease[58–60].

According to the European Society for Medical Oncology (ESMO), treatment options and recommendations for PC depend on several factors, including the size, location and stage of the tumor, and patients' overall health[59] (**Figure 1.9**). Before treatment decisions, PC is first classified according to its clinical stage, as localized or resectable disease, borderline resectable, locally advanced or metastatic, based on the degree of contact between the tumor and the vascular system[59].

For localized or resectable disease, treatment typically involves surgical resection followed by adjuvant chemotherapy, with either gemcitabine or 5-fluorouracil (5-FU)[59,60].

Borderline resectable PC is neither resectable nor unresectable but implies a greater chance of incomplete resection [59,61]. The preferred approach is neoadjuvant treatment protocols to achieve some degree of downstaging, improve patient selection for surgical resection, and early treatment of possible micromestastasis[59,61].

In patients with locally advanced disease - no metastasis, but surgical intervention is considered not beneficial due to extensive vascular involvement - the standard of care is gemcitabine monotherapy[59,62]. However, FOLFIRINOX (a combination therapy of folinic acid, 5-FU, irinotecan, and oxaliplatin) can also be considered for patients with good performance status – patients' functioning in daily life activities[62].

Patients with metastatic disease – primarily in the peritoneum, liver, and, in some cases, the vascular and/or the nervous system - generally qualify for systemic palliative chemotherapy[59,60]. There are three options of treatment according to the patient's performance status[59,60]. Patients with a performance status of 3/4 and with a very short life expectancy will be offered supportive care only[59,60]. Patients with a performance status of 2 and/or with high bilirubin levels may be treated with gemcitabine alone, however, gemcitabine plus nanoparticle albumin-bound paclitaxel (GnP) can also be considered[59,60]. For patients with a performance status of 0 or 1, the first line of chemotherapy is the FOLFIRINOX regimen with an Overall Response Rate (ORR) of 31.6%[63], and the second line is GnP, with an ORR of 9.4%[59,63].
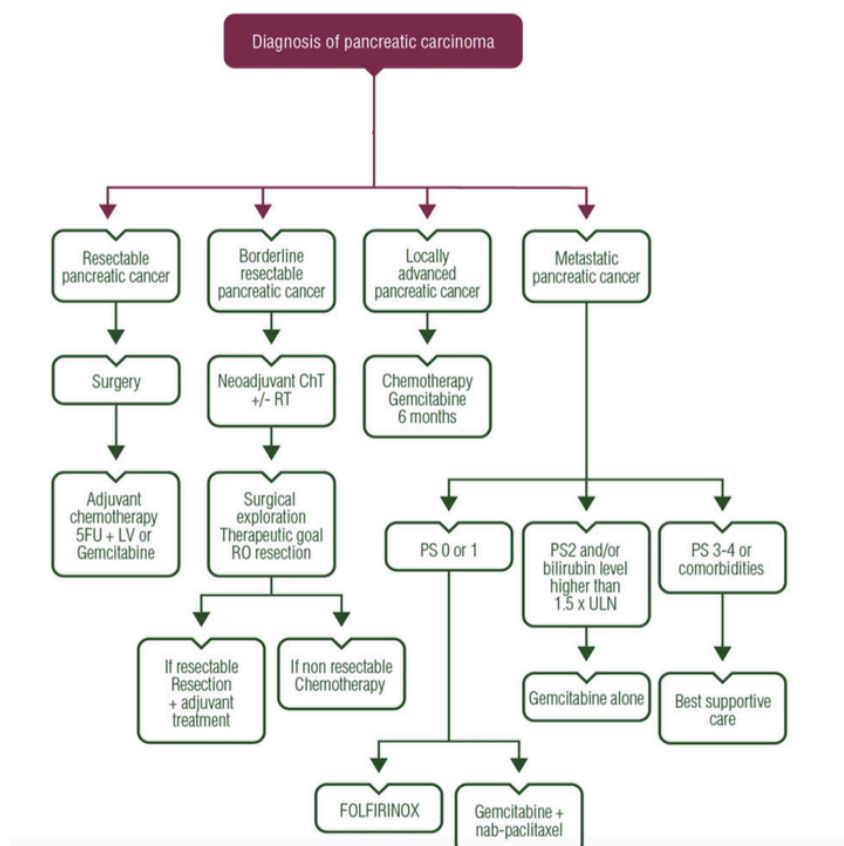
Figure 1. 25 - ESMO Clinical Guidelines for PC treatment. According to the degree of contact between the tumor and the vessels, PC can be categorized as localized or resectable, borderline resectable, locally advanced or metastastic. After the classification, specific treatment strategies are applied. Adapted from [59].

1.4.5.2. *Immunotherapy – a promising novel therapy or a failure?*

Over the last years, immunotherapy has revolutionized cancer treatment, and several approaches are being developed to boost the immune system to fight cancer, such as immune checkpoint inhibitors (ICIs)[1]. Under normal physiological conditions, the immune system has evolved self-tolerance mechanisms – immune checkpoints - to modulate T cell responses and prevent autoimmunity and inflammatory tissue damage[64]. Cytotoxic T lymphocyte antigen-4 (CTLA-4) and programmed cell death-1 (PD-1) are the most potent examples of T cell immune checkpoint molecules. However, tumors have exploited these mechanisms to acquire resistance to immune surveillance and escape from anti-tumor immune responses[65,66]. The introduction of ICIs, including anti-CTLA-4 and anti-PD-1 antibodies, into clinical practice transformed the prognosis of cancer patients with advanced melanoma and lung cancer by blocking these immune checkpoint pathways and enhancing anti-tumor immunity[67].

Regarding the PD-1/PD-L1 immune checkpoint, PD-L1 has been reported to be overexpressed in PC, and several studies correlate this overexpression with worse prognosis[68]. PD-1, which has been thought to be primarily expressed only on immune cells, was also described to be expressed by PC cells and was shown to contribute cell-autonomously to tumor growth[69]. Nevertheless, PD-1 expression levels are inconsistent, ranging from 12 to 90%, therefore predictive biomarkers for checkpoint inhibitors are needed to improve therapeutic outcomes[68]. Unfortunately, to date, attempts of using ICIs to treat PC have been unsuccessful when applied as single agents. This may be partly attributed to the unique immunosuppressive TME of PC, rich in fibroblasts and ECM proteins, reducing the interaction between effector T cells and malignant cells[65,66]. Due to the lack of clinical success with single agent checkpoint inhibitors, combination of anti-PD-1 and CTLA-4 antibodies as well as the combination of ICIs with chemotherapy are being assessed[70]. Currently, nivolumab (nivo) (anti-PD-1 antibody) is being evaluated in combination with GnP, in a phase I clinical trials for efficacy and safety[71]. So far, the reported results are an overall well-tolerated combination, with disease control in 12 of 17 patients with locally advanced or metastatic PC[71].

Besides ICIs, CAR (Chimeric Antigen Receptor) T cell therapies and cancer vaccines are being developed with the hope of inducing an anti-tumor immune response in PC[68,72,73].

In CAR T-cell therapy, tumor-specific T cells are isolated from the patient, genetically engineered to express CARs (that recognize cancer-specific antigens), expanded *ex vivo*, and re-infused into the patient to target malignancies[1]. This approach had impressive results in many hematological diseases malignancies, such as acute lymphoblastic leukemia (ALL) and has started to be investigated in solid tumor malignancies, including PC[68,73]. Phase I clinical trials are assessing the potential of CAR T-cells to target mesothelin, a tumor-associated antigen overexpressed in almost 80% of PC cases, and associated with an unfavorable prognosis[72,74]. Clinical trial results demonstrated an anti-tumor immune response in patients with metastatic PC, aside from the resolution of liver metastasis in one PC patient after one month of therapy[74].

Cancer vaccines involve administering tumor-associated antigens (TAAs) to stimulate the immune system to attack cancer cells[75]. GM-CSF cell-based vaccines are the most extensively evaluated and have been confirmed to deplete T-Regs[72,73,75]. Phase II clinical trials, have been assessing the efficacy of combining GM-CSF cell based-vaccines with immune checkpoint inhibitors (for example ipilimumab) in patients with metastatic PC[76]. Up to now, the combined treatment yielded a longer overall survival (OS) than that observed with ICIs applied as single agents[76]. Nevertheless, PC has a low-mutation burden with lack of neoantigens, which can be an obstacle regarding cancer vaccines therapy[65].

PC poses crucial challenges for immune therapeutic interventions, including the unique immunosuppressive TME of PC, low levels of antitumoral infiltrating T cells and low neoantigens levels. Despite this, some early clinical data have shown that the combination of different immunotherapeutic approaches or immunotherapy plus traditional therapy, like chemotherapy, may have a synergic effect in patients with advanced and metastatic PC[71,74,76]. Nevertheless, more multicenter, phase III clinical trials should be done, and since not all patients are eligible to immune targeted therapies, patients with more susceptibility should be identified and included[72].

1.4.6. Challenges in PC management - new biomarkers are still needed

The poor prognosis of PC is mainly attributed to an extremely challenging diagnosis, since patients are commonly diagnosed at advanced stages, where curative treatment options are still lacking[9]. Even for patients with early-stage PC, the diagnosis is still very difficult due to the lack of symptoms[9]. Therefore, there's an urgent need to develop biomarkers with diagnostic, predictive, and prognostic potential in PC patients[12]. The research for novel and accurate biomarkers is ongoing since there is still no molecular signature to be implemented in clinical routine[12].

Carbohydrate antigen 19-9 (CA 19-9) is the only biomarker approved by the National Comprehensive Cancer Network (NCCN) guidelines for the clinical management of PC[12,77]. CA 19-9 is synthesized in the pancreatic-biliary system and has been reported to increase in PC. However, CA 19-9 biomarker has some limitations: 1) its expression depends on Lewis blood group, therefore patients Lewis-negative cannot be followed by CA 19-9 expression, 2) the variable sensitivity (53%) and specificity (95%) may lead to false-negative results and mislead the diagnosis, and 3) CA 19-9 levels can be elevated in other gastrointestinal malignancies and in benign conditions [12,78].

New and more reliable diagnostic biomarkers have been explored for a better management and follow-up of PC patients, such as microRNAs, including miR-21, miR-155, and mi-R196, which were found to be upregulated in PC[12,79,80], and KRAS mutation[81]. However, the specific role of such miRNAs is still unknown, making their clinical application unlikely, and the diagnostic accuracy of KRAS mutation for PC is of variable sensitivity and specificity, since is detected in PC patients but also patients with chronic pancreatitis or benign pancreatic tumors[82,83].

To date, no reliable biomarkers exist to help predict PC patients' responses to the major therapeutic options. Thus, clinical decisions are based on a "trial-and-error"

approach to find the best treatment. Stromal markers, such as HA status, for Pegvorhyaluronidase alfa (PEGPH20) therapy, and PD-1/PD-L1 expression for immunotherapy, are being studied as potential predictive biomarkers[12].

Recent data revealed that high levels of certain inflammatory cytokines, including, IL-2, IL-6, IL-8, IL-10, and TNFα[84], and immune cells, such as MDSCs and T-Regs[85], are associated with a worse prognosis and poor survival rate in PC patients. Yet, there are still no sufficient data that confirm the reliability of these markers for prognosis, and they need to be investigated in the context of larger clinical trials.

A diverse array of biomarkers are currently being studied to find effective management of PC. However, these studies have been confronted with several obstacles that compromise the development of biomarkers, such as selection of early stage cases, requirement of large volume of samples, tumor biopsies frequently contain limited tumor cells or low-quality tumor content and non-specificity of molecular markers[12].

1.5. Zebrafish xenografts as a screening platform for pancreatic cancer therapy – Thesis Goals

Cancer is a highly individualized disease, but patients are treated according to standardized clinical guidelines, which are developed and approved based on average efficacy and safety rates[86,87]. Although some patients respond to this kind of approach, others do not and are subjected to ineffective treatment, eventual disease progression, unnecessary toxicity, and loss of therapeutic time, which in PC is even more critical[86,87]. Therefore, there is an urgent need to predict individual patient responses prior to treatment to determine the most accurate and effective therapy[86].

Currently, there are several different models able to directly challenge tumor cells in a personalized manner[86]. Two-dimensional (2D) cultured cancer cell lines is a fundamental model used in basic cancer research and in the development of oncology drugs[88]. Their usefulness is primarily linked to their ability to provide an indefinite source of biological material[88]. However, cancer cell lines lack the heterogeneity of the primary tumor as well as the tumor microenvironment[86,88]. Therefore this model is not ideal for recapitulating patient tumors and predicting the response to a given treatment[86,88].

Opposed to 2D cultures, 3-dimensional models, including spheroids, explants, and organoids, are able to architecturally and functionally mimic a particular organ/tissue[86,88]. Nevertheless, these models still lack many complex interactions observed in the TME and cannot reproduce therapy sensitivity as in a living organism[86,88].

Patient-derived xenografts (PDXs) can maintain both interindividual and genetic heterogeneity of the original tumor, and therefore, emerged as a powerful tool to predict drug efficacy[86–88]. Mouse PDXs (mPDXs) is the most widely used *in vivo* model and represent the gold standard in cancer biology for personalized screening[86–88]. However, the amount of patient sample required and the time frame required for tumor establishment (~1-10 months) are some of the limitations that make this model unfeasible for clinical practice[86,87].

In recent years, zebrafish has emerged as an alternate xenograft model to study human cancers, with several and unique advantages:

- adult zebrafish can produce hundreds of embryos per week;
- embryos optical transparency allows direct visualization of tumor-associated processes, such as implantation, migration, and micrometastasis formation, and single-cell resolution imaging;
- larvae small size allows for reduced number of cancer cells for successful transplantation (~500 cells per animal);
- compatible with biopsy samples;
- experiments have a short window of ~ 4 days;
- the absence of an active adaptive immune system until 8dpf, avoids the use of immunosuppressive agents and allows xenograft engraftment;
- the availability of several transgenic lines, enables the real-time monitorization of several cancer hallmarks, such as angiogenesis and innate-immune interactions;
- The human and zebrafish genomes have ~70% of homology and cancer-associated human genes are conserved structurally and functionally in zebrafish[89].

All of these features make the zebrafish larvae an attractive and feasible model to analyze patient-specific chemosensitivity and to study cancer development and interactions with the microenvironment[86,90].

Recently, my host laboratory proposed a fast *in vivo* assay– the zebrafish-larvae xenograft assay to determine the best therapeutic option for each patient, and help oncologists with their first clinical decisions. In some of the Lab latest work, results showed that zebrafish larvae xenografts have high cellular resolution to reveal inter-an intratumor functional cancer heterogeneity and differential tumor responses to standard therapy[87,91,92]. Moreover, proof-of-concept experiments showed that zebrafish patient-derived xenografts (zPDX or zAvatars) present similar responses to therapy as their matching patients[87]. The Lab is currently validating the predictive value of the assay by increasing the cohort of patients. This assay was established for colorectal and breast cancer, and currently more other cancer types are also being tested, including PC.

The main goal of my thesis project was to determine the **feasibility and sensitivity of the zebrafish xenograft model as a screening platform for PC therapy**. This concerned not only testing the common therapeutic options for PC, but also some novel therapies, including immunotherapy.

Hence, the main tasks of this project were:

(1) to establish zebrafish xenografts with two human PC cell lines: Panc-1 and MIA PaCa-2;
(2) to test the main treatment options for patients with advanced PC, FOLFIRINOX and GnP. Tumor responses were evaluated through the analysis of tumor size, proliferative index, and apoptotic levels;

(3) to test the alternative treatment options for patients with PC using the PD-1 inhibitor nivo and nivo plus GnP (phase 1 clinical trial ongoing for advanced PC), as PD-1 is expressed in both Panc-1 and MIA PaCa-2;

(4) to explore the cross-talk between PC tumor cells and the innate immune compartment.

2. Material and Methods

2.1. Experimental Workflow

Zebrafish xenografts were generated using human immortalized PC cell lines. Experimental workflow is schematically illustrated in **Figure 2.1.**
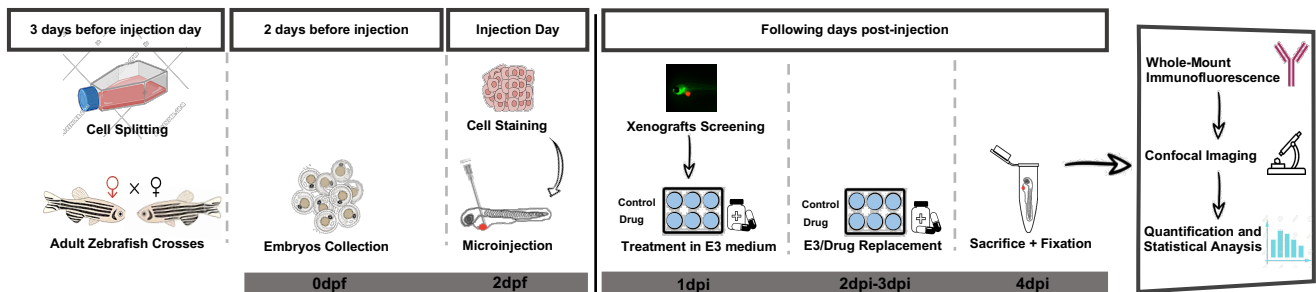
Figure 2. 1 - Experimental Outline. The generation of zebrafish xenografts was the foundation of this research project. Three days prior to injection day, PC cell lines were split, in order to achieve 70-80% confluence, and adult zebrafish crossed. On the next morning, zebrafish embryos were placed onto petri dishes and incubated at 28°C for the following 2 days. On injection's day, PC cell lines were labelled with a fluorescent dye and microinjected into the perivitelline space (PVS) of 2 days post-fertilization (dpf) zebrafish larvae. Injected zebrafish larvae were kept at 34°C until the next day. At 1 day post-injection (dpi), successfully injected zebrafish xenografts were screened according with the tumor size, and non-successful xenografts were discarded. After the screening, zebrafish xenografts were divided into two experimental conditions: control and treatment group. For the treatment group, drugs - FOLFIRINOX, GnP, nivo (also added to the cell suspension prior to injection) and nivo+GnP – were added to the E3 medium and replaced daily. At 4dpi, zebrafish xenografts were sacrificed and fixed. In fixed xenografts, whole-mount immunofluorescence technique was performed for specific targets and imaged by confocal fluorescent microscopy. After image acquisition, quantification and statistical analysis was carried out.

2.2. Cell Culture Techniques

2.2.1. Cell Lines and Culture

Panc-1 and MIA PaCa-2 cell lines, were kindly provided by Valérie Paradis, at Beaujon Hospital (Clichy, France). Fibroblast cell line, HS-5, was kindly provided by João Barata's Laboratory at Instituto de Medicina Molecular (Lisbon, Portugal). All cell lines were authenticated through short tandem repeat profile analysis and tested for mycoplasma.

All cell lines were adherently cultured and expanded in sterilized plastic T-flasks (Orange Scientific) using filtered Dulbecco's Modified Eagle Medium (DMEM, Biowest) supplemented with 10% Fetal Bovine Serum (FBS, Sigma Brazil) and 1% Penincillin-Streptomycin (P/S) 10,000 Units/mL (Hyclone). Cells were maintained in an incubator (inCu Safe) with a humified atmosphere at 5% CO_2 and 37°C.

2.2.2. Cell Thawing and Expansion

Cells were thawed and expanded for two weeks before injection and maintained in culture until passage 15.

To thaw frozen cells, cryovials were removed from -80°C and placed in a pre-warmed 37°C water bath. When the cell suspension was thawed, the cryovial was wiped with 70% ethanol and transferred into the laminar flow cabinet. Cell suspension

was then diluted in 10mL of warm culture medium and centrifuged at 1200rpm for 5 minutes. After centrifugation the cell pellet was resuspended in 1mL of culture medium and transferred into a sterilized T-25 flask.

For cell expansion and maintenance, cell passage was performed twice a week once cells achieve 70-80% confluence. Cells were washed with 1x Dulbecco's Phosphate Buffered Saline (DPBS, Biowest) and detached with TrypLE™ Express Enzyme (TrypLE, Gibco) at 37°C for 5 minutes (Panc-1), 4 minutes (MIA PaCa-2) and 2 minutes (HS-5). Subsequently, cells were counted by using Trypan Blue Exclusion Assay and cell concentration and cell viability were calculated according with **equation 1** and **2**, respectively (see section 2.2.3.). Finally, Panc-1, MIA PaCa-2 and HS-5 were seeded at $1,5\times10^4$ cell/cm^2, $1,3\times10^4$cells/cm^2 and 2×10^4cells/cm^2, respectively, into sterilized T-flasks with pre-warmed (37°C) culture medium.

2.2.3. Cell Counting – Trypan Blue Exclusion Assay

Trypan Blue is a membrane-impermeable dye that selectively stains dead cells, as it can only pass a damaged cell membrane, after which it binds intracellular proteins and gives cells a bluish color. Trypan Blue Exclusion Assay is used to determine the number of live cells (unstained) and dead cells (blue) present in a cell suspension[93].

To conduct this assay, cells were diluted at 1:100 with 1% Trypan Blue (Sigma Aldrich) and counted with a hemocytometer (Neubauer Chamber, BlauBrand) to assess cell viability and cell concentration. Cell viability and cell concentration were calculated according with **equation 1** and **2**, respectively.

Equation 1:

$$Cell\ concentration\ (cells\ mL^{-1}) = \frac{n^{\underline{o}}\ of\ live\ cells}{n^{\underline{o}}\ of\ squares} \times 10^{dilution\ factor} \times 10^4\ mm^3 mL^{-1}$$

10^4 is a constant that takes into account the sample volume present in each square

Equation 2:

$$Cell\ viability\ (\%) = \frac{n^{\underline{o}}\ of\ live\ cells}{n^{\underline{o}}\ of\ live\ cells + n^{\underline{o}}\ of\ dead\ cells} \times 100$$

2.2.4. Cell Freezing

Cell lines in continuous culture are likely to suffer genetic alterations and microbial contamination or cross contamination with other cell lines. Therefore, it is important that they are frozen with few passage numbers (2-4) and cryopreserved for long-term maintenance.

Primarily, cells were washed with DPBS 1x and detached from the T-flask with TrypLE. Detached cells were then harvested, transferred for a 10mL falcon and centrifuged at 1200rpm for 4 minutes. After centrifugation, the supernatant was discarded and the cells were resuspended in freezing media, composed by 90% FBS and 10% Dimethyl Sulfoxide (DMSO, Sigma-Aldrich), to guarantee a slowly cooling rate and prevent the risk of ice crystals formation, which can damage the cells. Cell suspension was distributed into several cryovials (Corning), which were placed in a freezer container (Thermo Fisher Scientific) at -80°C, for a gradient cell freezing. The next day, cryovials were transferred to the vapor phase of liquid nitrogen container (K Series Cryostorage System) at -196°C or stored in a proper box at -80°C.

2.2.5. Cell Bank

In order to minimize all the potential risks of maintaining cell lines in continuous culture and to ensure the robustness and reproducibility of experimental work, our lab implemented a two-tiered cell banking system composed by a working cell bank at -80°C and a master cell bank stored in the vapor phase of liquid nitrogen. The working cell bank was generated through the expansion of cells from the master cell bank. Whenever a working cell bank was finished, a new vial from the master cell bank was thawed for the generation of a new working cell bank. Both cell banks had cells with low passage numbers (2-4).

2.3. Animal Model – Zebrafish
2.3.1. Zebrafish Care and Handling

In vivo experiments were performed using the zebrafish (*Danio rerio*) model, which were handled according to European Animal Welfare Legislation, Directive 2010/62/EU (European Comission 2016) and standard protocols.

Adult zebrafish were maintained in standard size tanks, with 3.5L, supported by a water recycling system with a maximum number of 35 fish per tank (including males and females). Water parameters, such as temperature, pH, salinity and dissolved gases were constantly monitored to be kept under the physiological range[94]. Besides, fish holding rooms were kept at controlled temperature (25°C) and humidity (50-60%) and under a 14 hours light plus 10 hours dark automatic cycle[94].

2.3.2. Crossing of Adult Zebrafish and Embryos Harvesting

For each *in vivo* experiment, adult zebrafish were crossed three days in advance. Crosses were performed into slopping breeding tanks that mimics the shallow waters where zebrafish mate, and allow the eggs to fall while protecting them from being eaten. Furthermore, synthetic algae were also added into the breeding tanks to promote environment enrichment. On the following morning, adult zebrafish mate and breed, and afterward, they were transferred back to their original tanks. The embryos were carefully collected with strainers, washed with E3 medium (zebrafish embryo medium) (composition in **Table 8.1** Appendix) and transferred to petri dishes

(approximately 50 embryos per dish) filled with E3 medium. Lastly, all petri dishes were incubated at 28°C for the next two days.

2.3.3. Zebrafish Lines

During this research project, different transgenic and mutant zebrafish lines were used accordingly with the goal of each experiment.

Transgenic zebrafish lines

The transgenic zebrafish lines used in this research project were:
- o Tg(Fli1:enhanced green fluorescent protein [eGFP]), which allows the visualization of blood and lymphatic vessels, through the expression of eGFP linked to fli1 (endothelial marker) promoter[95].
- o Tg(mpx:green fluorescent protein [GFP]) and Tg(mpeg:loss red loss green [LRLG]), that specifically label neutrophils in green and macrophages in red, respectively[96].
- o Tg(mpeg:LRLG;TNFα:GFP), which is used to discriminate macrophages subsets. This transgenic labels macrophages in red (mpeg$^+$), inflammatory cells in green (TNFα$^+$) and inflammatory macrophages in yellow (mpeg$^+$ TNFα$^+$)[97].

Mutant zebrafish lines

The mutant zebrafish lines used in this research project were:
- o Nacre, which has complete lack of melanocytes due to a mutation in the gene enconding the *mitfa* gene[98].
- o Panther, in which macrophages migration is compromised due to a mutation in *csf1ra* [99].
- o Runx^{w84x}, which carries a truncation mutation, W84X, in *runx1* gene. Mutant embryos have normal primitive hematopoiesis but blockage of definitive hematopoiesis (low neutrophils and high macrophages)[100].

2.4. In vitro Experiments

Firstly, square (VWR Borosilicate cover glass, 20x20mm, Thickness no.1) and round (VWR Borosilicate cover glass, 13mm diameter, Thickness no.1.5) glass coverslips were sterilized in 70% Ethanol for 20 minutes, followed by immersion in sterile Milli-Q water. Then, coverslips were left in sterilized petri dishes for 30 minutes with UV lights on.

Sterile square and round coverslips were placed in 6-well and 24-well plates, respectively, and seeded with 1) Panc-1 cells (15.3x10^4; 3.04 x10^4 cells/cm^2), 2) HS-5 cells (19.2 x10^4; 3.8 x10^4 cells/cm^2) and 3) Mixture of Panc-1 and HS-5 in equal proportions – "MIX" 1:1 (15.3x10^4; 3.04 x10^4 cells/cm^2), diluted in DMEM in a final volume of 500μL/well and 1mL/well, respectively.

The plates were incubated in a humidified atmosphere containing 5% CO$_2$ at 37°C, for 3 days. After three days, culture media was discarded, wells were washed with

DPBS 1x, fixed with 4% formaldehyde (FA, Thermo Scientific) for 24 hours and submitted for histophatological analysis (see section 2.9.).

2.5. *Zebrafish Xenografts Experiments*

2.5.1. *Cell Labelling*

Cells were labelled with fluorescent lipophilic dyes diluted in DPBS 1x and protected from the light. Depending on the transgenic zebrafish line used, cells were labelled with Vybrant CM-DiI (Vybrant^TM CM-DiI, Thermo Fisher Scientific), at a concentration of 4μL/mL, or Deep Red dye (CellTracker^TM, Thermo Fisher Scientific), at a concentration of 1μL/mL.

PC and Fibroblast cell lines

Cells with a confluence of 70-80%, were washed with DPBS 1x and stained in a T-flask with a fluorescent dye diluted in DPBS 1x for 15 minutes at 37°C. Subsequently, cells were detached from the T-flask with TrypLE, collected to 10mL falcons and centrifuged at 1200rpm for 4 minutes. After centrifugation, the supernatant was discarded and the cell pellet was resuspended in DMEM and transferred into 1,5mL eppendorf. Cells were counted by using Trypan Blue Exclusion Assay and cell concentration and cell viability were calculated according with **equation 1** and **2**, respectively (see section 2.2.3.). Then, total cell number, regarding the volume in the eppendorf, was calculated through **equation 3**. Cells were centrifuged one last time at 1200rpm for 4 minutes, and resuspended in a final volume, given by **equation 4**, to achieve a final a concentration of 0,25x10^6cells/μL (Panc-1) or 0,5x10^6cells/μL (MIA PaCa-2). For the mix between Panc-1 and HS-5 cell lines, both cell lines were mixed in equal proportions (1:1) to achieve a final concentration of 0,5x10^6cells/μL.

Equation 3:

$$Total\ Cell\ Number = Cell\ concentration\ (cells\ mL^{-1}) \times Volume\ in\ eppendorf\ (mL)$$

Equation 4:

$$Final\ volume\ (\mu L) = \frac{Total\ Cell\ Number\ (cells)}{0,5\ or\ 0,25 \times 10^6 (cells\ \mu L^{-1})}$$

2.5.2. Pre-Injection tasks: zebrafish larvae care, glass needles and agarose plates

At 2dpf, zebrafish larvae are at the right development stage for enrolling the assay, but before the injection procedure, some essential tasks were performed:

- o Dead zebrafish larvae were discarded, while live zebrafish were kept in E3 medium at 28°C. Live zebrafish inside the chorion were also kept in E3 medium at 28°C, however pronase (composition in Appendix **Table 8.1**) , an enzymatic digester, could be added to the E3 medium to speed up the process. After approximately two hours, pronase was removed and replaced by E3 medium;
- o For zebrafish injection, needles were prepared from glass capillaries (World Precision Instruments, Borosilicate Glass Capillaries, 1mm thickness) using a Laser-Based Micropipette Puller (Sutter Instrument P-2000);
- o To stabilize zebrafish larvae during injection, 3% agarose plate with straight lines was made.

2.5.3. Injection of cancer cells in zebrafish larvae

Firstly, zebrafish larvae were anesthetized with Tricaine 1X (composition in Appendix **Table 8.1**) and then transferred to the agarose plate. With the help of a handmade hairpin, anesthetized zebrafish larvae were aligned along the straight lines of the agarose plate. Subsequently, fluorescently labelled cancer cells were loaded into a glass needle, which was attached to a pneumatic injector (World Precision Instruments, Pneumatic Pico pump PV820) controlled by a foot pedal. Cancer cells were microinjected into the PVS of zebrafish larvae under a fluorescence microscope (Zeiss Axio Zoom. V16) to monitor the procedure. Followed injection, zebrafish xenografts were transferred to petri plates with Tricaine 1X , for approximately 15 minutes, in order to keep the larvae and the tumor stable during the recovery phase/wound healing. After this period, Tricaine 1X was replaced by E3 medium and zebrafish xenografts were incubated at 34°C, a compromised temperature between the optimal temperature for human cell growth and zebrafish correct development, until the end of the experiment.

2.5.4. Zebrafish xenografts screening, anticancer drugs administration and fixation

At 1 day post injection (dpi), zebrafish xenografts were screened under a fluorescence microscope. Zebrafish xenografts with severe edema, cells in the yolk, cell debris or non-injected larvae were sacrificed with Tricaine 25x (composition in **Table 8.1** Appendix). Zebrafish xenografts successfully injected, were grouped according to tumor size, which was compared with the size of the eye: smaller than the eye (+), size of the eye (++) and bigger than the eye (+++) (**Figure 2.2**).
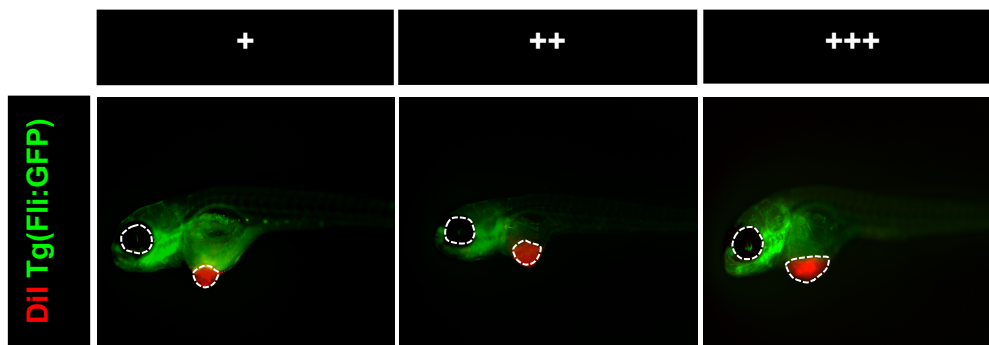
Figure 2. 4 - Zebrafish xenografts classification according to the tumor size. At 1dpi, injected zebrafish were screened according to tumor size and divided into three groups: smaller than the eye (+), size of the eye (++) and bigger than the eye (+++).

After the screening, zebrafish xenografts were randomly divided into two groups: control and treatment group. Larvae from the control group were kept in E3 medium, while larvae from the treatment group were kept in E3 medium supplemented with FOLFIRINOX, GnP, nivo or nivo+GnP. Both groups were kept at 34°C and the medium was renewed daily until the end of the experiment (4dpi).

At 4dpi, zebrafish xenografts were sacrificed with Tricaine 25x and fixed with 4% FA overnight at 4°C. For transgenic zebrafish lines [*Tg(mpx:GFP)* and *Tg(mpeg:LRLG;TNFα:GFP)*], fixation was performed with PIPES 1,5% (composition in **Table 8.2** Appendix) for optimal fluorescent signal preservation, as 4% PFA tends to reduce both GFP and mcherry signals. After 24 hours in fixative, zebrafish xenografts were transferred to Methanol 100% (MeOH, VWR Chemical) and stored at -20°C.

2.5.4.1. *Anticancer Drugs Administration*

All the drugs used in this project were kindly provided by the hospital pharmacy at the Champalimaud Foundation. For each drug, maximum tolerated concentration (MTC) for zebrafish larvae was determined by using the patient maximum plasma concentration as a reference. Group of 50 zebrafish larvae with 3dpf were exposed to different drug concentrations for three consecutive days, replaced daily. Toxicity was evaluated daily by counting the total number of dead fish and assessing presence of cardiac edema and curved tail. Working concentration corresponded the highest and with minimal toxicity (pathology) in the zebrafish. Stock and working concentrations of each drug are described in detail in **Table 8.3** in the Appendix section.

2.6. *Whole-mount Immunofluorescence Technique*

On day one of the immunofluorescence protocol, zebrafish xenografts stored in MeOH at -20 °C, were first submitted to a rehydration process through MeOH series 100% - 75% - 50% - 25% before the permeabilization step. Zebrafish xenografts stored in 4% FA at 4°C went directly to the permeabilization step.

Zebrafish xenografts were permeabilized 4x5 minutes with PBS-Triton 0,1% (Carl Roth), washed with sterile water for 5 minutes and incubated in 100% acetone (Fisher

Chemicals) for 7 minutes at -20 °C. Then, larvae were washed 2x5 minutes with PBS-Triton 0,1% and blocked for one hour at room temperature (RT) in a blocking solution, PBDX_GS (composition in **Table 8.2** Appendix). Subsequently, larvae were incubated with specific primary antibodies diluted at 1:100 in PBDX_GS for one hour at RT and then overnight at 4°C.

On day two, larvae were washed 2x10 minutes in PBS-Triton 0,1% followed by 4x30 minutes in PBS-Triton 0,1% and incubated with specific secondary antibodies and DAPI (Roche) diluted at 1:400 and 1:100, respectively, in PBDX_GS for one hour at RT and then overnight at 4°C. To preserve the fluorescence signal, samples were protected from the light until microscopy observation.

On day three, larvae were washed 4x15 minutes in PBS-Tween 0,05% (Thermo Fisher Scientific) and fixed with 4% FA for 20 minutes. Finally, larvae were washed 4x5 minutes in PBS-Tween 0,05% and mounted in mounting media (Mowiol, Sigma-Aldrich) into coverslips for confocal microscopy imaging. The coverslips were stored at 4°C into disposable cardboard slide trays (Fisher Scientific).

2.7.   Confocal Microscopy and Analysis of Imaged-Zebrafish Xenografts

Zebrafish xenografts were imaged in a Zeiss LSM710 fluorescence confocal microscope with an objective LD LCI Plan-Apochromat 25x/0.8 Imm Corr DIC M27 (Zeiss). For fixed samples, sequential images were acquired along tumor's depth with a 5μm interval using the z-stack function.

After image acquisition, quantification analysis was performed using the ImageJ software (V. 1.52p) Cell Counter Plugin. To assess tumor size, three representative slices of the tumor, from the top, middle and bottom, per z-stack per xenograft were analyzed and a proxy of total cell number (DAPI nuclei) was estimated by **equation 5**. To present the tumor size as a fold induction, the absolute numbers obtained for controls and treated xenografts were normalized to the control average.

Equation 5:

$$Tumor\ size\ (DAPI\ nuclei) = \frac{AVG\ 3\ slices\ counted\ \times\ total\ number\ of\ slices}{1.5}$$

The number of mitotic figures, activated caspase 3-positive cells, macrophages, neutrophils, M1-like and M2-like macrophages were counted in every slice, starting from the first and finishing in the last slice for tumor size counting. To calculate the percentage for each, the absolute numbers were divided by tumor size.

Implantation potential was evaluated by scoring the number of zebrafish xenografts with tumor in the PVS.

2.8. Histopathology

To characterize morphological features of PC cells and fibroblasts in single and mixed cell cultures, after fixation coverslips were stained with hematoxylin and eosin (H&E), mounted onto glass slides and examined by a pathologist in an Axioscope 5 microscope (Zeiss). Cell density, evidence of apoptosis/necrosis, mitotic activity and other cellular features were scored. Representative microphotographs were captured with an Axiocam 208 color camera (Zeiss).

To characterize morphological features of tumor xenografts in zebrafish larvae, after fixation larvae were embedded in paraffin, sectioned through their sagittal plane at 4µm and stained with H&E. Slides were examined by a pathologist in an Axioscope 5 microscope (Zeiss) and representative microphotographs were captured with an Axiocam 208 color camera (Zeiss).

2.9. Statistical Analysis

Statistical analysis was performed using the GraphPad Prism software (version 8.2.1 for macOS).

All data were challenged by two normality tests: the D'Agostino & Pearson and the Shapiro-Wilk normality tests. A Gaussian distribution was assumed only for datasets that pass both normality tests and were analyzed by an unpaired t test with Welch's correction. Datasets that do not pass the normality test were analyzed by an unpaired and non-parametric Mann-Whitney test.

For all the statistical analysis, P value (P) was from a two-tailed test with a confidence interval of 95%. Difference was considered statistically significant whenever P<0,05 and statistical output was represented by stars as follows: non-significant (ns)>0.05, *≤0.05, **≤0,01, ***≤0.001, ≤****0.0001. Results are represented as AVG ± standard error of the mean (SEM).

3. Results

3.1. *Human PC cell lines display different engraftment rates*

We started by selecting two human PC cell lines : Panc-1 and MIA PaCa-2. Both cell lines are commonly used to study PC carcinogenesis, chemotherapy responses and also immunotherapy with nivolumab (i.e. that express PD-1).

The Panc-1 cell line was established from a patient with adenocarcinoma of the head of the pancreas with metastasis to one peripancreatic lymph node. The MIA PaCa-2 cell line was established from a patient with adenocarcinoma of the body and tail of the pancreas. Both cell lines are of epithelial origin but also express the mesenchymal marker vimentin[101]. Regarding their genetic profile, both have missense mutations in KRAS and TP53 genes, the two most common mutated genes in patients with PC, and express PD-1, the target of nivolumab[69,101].

Before assessing the effect of the different therapeutic options, we started by characterizing their engraftment rates. Engraftment is described as the presence of a tumor mass in the site of injection (PVS) at 4dpi, and the percentage of engraftment is calculated according to **equation 6.**

Equation 6:

$$\%\text{Engraftment} = \frac{number\ of\ xenografts\ with\ tumor\ (4dpi)}{number\ of\ total\ xenografts\ (at\ 4dpi)} \times 100$$

To achieve this, cells were fluorescently labelled with CM-DiI. Panc-1 cell line has a grape-like morphology and they spontaneously form aggregates short after dissociation, which hampers injection due to capillary clogging. Thus, we tried several strategies to try to avoid aggregates. We first resuspended cells in PBS EDTA 2mM but there was still constant clogging of the needle. We then tried resuspension in higher concentration of PBS EDTA 3mM but it was toxic to both Panc-1 cells and the zebrafish larvae, so we had to use the PBS EDTA 2M condition. MIA PaCa-2 cell line was resuspended in PBS EDTA 1mM and it was easier to inject.

At 1dpi, zebrafish xenografts were screened to select the successfully injected xenografts and sacrifice the badly injected or the xenografts with cardiac edema. Unfortunately, 73.38% of Panc-1 xenografts (see **Table 8.4** in Appendix) and 84.31% of MIA PaCa-2 xenografts showed severe cardiac edema (**Figure 3.1 A,D,G**). At 4dpi, the engraftment rate was evaluated and Panc-1 and MIA PaCa-2 cells revealed an implantation capacity of 52.52% and 7.09%, respectively (**Figure 3.1 B,C,F,H**).

To try to increase the implantation rate of both cell lines, we resuspended the cells in 60% of FBS (DMEM). FBS is the most widely used growth supplement for cell culture media, and it has a rich content of growth-promoting factors, which could help implantation. At 1dpi, the percentage of Panc-1 and MIA PaCa-2 zebrafish xenografts with severe cardiac edema decreased to 55.73% and 65.10%, respectively (**Figure 3.1 D,G**), but engraftment did not improve (46.77% and 2.27%, respectively) (**Figure 3.1 F,H**). Therefore, we decided to use PBS EDTA 2mM (for Panc-1 cell line), and

PBS EDTA 1mM (for MIA PaCa-2 cell line) for the subsequent experiments, since high concentrations of FBS may be also toxic for the cells.
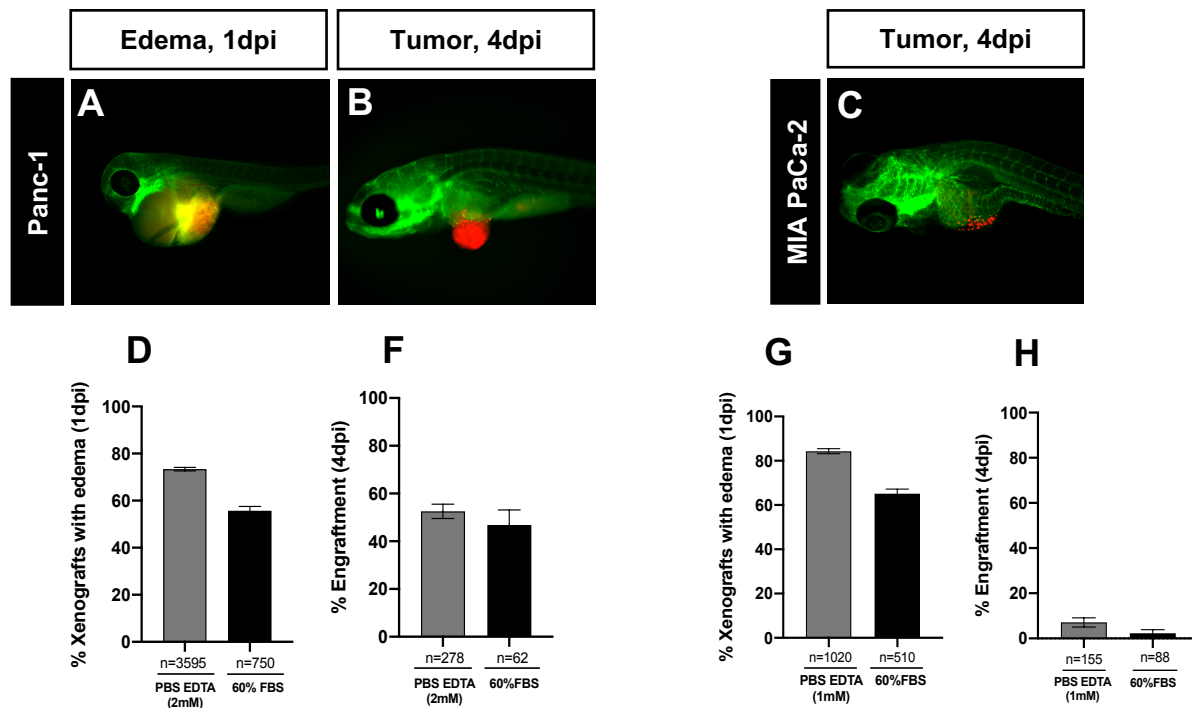
Figure 3. 1 - Engraftment analysis of the human PC cell lines Panc-1 and MIA PaCa-2 in zebrafish larvae. Panc-1 and MIA PaCa-2 cell lines were fluorescently labelled with CM-DiI (red), resuspended in PBS-EDTA 2mM and PBS-EDTA 1mM, respectively, or in 60% of FBS (experimental condition), and injected into the PVS of 2dpf zebrafish larvae. At 1dpi, zebrafish xenografts with severe edema were discarded (**A,D,G**) and successfully implanted xenografts were kept at 34°C until the end of the experiment. At 4dpi, the presence of tumor - %Engraftment - (**B,C,F,H**) was evaluated in both conditions. All results (**D,F,G,H**) are expressed in AVG±SEM, and are from three (PBS-EDTA 2mM, PBS-EDTA 1mM) and one (60%FBS) independent experiments.

Because of time constraints, we decided to continue the project with only Panc-1 cell line because at least approximately 52% of zebrafish xenografts had a tumoral mass at 4dpi, allowing for future experiments to be done.

Collectively, these results showed that Panc-1 and MIA PaCa-2 cell lines present very different engraftment potentials in zebrafish larvae.

3.2. Histomorphological features of Panc-1 zebrafish xenografts

To better characterize morphological changes overtime in Panc-1 zebrafish xenografts and characterize the xenografts with edema, xenografts with edema and without edema were fixed and processed for histopathology.

At 1dpi, Panc-1 zebrafish xenografts displayed severe cardiac edema, occasionally with multifocal hemorrhage (arrow, **Figure 3.2 A**). At high magnification, there was marked single-cell necrosis of tumor cells with nuclear fragmentation – karyorrhexis (arrowhead, **Figure 3.2 A'**). Several studies have shown that PC cells can trigger inflammation by producing and secreting proinflammatory cytokines and growth factors, essential for PC progression[53,55]. Regarding clinical features of PC patients,

numerous studies associated the presence of proinflammatory cytokines, such as IL-1, IL-6, IL-8, and TNFα, with cancer cachexia – a systemic inflammatory response that promotes skeletal muscle loss and insulin resistance - and worse prognosis[102]. In this way, this pathological condition displayed by zebrafish xenografts may be correlated with proinflammatory cytokines released by necrotic Panc-1 cells, and possibly correspond to the cancer cachexia that PC patients exhibit.

Larvae that did not develop severe edema, that did not die and in which the tumor engrafted at 4dpi, showed solid tumor masses often in close proximity with the zebrafish pancreas (arrow, **Figure 3.2 B**). There was no evidence of edema and at higher magnification tumor was composed by a densely packed population of tumor cells with frequent mitosis (arrow, **Figure 3.2 B'**).

Overall, these results suggested that the presence of severe edema, at 1dpi, in zebrafish xenografts can be an inflammatory response linked to the necrosis of Panc-1 cells, which does not occur at 4dpi. Moreover, our results show that PC cells that successfully implant in zebrafish larvae can undergo cell division.
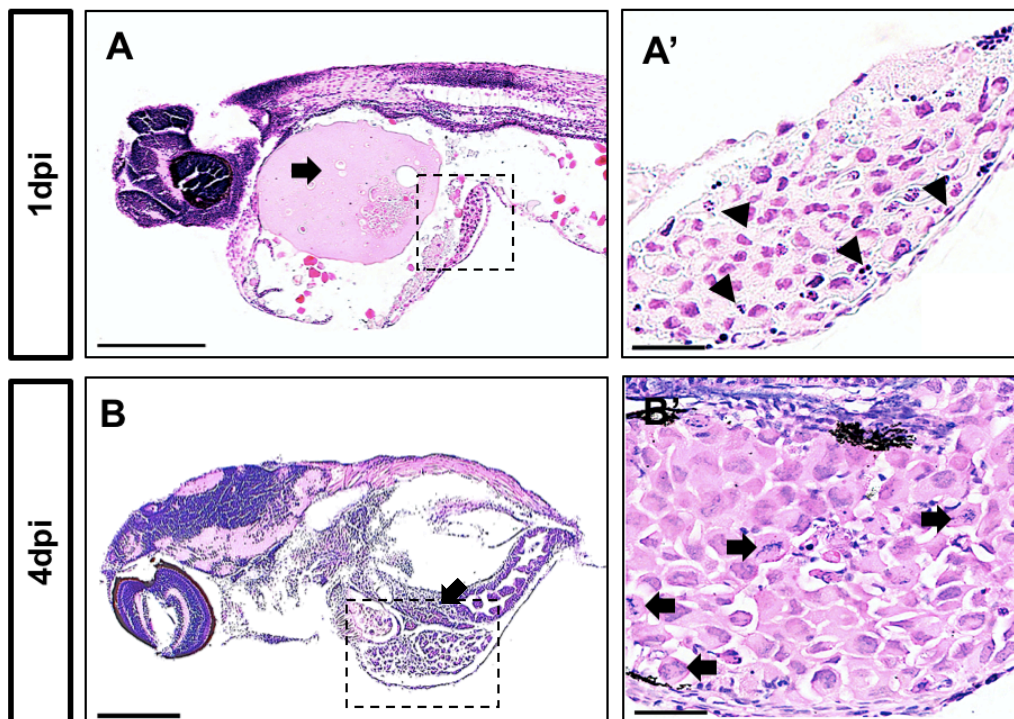
Figure 3. 2 - Representative microphotographs of Panc-1 zebrafish xenografts at 1dpi and 4dpi.
(**A**) low magnification of a larvae at 1dpi displaying severe edema (arrow). (**A'**) high magnification of the engrafted Panc-1 cells at 1dpi, showing multifocal and marked single cell necrosis (arrowhead) and occasional hemorrhage. (**B**) low magnification of larvae at 4dpi, showing a solid tumor mass in close proximity with the zebrafish pancreas (arrow), without edema or hemorrhage. (**B'**) high magnification of the engrafted Panc-1 cells at 4dpi, showing a population of tumor cells with frequent mitosis (arrow). PFA-fixed, paraffin-embedded and H&E-stained 4μm sections.

3.3. Exploring the role of fibroblasts in PC progression

One of the most well-establish features of PC microenvironment is the dense desmoplastic stroma, composed by stromal cells and ECM[49]. The key contributor to PC desmoplasia is CAFs, primarily PSCs, which aberrantly secrete ECM proteins[50].

Therefore, we tested whether the co-injection of Panc-1 cells with fibroblasts could potentially increase the engraftment rate.

To assess this, two experimental conditions were used to generate zebrafish xenografts (**Figure 3.3 A**):

(1) injection of Panc-1 cells (control condition);

(2) co-injection of Panc-1 cells with HS-5, a human fibroblast cell line derived from the bone marrow.

At 1dpi zebrafish xenografts were screened and a tumor mass was hardly visible. To confirm this, zebrafish xenografts were prepared for confocal microscopy to evaluate and compare the implantation potential of Panc-1 cells with and without HS-5 cells. Surprisingly, confocal imaging revealed that Panc-1 plus HS-5 did not engraft into the zebrafish larvae (**Figure 3.3 C**), in contrast with the control condition (Panc-1 cells only, **Figure 3.3 B**), in which a tumor mass was clearly visible.
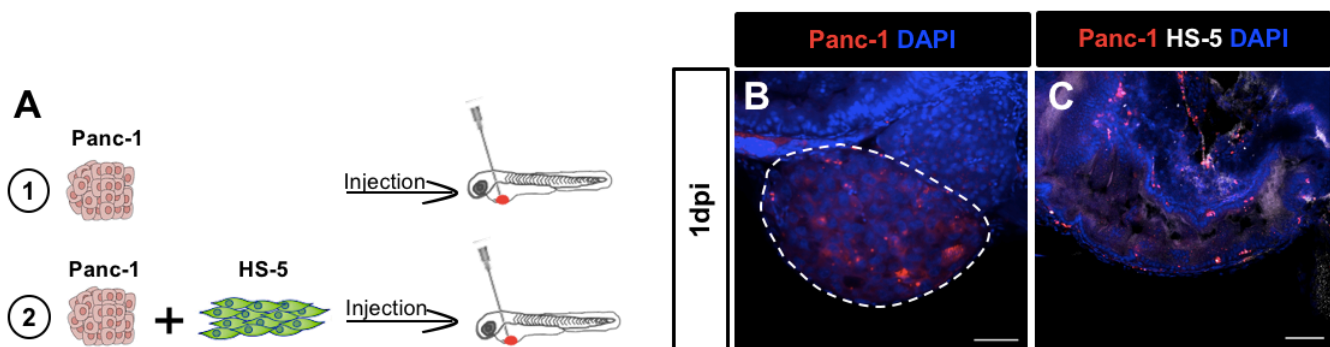
Figure 3. 3 - Confocal microscopy reveals the absence of Panc-1 cells and human fibroblasts (HS-5 cells) co-injected in zebrafish larvae, at 1dpi. Panc-1 cell line and HS-5 were fluorescently labelled with CM-DiI and Deep Red Dye, respectively. Panc-1 cells were injected alone (**A1**) and co-injected with HS-5 cells (**A2**), into the PVS of 2dpf zebrafish larvae. At 1dpi, zebrafish xenografts were imaged by fluorescent confocal microscopy to evaluate the implantation of Panc-1 cells with (**C**) or without HS-5 cells (**B**). The dashed line represents the tumor area. Scale bar represent 50µm. Confocal image is anterior to the left, posterior to right, dorsal up and ventral down.

The absence of both Panc-1 and HS-5 cells in the zebrafish xenograft model, may result from direct interactions between these cells, or be dependent on the zebrafish microenvironment. Therefore, to discriminate these two hypothesis, an *in vitro* assay was performed. If the absence of both cell lines is exclusively dependent on their direct interaction, it is expected to observe similar results also in the *in vitro* setting.

In this experiment, we compared the behavior of the monocultures of Panc-1 and HS-5 cells, with the co-culture of both cell lines. Each condition was seeded with DMEM and after three days, cells were fixed in 4% FA and smears submitted for histopathology.

HS-5 monoculture was characterized by a population of small sized stellate cells, with scant cytoplasm and small round to elongated nucleus (**Figure 3.4 A**). Panc-1 monoculture was characterized by a population of cells with various sizes and shapes – anisocytosis – often with very large nucleus (**Figure 3.4 B**). The mixed culture is very similar to Panc-1 cells in pure culture, with few spindle-shape cells, compatible with HS-5 cells (**Figure 3.4 C**). Overall, these results showed no significant differences between monoculture vs. co-culture that could explain the results obtained *in vivo*, suggesting that the zebrafish microenvironment might be promoting the clearance of both Panc-1 and HS-5 cells.
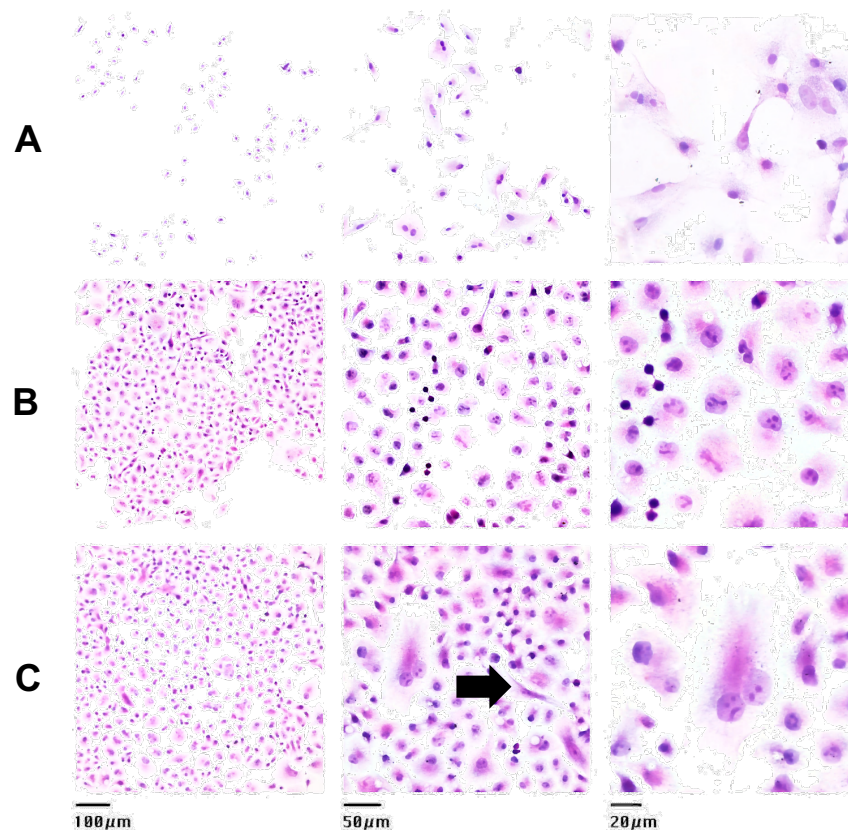
Figure 3. 4 - **Representative microphotographs of HS-5 and Panc-1 cells in pure and mixed culture.** (**A**) HS-5 cells in pure culture was characterized by a population of small sized spindle or stellate cells, with scant cytoplasm, small round to elongated nucleus with dense chromatin, with poorly defined cell borders and low cell density. (**B**) Panc-1 cells in pure culture corresponded to a population of cells with marked anisocytosis and anisokaryosis: round to polygonal to stellate in shape, from small to large-sized; indistinct borders and often with very large nucleus with multiple evident nucleoli. (**C**) HS-5 and Panc-1 cells in mixed culture was very similar to Panc-1 cells in pure culture, where only rare spindle-shape cells, compatible with fibroblasts, can be seen (arrow). PFA-fixed, H&E-stained cells, cultured on coverslip.

In summary we were not able to improve the engraftment rate and had to move with these not so ideal conditions.

3.4. PC zebrafish xenografts show sensitivity to the standard chemotherapy

After optimizing the establishment of PC zebrafish xenografts, we tested whether zebrafish xenografts could be used to measure different responses to therapy. We assessed the main therapeutic options in advanced PC guidelines: FOLFIRINOX (first line of chemotherapy) and GnP (second line of chemotherapy).

To address this, Panc-1 zebrafish xenografts were generated and randomly distributed between treatment groups at 1dpi: Control (non-treated xenografts), FOLFIRINOX and GnP. After three days of treatment (4dpi), zebrafish xenografts were fixed and prepared for confocal imaging to assess mitotic index, cell death by apoptosis (activated caspase3) and tumor size (**Figure 3.5**).

In Panc-1 tumors, both FOLFIRINOX and GnP treatment significantly reduced the mitotic index (FOLFIRINOX: ~42% reduction, **P=0.0042; G+P: ~51% reduction, ***P=0.0006; **Figure 3.5 D**). A significant induction of apoptosis was also observed with both treatments, wherein GnP revealed a slightly higher tendency to induce apoptosis (****P<0.0001; **Figure 3.5 A'-C', E**).

FOLFIRINOX treatment significantly reduced the tumor size of Panc-1 tumors (FOLFIRINOX: ~24% tumor shrinkage, **P=0.0097). However, despite the cytotoxic effects of GnP regarding apoptosis induction, GnP showed a tendency to decrease tumor size, but not statistically significant (GnP: ~18%tumor shrinkage; P=0.0661) (**Figure 3.5 F**). Based on previous studies[87,91], we may speculate that if we increase the duration of the GnP treatment this would result in a significantly shrinkage of the tumor size.

In summary, our results demonstrate that zebrafish Panc-1 xenografts are sensitive to the main therapeutic options approved for advanced PC.
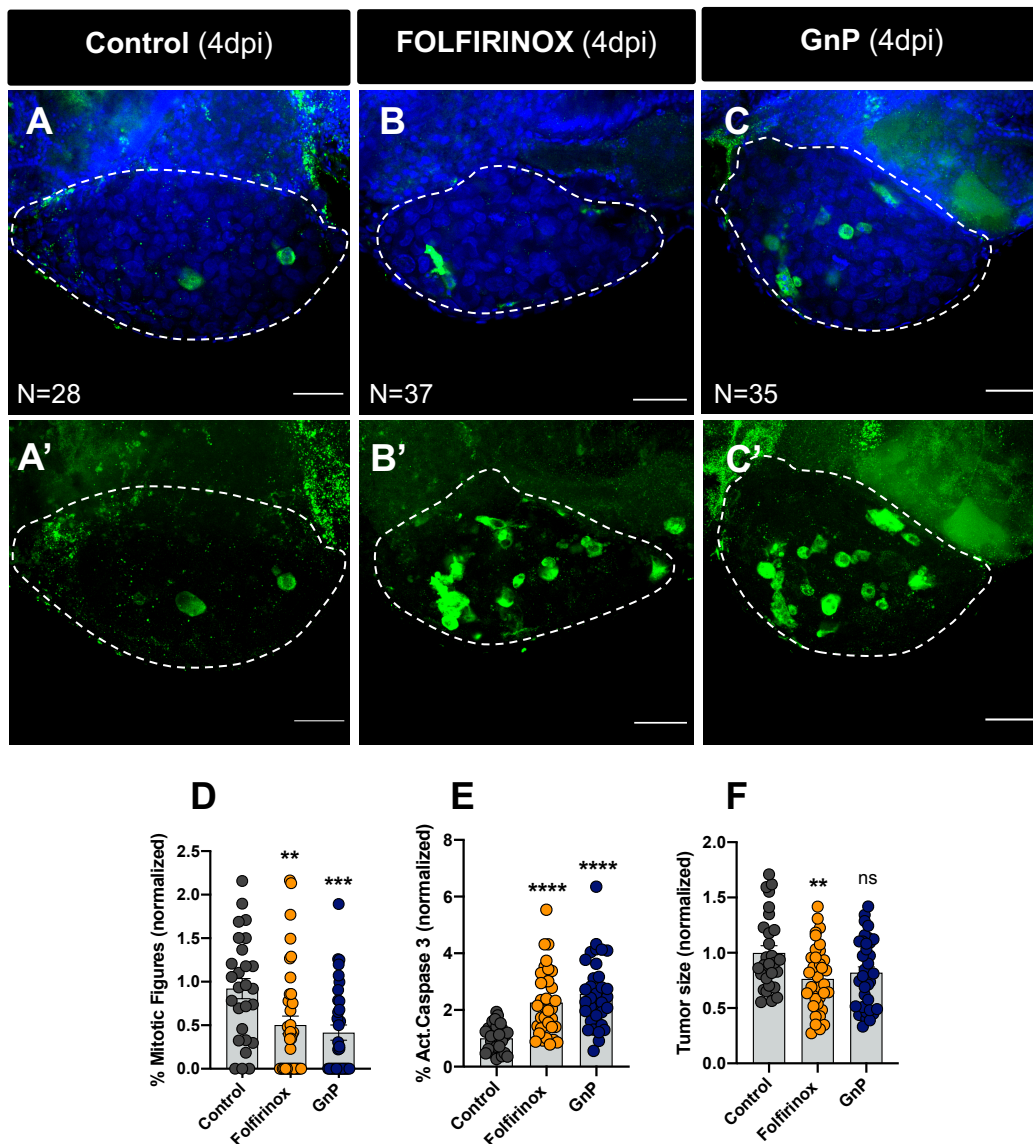
Figure 3. 5 - Zebrafish xenografts reveal cellular sensitivity to the major therapeutic options for PC – FOLFIRINOX and GnP chemotherapy. 2dpf zebrafish larvae were injected with fluorescently labelled Panc-1 cells in the PVS (not shown). At 1dpi, successfully implanted xenografts were submitted to FOLFIRINOX (**B**) or GnP (**C**) treatment for three consecutive day, and compared to control nontreated xenografts (**A**). Maximum Z projections of Activated Caspase3 (**A'- C'**). At 4dpi, zebrafish xenografts were sacrificed and fixed, 3 days posttreatment (3dpT), subjected to whole-mount immunofluorescence and imaged by confocal fluorescent microscopy. Mitotic Figures (**D**, **P=0.0042, ***P=0.0006), apoptotic index (% of Activated Caspase3 in green) (**E**, ****P<0.0001) and tumor size (number of tumor cells, DAPI in blue) (**F**, **P=0.0097) were analyzed and quantified). All results (**D-F**) are expressed in AVG±SEM. Statistical analysis was performed using Mann-Whitney test. Statistical results: (ns) > 0.05, *P≦0.05, **P≦0.01, ***P≦0.001, ****P≦0.0001. The number of zebrafish xenografts analyzed is indicated in the representative images, and are the results from 3 independent experiments. The dashed line represents the tumor area. Scale bars represent 50μm. All images are anterior to the left, posterior to right, dorsal up and ventral down.

3.5. PC zebrafish xenografts respond to PD-1 inhibitor monotherapy and in combination with chemotherapy

Several PC cell lines, including Panc-1 cell line, were previously documented to express PD-1, which was shown to enhance PC growth *in vitro* and in immunocompromised mouse models[69]. Additionally, the same study showed that PD-1 inhibitors, including the monoclonal antibody nivo, have direct cytotoxic effects in PC cells and tissues, independent of T cell activity[69].

Based on Fior et al. 2017[87] and Rebelo de Almeida et al. 2020[92], which demonstrate that zebrafish xenografts could be used to asses responses to biological targeted therapies – cetuximab and bevacizumab, respectively - we decided to investigate whether zebrafish xenografts could display different tumor responses to nivo and to a combinatory treatment that is currently being evaluated in a phase I clinical trial, nivo+GnP[71].

To test this, Panc-1 zebrafish xenografts were generated and randomly distributed into four experimental conditions at 1dpi:
- Control (non-treated xenografts);
- GnP;
- nivo;
- nivo+GnP.

Similar to the other monoclonal antibodies (cetuximab and bevacizumab), we found that to observe a clear phenotype, not only tumor cells had to be resuspended in nivo prior to injection but also xenografts had to be incubated with the antibody in the E3-fish water for three consecutive days.

After three days of treatment (4dpi), zebrafish xenografts were fixed and processed for confocal microscopy to evaluate the impact of these therapies in mitotic index, cell death by apoptosis (activated caspase3) and tumor size (**Figure 3.6**).

GnP significantly induced a reduction in mitotic figures, contrary to nivo monotherapy despite the decreasing tendency. Nevertheless, when nivo was combined with GnP, a reduction of tumor cells undergoing mitosis was clearly observed (GnP: ~51% reduction, ***$P=0.0006$; nivo: ~37% reduction, $P=0.0705$; nivo+GnP: ~73% reduction, ****$P<0.0001$; **Figure. 3.6 E**).

All treatment regimens significantly induced apoptosis, but nivo monotherapy had a 2.5-fold induction (****$P<0.0001$; **Figure 3.6 A'-D', F**).

Regarding tumor size shrinkage, GnP treatment did not reduce tumor size, but nivo monotherapy had the most significant effects regarding tumor size. However, the combinatory treatment, nivo+GnP, did not have any synergic effect on tumor size reduction (G+P: ~18% tumor shrinkage, $P=0.0661$; nivo: ~25% tumor shrinkage, **$P=0.0040$; nivo+GnP: ~23% tumor shrinkage, *$P=0.0113$). Considering the impact of the combinatorial treatment on cell proliferation and cell death, an additional day of treatment could be reflected in tumor size reduction.

Overall, our data showed that nivo treatment exhibit cytotoxic effects in Panc-1 zebrafish xenografts, but an addictive effect is not observed when in combination with GnP.

Besides, these results highlight the potential of zebrafish xenografts as a promising *in vivo* model to screen nivo treatment in a personalized manner.
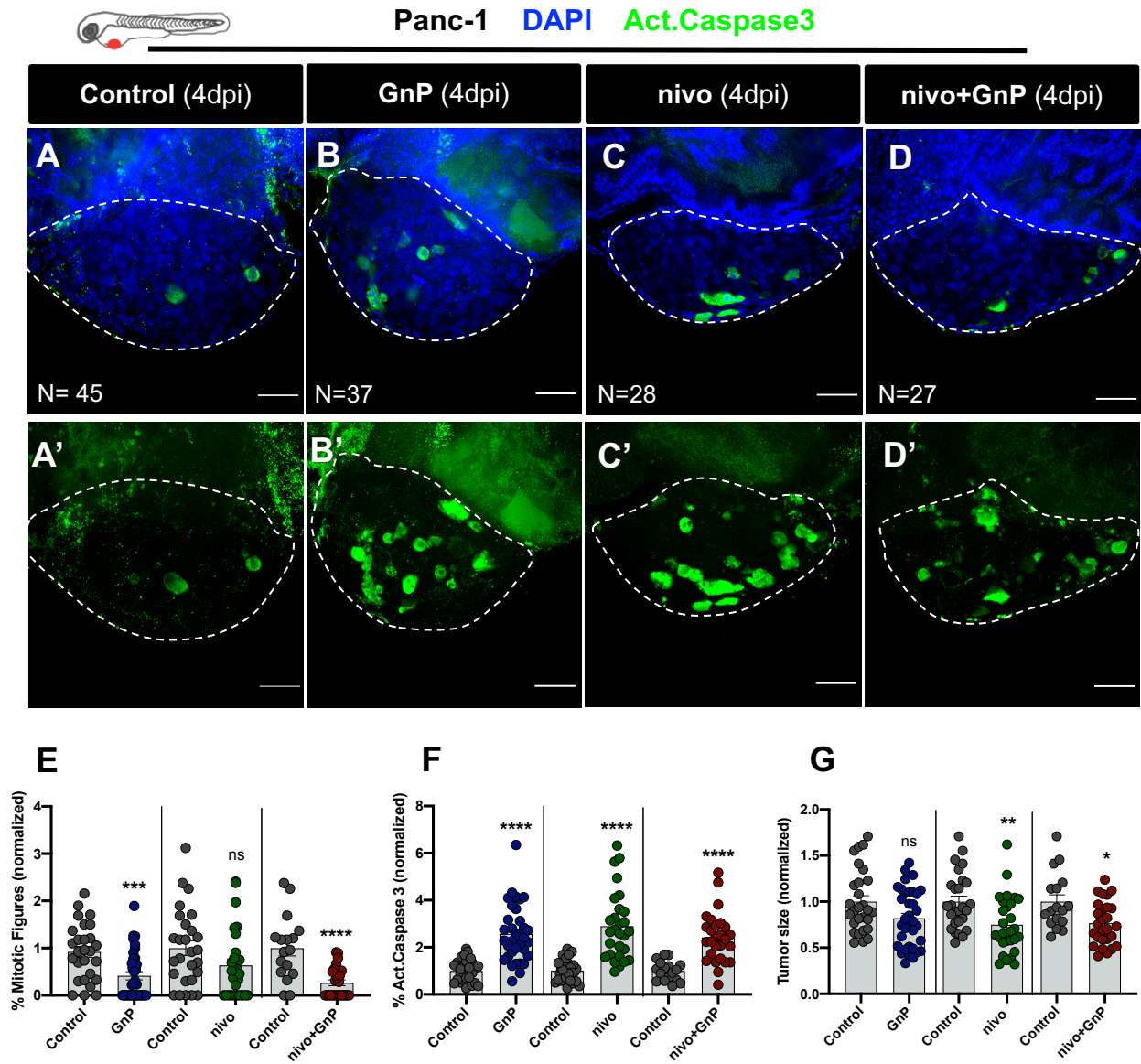
Figure 3. 6 - Zebrafish xenografts reveal tumor responses to PD-1 inhibitor monotherapy and in combination with GnP chemotherapy. 2dpf zebrafish larvae were injected with fluorescently labelled Panc-1 cells in the PVS (not shown). At 1dpi, successfully implanted xenografts were treated with GnP (**B**), nivo (**C**) or nivo+GnP (**D**) for three consecutive days, and compared to control nontreated xenografts (**A**). Maximum Z projections of Activated Caspase3 (**A'-D'**). At 4dpi, zebrafish xenografts were sacrificed and fixed, submitted to whole-mount immunofluorescence and imaged by confocal fluorescent microscopy. Mitotic Figures (**E**, ***P=0.0006, ****P<0.0001), apoptotic index (% of Activated Caspase3 in green) (**F**, ****P<0.0001) and tumor size (number of tumor cells, DAPI in blue) (**G**, *P=0.0013, **P=0.0040) were analyzed and quantified. All results (**E-G**) are expressed in AVG±SEM. Statistical analysis was performed using Mann-Whitney test. Statistical results: (ns)>0.05, *P≦0.05, **P≦0.01, ***P≦0.001, ****P≦0.0001. The number of zebrafish xenografts analyzed is indicated in the representative images, and are the results from 3 independent experiments. The dashed line represents the tumor area. Scale bars represent 50µm. All images are anterior to the left, posterior to right, dorsal up and ventral down.

3.6. Characterization of neutrophil population in the TME of Panc-1 xenografts

Although Panc-1 cell line express PD-1, we also hypothesized whether nivo was acting through modulation of the innate immune system. Therefore, to unravel the mechanisms behind the cytotoxic effects of nivo, it is essential to first understand the intricate interactions between Panc-1 cells and the TME.

As previously mentioned, at the stage of the assay (2dpf to 6dpf), only the innate immune system is at play, adaptive immunity is only matured after 4-6 weeks postfertilization[103]. Thus, we focused in characterizing the main immune populations present at this stage: neutrophils and macrophages.

We first started by characterizing the neutrophils populations in the TME of Panc-1 xenografts over time. To address this, Panc-1 cells were injected into *Tg(mpx:GFP)* a zebrafish transgenic line with GFP under the mpx⁺ promoter, a marker for neutrophils-specific myeloperoxidase (MPO)[96]. At 6hpi, 1dpi and 4dpi, zebrafish xenografts were imaged by confocal microscopy and the neutrophils present in the TME were quantified (**Figure 3.7**).

For each xenograft the percentage of neutrophils (%mpx) was calculated by the ratio of the total number of neutrophils divided by the total number of tumor cells (**Figure 3.7 D,F**).

Collectively, our results showed that from 6hpi to 1dpi, there was a significant decrease in the percentage of neutrophils, but at 4dpi, a drastic increase in the percentage of neutrophils was observed (6hpi: ~4%; 1dpi: ~2%; 4dpi: ~9%; **Figure 3.7 E**). Interestingly, our results also revealed that at 4dpi, ~80% of the neutrophils population were in the periphery of the tumor, lining the tumor margin (**Figure 3.7 G**).

Figure 3. 7 - Neutrophil populations in the TME of Panc-1 xenografts over time. Panc-1 cell line was fluorescently labelled with CM-DiI and injected into the PVS of *Tg(mpx:GFP)* zebrafish transgenic line with 2dpf (not shown). Successfully implanted xenografts were sacrificed and fixed at 6 hours post-injection (6hpi) (**A**), 1dpi (**B**) and 4dpi (**C**), to be visualized by fluorescent confocal microscopy. The absolute number of neutrophils (**D**, ***P=0.0004, ****P<0.0001) and neutrophils in the periphery of the tumor (**F**, *P=0.0179, ****P<0.0001) was quantified, and the respective percentage calculated (**E**, *P=0.0102, ****P<0.0001) (**G**, ***P=0.0002, ****P<0.0001). The absolute number of innate cells and the respective percentage were compared between 6hpi, 1dpi and 4dpi. All results (**D-G**) are expressed in AVG±SEM. Statistical analysis was performed using Mann-Whitney test. Statistical results: (ns)>0.05, *P≦0.05, **P≦0.01, ***P≦0.001, ****P≦0.0001. The number of zebrafish xenografts analyzed is indicated in the representative images, and are the results from 4 independent experiments. Scale bars represent 50μm. All images are anterior to the left, posterior to right, dorsal up and ventral down.

3.7. Characterization of macrophage population in the TME of Panc-1 xenografts

In addition to neutrophils, macrophages are also a major component of the innate immune system.

In order to characterize the macrophages population in the TME of Panc-1 xenografts over time, Panc-1 cells were injected into *Tg(mpeg:LRLG;TNFα:GFP)* zebrafish transgenic line, which allows the identification of macrophages in red (mpeg$^+$). At 6hpi, 1dpi and 4dpi, zebrafish xenografts were imaged by confocal microscopy and macrophages were quantified (**Figure 3.8**).

For each xenograft the percentage of macrophages (%mpeg), was calculated as the ratio of the total number of macrophages divided by the total number of tumor cells (**Figure 3.8 D,F**).

From 6hpi to 1dpi there was a significant increase in the percentage of macrophages. From 1dpi to 4dpi the percentage of macrophages tended to decrease, although the difference was not significant (6hpi: ~14%; 1dpi: ~20%; 4dpi: ~15%) (**Figure 3.8 E**).

In terms of the percentage of macrophages in the periphery of the tumor, at 6hpi ~66% of macrophages population was lining the tumor margin; at 1dpi half of the population was in the periphery and the other half inside the tumor; and at 4dpi, ~67% of macrophages were again in the periphery of tumor. In other words, it seems that, at 6hpi the macrophages in the periphery are "scanning" the surroundings, then at 1dpi, half of the population infiltrates the tumor, and later, at 4dpi, most macrophages get back to their original positions (in the periphery).

Finally we compared the percentage of macrophages and the percentage of neutrophils overt-time, and it is clear that macrophages are more abundant in Panc-1 TME than neutrophils, primarily at 6hpi and 1dpi (6hpi: mpeg=~14%, mpx=~3%; 1dpi: mpeg=~20%, mpx=~2%) (**Figure 3.7 E** and **Figure 3.8 E**).
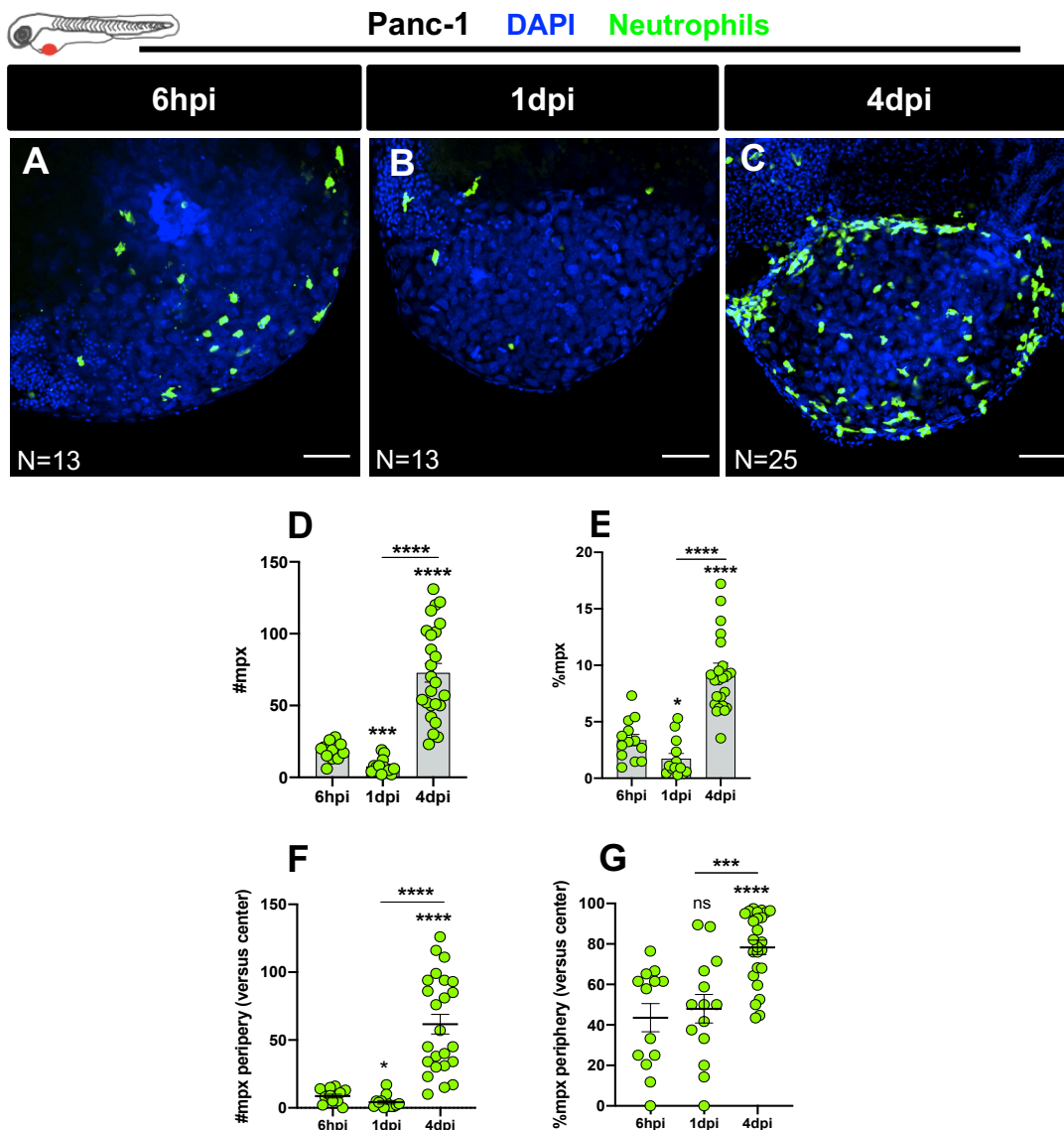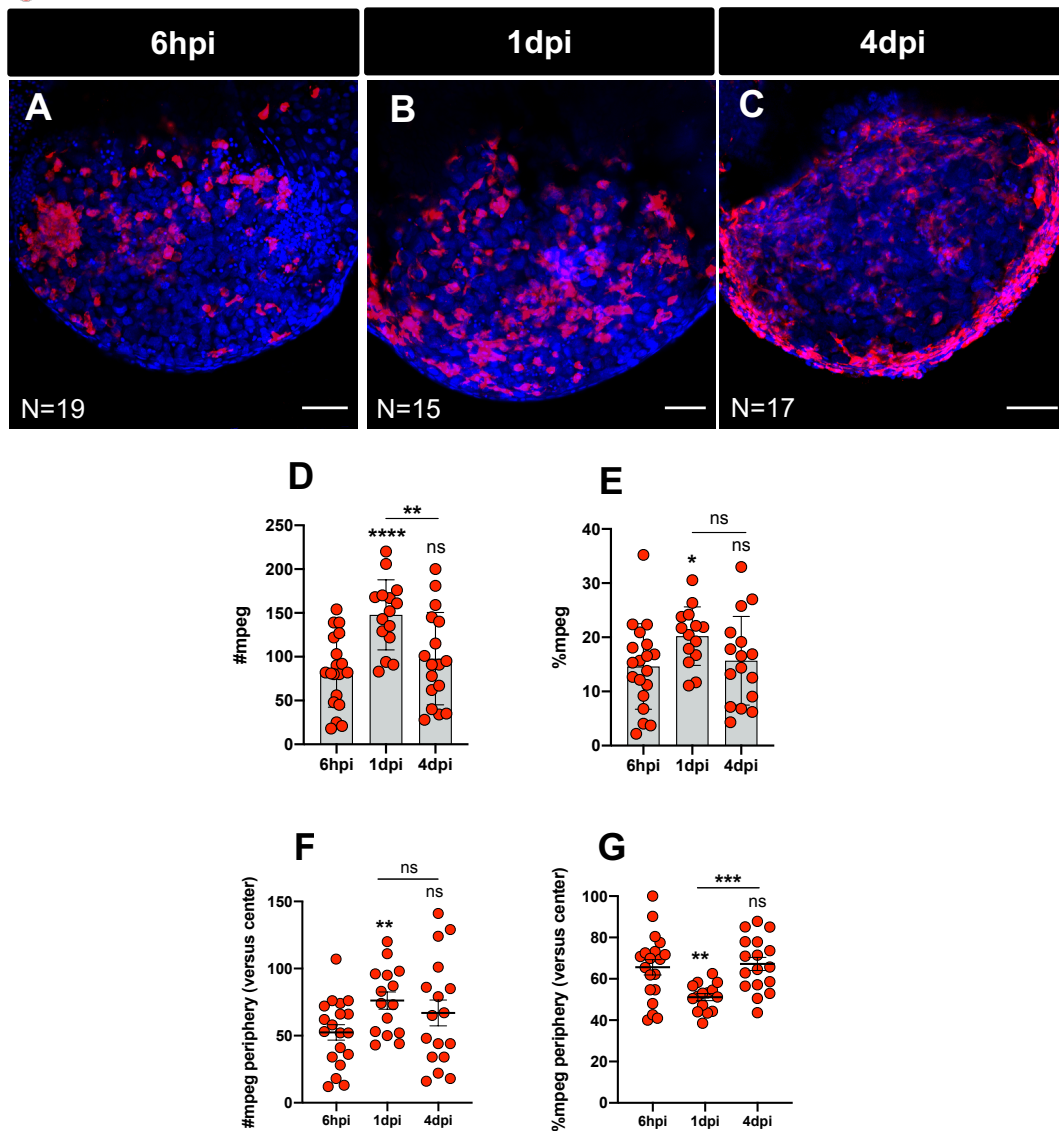
Figure 3. 8 - Macrophage populations in the TME of Panc-1 xenografts over time. Panc-1 cell line was fluorescently labelled with Deep Red Dye and injected into the PVS of *Tg(mpeg:LRLG;TNFα:GFP)* zebrafish transgenic line with 2dpf (not shown). Successfully implanted xenografts were sacrificed and fixed at 6hpi (**A**), 1dpi (**B**) and 4dpi (**C**), to be visualized by fluorescent confocal microscopy. The absolute number of macrophages (**D**, **P=0.0049, ****P<0.0001) and macrophages in the periphery of the tumor (**F**, **P=0.0097) was quantified and the respective percentage calculated (**E**, *P=0.0219) (**G**, **P=0.0016, ***P=0.0002). The absolute number of innate cells and the respective percentage were compared between 6hpi, 1dpi and 4dpi. All results (**D-G**) are expressed in AVG±SEM. Statistical analysis was performed using Welch's t test. Statistical results: (ns)>0.05, *P≦0.05, **P≦0.01, ***P≦0.001, ****P≦0.0001. The number of zebrafish xenografts analyzed is indicated in the representative images, and are the results from 5 independent experiments. Scale bars represent 50µm. All images are anterior to the left, posterior to right, dorsal up and ventral down.

Interestingly we also found that macrophages form networks of interconnected macrophages surrounding PC cells, mainly at 1dpi and 4dpi (**Figure 3.9**), which we do not know what it means but macrophages can form different cellular structures to fight infections or fuel these infections, such as in granuloma formation in tuberculosis[104].
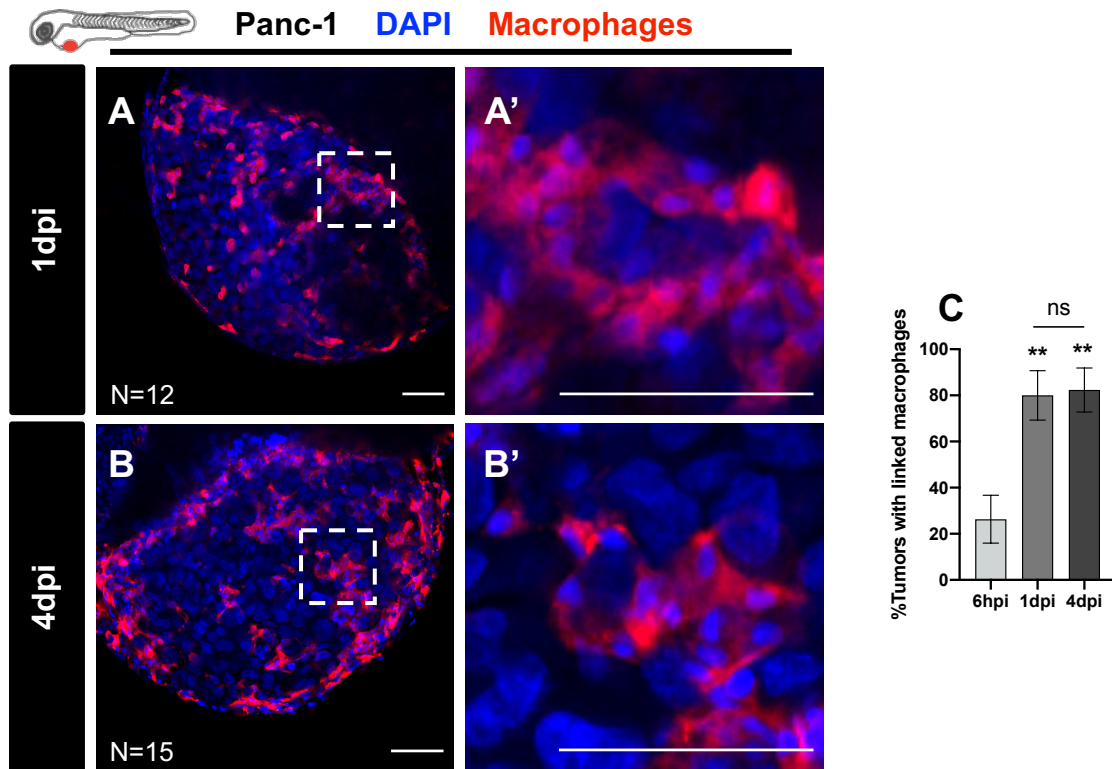
Figure 3. 9 - Macrophage populations tend to form network-like structures in the TME of Panc-1 xenografts, primarily at 1dpi and 4dpi. Panc-1 cell line was fluorescently labelled with Deep Red Dye and injected into the PVS of *Tg(mpeg:LRLG;TNFα:GFP)* zebrafish transgenic line with 2dpf. Successfully implanted xenografts were sacrificed and fixed at 6hpi, 1dpi (**A**) and 4dpi (**B**), to be visualized by fluorescent confocal microscopy. (**A'**) and (**B'**) are zoom in images of (**A**) and (**B**), respectively. Tumors with linked macrophages were analyzed and quantified (**P=0.0049, **P=0.0011, **C**). Result (**C**) is expressed in AVG±SEM. Statistical analysis was performed using Mann-Whitney test. Statistical results: (ns)>0.05, *P≦0.05, **P≦0.01, ***P≦0.001, ****P≦0.0001. The number of zebrafish xenografts analyzed is indicated in the representative images, and are the results from 3 independent experiments. Scale bars represent 50µm. All images are anterior to the left, posterior to right, dorsal up and ventral down.

Macrophages are highly plastic and multifaceted cells, able to constantly alter their functional state in response to the TME[105]. Activated macrophages, can be polarized into two different phenotypes with distinct immune functions: M1-like phenotype (pro-inflammatory/ anti-tumoral phenotype) or M2-like phenotype (anti-inflammatory/ pro-tumoral). M1-like macrophages are characterized by the expression and secretion of pro-inflammatory cytokines, primarily TNFα, and are considered the "good macrophages", crucial for host defense and tumor cell killing[106]. In contrast, M2-like macrophages secrete anti-inflammatory cytokines and are considered the "bad macrophages" and "friends" of cancer cells, because they support angiogenesis and express immunosuppressive molecules[106]. In PC, the density of macrophages is

strongly correlated with a reduced survival, and are typically associated with a M2-like polarization state[107].

To investigate the presence of M1-like and M2-like macrophages in Panc-1 TME, the same zebrafish transgenic line was used, *Tg(mpeg:LRLG;TNFα:GFP)*, which allows the identification of M1-like macrophages in yellow, as double positive cells (mpeg$^+$ TNFα$^+$), and M2-like macrophages as mpeg$^+$ TNFα$^-$.

For each xenograft the percentage of macrophages M1-like (%M1) and M2-like (%M2) cells was calculated as the ratio of the total number of M1-like and M2-like cells divided by the total number of tumor cells (**Figure 3.10 D**).

According to our results, it was also possible to distinguish two populations of macrophages in the Panc-1 TME, in different ratios over-time. At 6hpi, Panc-1 TME was significantly enriched in M2-like macrophages (~62% compared to ~38% of M1-like macrophages, **Figure 3.10 A,E**). Subsequently, at 1dpi, a significant switch occurred, in which the percentage of M1-like macrophages increased to 62% while the percentage of M2-like macrophages decreased to ~38% (**Figure 3.10 B,E**). However, at 4dpi, another shift occurs, wherein M2-like macrophages dominate Panc-1 TME, like at 6hpi (~61% compared to ~39% of M1-like macrophages, **Figure 3.10 C,E**).

Overall, these results highlight the plasticity and dynamics of macrophages functions over-time in Panc-1 TME.
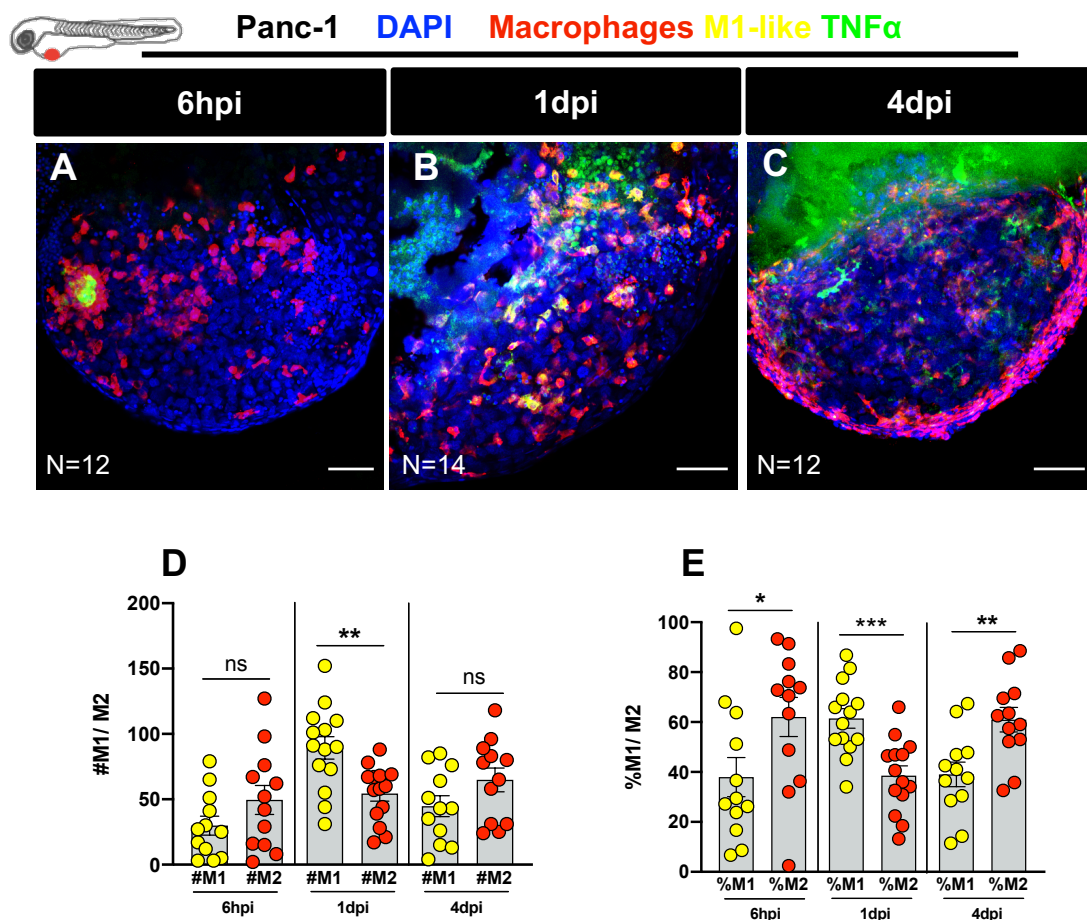
Figure 3. 10 - M1-like and M2-like macrophage populations in the TME of Panc-1 xenografts, over time. Panc-1 cell line was fluorescently labelled with Deep Red Dye and injected into the PVS of *Tg(mpeg:LRLG;TNFα:GFP)* zebrafish transgenic line with 2dpf (not shown). Successfully implanted xenografts were sacrificed and fixed at 6hpi (**A**), 1dpi (**B**) and 4dpi (**C**), to be visualized by fluorescent confocal microscopy. The absolute number of M1-like and M2-like cells was quantified (**D**, **P=0.0026) and the respective percentage calculated (**E**, *P=0.041, **P=0.0045, ***P=0.0003). The absolute number of M1-like and M2-like cell, and the respective percentage were compared between 6hpi, 1dpi and 4dpi. All results (**D,E**) are expressed in AVG±SEM. Statistical analysis was performed using Welch's t test. Statistical results: (ns)>0.05, *P≦0.05, **P≦0.01, ***P≦0.001, ****P≦0.0001. The number of zebrafish xenografts analyzed is indicated in the representative images, and are the results from 3 independent experiments. Scale bars represent 50µm. All images are anterior to the left, posterior to right, dorsal up and ventral down.

3.8. Macrophages and neutrophils exert opposite roles in Panc-1 tumors

To address the role of macrophage and neutrophil populations in the implantation/ clearance of Panc-1 tumors, it is essential to perform loss- and gain-of-function experiments. These experiments were performed using hippomorphic mutant zebrafish lines, and the one of the two following phenotypes is expected:

(1) if an immune population responsible for tumor rejection (anti-tumor activity) is ablated, it is expected to lead to an increase in the engraftment capacity of Panc-1 cells;

(2) if an immune population responsible for tumor maintenance (pro-tumor activity) is ablated, it is expected a reduction in the engraftment capacity.

Therefore, to perform these engraftment studies, Panc-1 cells were injected into zebrafish mutant lines for macrophages (csf1ra[j4blue] panther mutants)[99] and for neutrophils (runx1[w84x] mutants)[100], and compared to wild-type zebrafish hosts.

At 4dpi, zebrafish xenografts were imaged by confocal microscopy and engraftment and tumor size were quantified (**Figure 3.11**).

Although we could not detect a significant impact of the downregulation of macrophages and neutrophils on engraftment, we could detect a significant impact on Panc-1 tumor size.

In panther mutants, the tumor size significantly decreased, suggesting that macrophages are important for the maintenance and survival of Panc-1 tumors (~31% tumor reduction, *P=0.0316, **Figure 3.11 A,B,E**). While in runx mutants, Panc-1 tumor size significantly increased, suggesting that neutrophils have an important role in tumor clearance (~35% tumor increase, *P=0.0500, **Figure 3.11 C,D,F**).

Collectively, our data highlights the importance of macrophages and neutrophils in the maintenance and clearance of Panc-1 tumors, respectively. However, these results correspond to only one independent experiment, so, at least, two more experiments with a more robust sample should be done to validate both phenotypes.
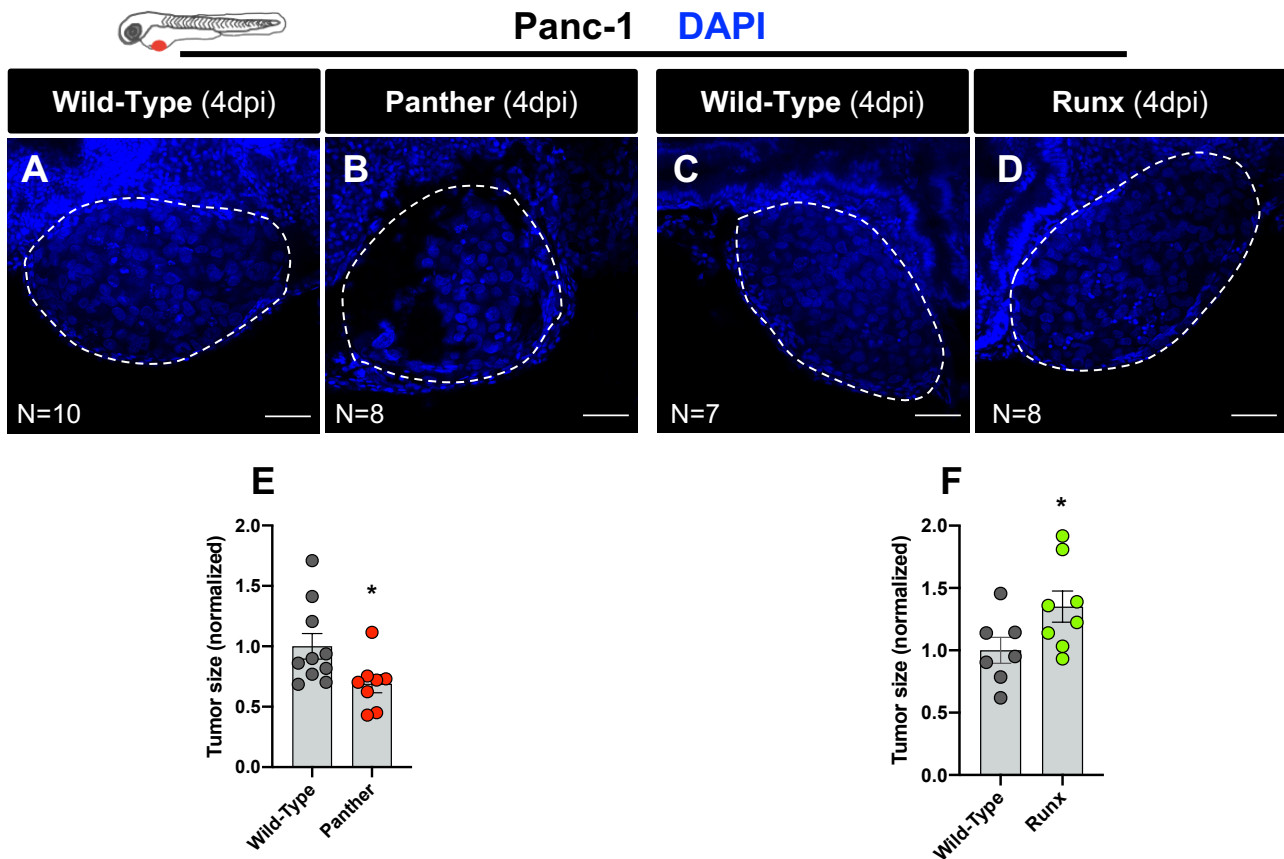
Figure 3. 11 - Macrophages contribute to Panc-1 tumors survival while neutrophils play a role in the clearance of Panc-1 tumors. Panc-1 cell line was fluorescently labelled with Deep Red Dye (not shown) and injected into the PVS of 2dpf zebrafish mutant line for macrophages (panther mutants), 2dpf zebrafish mutant line for neutrophils (runx mutants) and 2dpf *Tg(mpeg:LRLG)* zebrafish transgenic line (wild-type for macrophages and neutrophils). At 4dpi, zebrafish xenografts were imaged by confocal microscopy (**A-D**) and the tumor size was quantified (**E**, *P=0.0316) (**F**, *P=0.0500). All results (**E,F**) are expressed in AVG±SEM. Statistical analysis was performed using Welch's t-test. Statistical results: (ns) > 0.05, *P≦0.05, **P≦0.01, ***P≦0.001, ****P≦0.0001. The number of zebrafish xenografts analyzed is indicated in the representative images, and are the results from one independent experiment. The dashed line represents the tumor area. Scale bars represent 50µm. All images are anterior to the left, posterior to right, dorsal up and ventral down.

3.9. Reduction of macrophages do not contribute for the engraftment of MIA PaCa-2 tumors

The previous results revealed that the innate immune system modulates the size of Panc-1 tumors. Thus, we questioned whether the innate immune system could also be regulating MIA PaCa-2 tumors, which showed very low engraftment rates.

We started by exploring the role of macrophages by injecting MIA PaCa-2 cells into panther mutants and comparing their engraftment with wild-type controls. At 4dpi, the presence of a tumor mass was evaluated in both wild-type and mutant xenografts (**Figure 3.12**). The engraftment percentage in panther mutants was very similar compared to the wild-type transgenic, 1.82% and 2.17%, respectively, suggesting that macrophages do not play a major role in the rejection of MIA PaCa-2 tumors. However, this assay was performed only once, and the panther mutants are hypomorphs, which

means they only have a reduction on the numbers of macrophages – in particular in resident macrophages[99]. Thus further experiments are needed to exclude the role of macrophages in the clearance of these tumors.
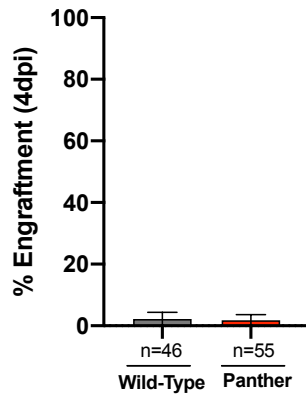
Figure 3. 12 - Macrophages seem to not play a role in the clearance of MIA PaCa-2 tumors. MIA PaCa-2 cell line was fluorescently labelled with Deep Red Dye (not shown) and injected into the PVS of 2dpf zebrafish mutant line for macrophages (panther mutants) and 2dpf *Tg(mpeg:LRLG)* zebrafish transgenic line (wild-type for macrophages). At 4dpi, the presence of tumor - %Engraftment - was evaluated in both wild-type and mutant zebrafish xenografts. Result is expressed in AVG±SEM, and is from one independent experiment.

4. Discussion

Cancer is a very complex and heterogeneous disease characterized by cancer cells' ability to sustain chronic proliferation and spread from the primary tumor to surrounding and distant tissues[2,3]. The heterogeneity of the disease is described by differences between cancer cells from different patients – inter-heterogeneity - and between cancer cells within a single patient – intra-heterogeneity[6]. This complexity and variability fuel drug resistance, and constitute the major obstacle for standard and precision medicine[6].

PC, one of the most aggressive solid malignancies, is ranked as the seventh most common cause of global cancer deaths, with 432.242 deaths reported in 2018 (4.5% of all cancer-related deaths)[11]. Early-stage PC is usually clinically silent. Therefore 80-90% of PC patients have advanced disease at the time of diagnosis where curative therapeutic options are lacking[16]. The main front line option for advanced PC is still chemotherapy: FOLFIRINOX or GnP[59]. However, there are no specific and sensitive predictive biomarkers for the current therapies used in PC, so it is difficult to know which patients are eligible for a given therapy[12].Thus, patients are treated according to international guidelines based on large randomized clinical trials that compare average response rates. This approach may be efficient to some patients, but not for others, and they are consequently subjected to ineffective treatments and unnecessary toxicity. Immunotherapy is also being studied for PC treatment, but the immunosuppressive microenvironment is one of the main reasons for the failure of this approach[65,66]. Besides, every patient is unique meaning that targeted drugs are often effective on only a portion of patients deemed susceptible. Thus, there is a huge need for a functional and predictive *in vivo* test, that can directly challenge tumor cells to the available therapeutic regimens. Such test would help medical doctors in their clinical decisions to provide the most efficient therapy to a single patient at a single time-point of the disease.

The zebrafish Avatar Test developed by my host laboratory – Dr. Rita Fior and her colleagues at Champalimaud Foundation - showed the ability of zebrafish larvae xenografts to reveal differential chemosensitive profiles in a one-week assay[87,91,92]. The ultimate goal of my thesis project, was to test the feasibility of zebrafish larvae xenografts as an *in vivo* screening platform for PC therapy. The cytotoxic effects of nivolumab as a monotherapy and in combination with GnP were also evaluated.

PC cell lines display differential implantation capacities in zebrafish embryos

With the aim of testing zebrafish xenografts as a screening platform for PC therapy, we selected two established human PC cell lines: Panc-1 and MIA PaCa-2.

First we started by characterizing the engraftment rate of each cell line.

At 1dpi, more than half of Panc-1 and MIA PaCa-2 xenografts displayed severe cardiac edema (**Figure 3.1** and **3.2**), with a lot of single-cell necrosis and without immune cells infiltrates. The aggressive behavior of PC has been correlated with the overexpression of pro-inflammatory cytokines (IL-1, IL-6, IL-8, and TNFα) secreted by

PC cells, essential for tumor progression and development[55]. These pro-inflammatory cytokines were also reported to be associated with a systemic inflammatory response, which is commonly presented by PC patients, called cancer cachexia[102,108]. Cancer cachexia is characterized by host nutritional depletion as result of anorexia and skeletal muscle wasting. Besides, immunosuppression (reduction in macrophages, dendritic and NK cells) is also a large problem of PC patients with cancer cachexia which increases infections susceptibility and morbidity[108].

Although we do not have enough evidence, the cardiac edema displayed by zebrafish xenografts at 1dpi may be associated with pro-inflammatory cytokines release by PC cells undergoing necrosis. Transcriptome analysis could be done to unravel the players responsible for this pathological condition.

At 4dpi, Panc-1 xenografts revealed an engraftment rate of 52.52%, while only 2.27% of MIA PaCa-2 tumors implanted (**Figure 3.1**). Literature was reviewed in order to understand if the low engraftment capacity of MIA PaCa-2 cell line was in agreement with other studies. According to Wang et al. 2015[109], MIA PaCa-2 cell line was successfully transplanted into zebrafish embryos, but the site of injection was in the yolk sac. However, these authors do not show quantification of engraftment and the tumors they use to screen drugs are very small[109], and in our assay very small sized tumors were not considered.

Generation of PC zebrafish xenografts with a fibrotic stroma

PC is characterized by extensive desmoplastic stroma that contributes to tumor progression[48,49]. In order to mimic this microenvironment and to evaluate if fibroblasts could improve engraftment of PC cells, fibroblasts (HS-5) were co-injected with Panc-1 cells into zebrafish embryos. Surprisingly, instead of improving engraftment, we observed the opposite, Panc-1 in the presence of HS-5 cells did not engraft (**Figure 3.3**). A previous study performed in mouse xenograft models, was able to successfully transplant PC with fibroblast cells[110]. However HS-5 cell line was not used in these study, which might explain the unsuccessful transplantation in our experiments. Instead, PC cells were orthotopically co-injected with a human immortalized pancreatic stellate cell (PSC) line, hPSC21-S/T, which resulted in tumor size increase[110].

HS-5 is a fibroblast cell line derived from the bone marrow. In contrast, hPSC21-S/T cell line is derived from resident PSCs from pancreatic tissues. These differences in the origin of HS-5 and PSC cell line, might have a significant impact in their interactions and engraftment potential. Therefore, human immortalized PSCs cell lines should be co-injected with PC cell lines in future experiments, to evaluate if it is possible to generate desmoplastic tumors as described in the previous study[110].

To discriminate whether the clearance of both cell lines was totally dependent of the direct interactions between them, or dependent on the zebrafish microenvironment, the behavior of Panc-1 and HS-5 monocultures and co-cultures was compared *in vitro* (**Figure 3.4**). Cell smears, analyzed by pathology, showed no differences between mono- and co-cultures, suggesting that the clearance of Panc-1 plus HS-5 may be dependent on the zebrafish microenvironment. Further analysis should be carried out to better understand the interaction between PC cells and fibroblasts. A previous *in vitro* study demonstrated that PSCs secretions increased Panc-1 cells proliferation and migration, and, at the same time, inhibited cancer cells apoptosis[111]. Although with did not use PSCs in this project, different parameters could be analyzed and compared between Panc-1 and HS-5 mono and co-cultures, such as, total cell numbers, cell proliferation (mitotic figures) and apoptosis (activated caspase3-positive cells).

Certain human pancreatic cancer cell lines, such as the Panc-1 cell line, are known to induce the recruitment of host fibrogenic cells and generate fibrotic tumors by themselves, without co-injection of PSCs[112]. For example, a previous study reported the induction of stroma in nude mice after orthotopic injection of Panc-1 cells[113], and another study reported the production of desmoplastic tumors after injection of Capan-2 cells in nude mice[114].

LeBert et al. 2018, developed a transgenic zebrafish line, the *Tg(-2vim:EGFP),* through the generation of a vimentin expression reporter by driving EGFP from the vimentin promoter[115]. At 4dpf, EGFP expression was reported in ganglion cells, spinal cord neurons, the opercule and fibroblasts[115]. This transgenic zebrafish could be used in the future, to investigate whether PC cells could induce the recruitment of zebrafish fibroblasts, and characterize the changes in the recruitment of fibroblasts upon treatment with the drugs tested in this project.

PC zebrafish xenografts as an *in vivo* screening platform for chemo- and immunotherapy

In order to test whether zebrafish xenografts could discriminate different sensitivities to the available therapies approved for advanced PC, Panc-1 cells were used to generate zebrafish xenografts and then were challenged with FOLFIRINOX and GnP therapies(**Figure 3.5**).

After three consecutive days of treatment, both antineoplastic drugs significantly impaired the number of cancer cells underdoing mitosis, and were also able to significantly induce apoptosis. FOLIFIRINOX treatment promoted shrinkage of the tumor mass, however this phenotype was not observed with GnP, despite the decreasing tendency.

To the best of our knowledge, there is only one study that challenged PC cells to the major therapeutic options for advanced PC. Morelli L et al. 2020[116] evaluated the use of zebrafish xenografts as Avatars for PC patients. Preliminary results[116] showed a statistically significant reduction of the relative tumor area with both FOLFIRINOX and GnP schemes. This is the first study[116] to establish a treatment correlation

between zebrafish xenografts and matched PC patients, and emphasizes the robustness of zebrafish embryos for personalized medicine.

Nivo is a checkpoint inhibitor that blocks the interaction between PD-1 receptor, (expressed on activated T cells), and its ligands, PD-L1 and PD-L2 (expressed by tumor cells and infiltrating immune cells), thereby promoting anti-tumor immunity[117]. Our data revealed that zebrafish PC xenografts can also respond to nivo (**Figure 3.6**). Nivolumab significantly induced cellular apoptosis and tumor size reduction, however only the combined treatment significantly reduced mitotic index. Since at this larvae stage the adaptive immune system is not yet developed, it may be hypothesized that (**Figure 4.1**):

- nivo might be having a direct cytotoxic effect on Panc-1 cells by PD-1 blockage, as demonstrated by Gao et al. 2018[69]. Gao et al. 2018[69] showed that Panc-1 cells express PD-1 which contributed to tumor growth, and ICIs (including nivo) were cytotoxic to PC cells, *in vitro* and *in vivo*, independent of immune responses. Therefore, in order to confirm nivo cytotoxicity through blockade of PD-1 expressed on Panc-1 cells, PD-1 expression must be evaluated in this cell line, by immunohistochemistry or *in vitro* immunofluorescence. We can also challenge Panc-1 cells to nivo *in vitro,* to confirm the results presented by Gao et al. 2018[69].

- nivo might be acting through the innate immune system by modulating the macrophage population. Gordon SR et al. 2017[118], showed that PD-1 expression is a key factor in maintaining macrophages in M2-polarized state, and that PD-1 blockade may repolarize TAMs towards a M1-activated state[118]. To address if nivo is working through macrophages polarization, we may inject PC cells into zebrafish panther mutants and challenged them with nivo. Chemical methods should also be used, such as L-Clodronate which depletes not only the resident macrophages but also the ones derived from the definitive wave[105]. If nivo therapeutic effects are dependent on macrophages, the expected result is the absence of cytotoxicity.
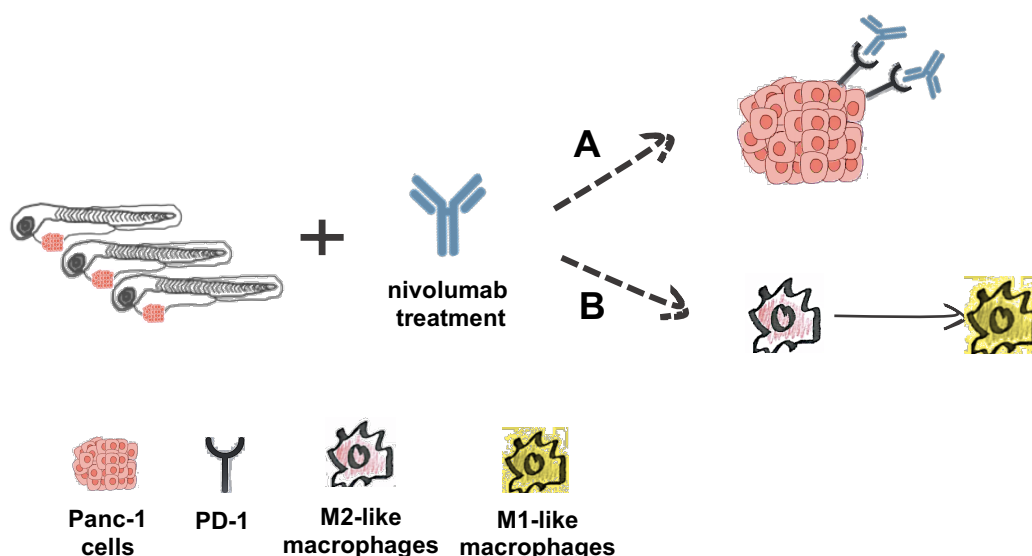
Figure 4. 1 – Illustrative scheme of the possible mechanisms of nivolumab cytotoxicity on Panc-1 tumors. (A) nivolumab blocks PD-1 expression on Panc-1 cells. **(B)** nivolumab treatment repolarizes M2-like macrophages into M1-like macrophages.

The innate immune TME of zebrafish PC xenografts

To understand the underlying mechanisms behind the cytotoxic effects of nivo in Panc-1 zebrafish xenografts, we decided to start studying the cross-talk between the innate immune system of zebrafish larvae and cancer cells.

Zebrafish embryos have a highly conserved innate immune system, primarily composed by macrophages and neutrophils with phagocytic capacity by 30hpf[105].

Regarding neutrophils population, our results showed that from 6hpi to 1dpi, the percentage of neutrophils decreased significantly. However, at 4dpi there was a huge increase in the percentage of neutrophils in which approximately 80% were lining the tumor margins (**Figure 3.7**). To explore the role of neutrophils in Panc-1 tumorigenesis, ablation of neutrophils, using the zebrafish runx mutant, showed an increase in the tumor size, suggesting that neutrophils are important for the clearance of Panc-1 tumors (**Figure 3.11**). It was shown by Dianrong et al. 2020[119], that the effect of neutrophils on Panc-1 cells was dependent on concentration. A low concentration of neutrophils mainly promoted the migration ability of PC cells by cytokines release, while a high concentration of neutrophils showed lethal effects towards cancer cells.

Macrophages are one of the most abundant immune cells in the TME and their presence is strongly correlated with a poor survival in breast, lung, bladder and PC[105,107]. According to our results, Panc-1 microenvironment is richer in macrophages than neutrophils at all time points studied (6hpi, 1dpi and 4dpi) (**Figure 3.8**), and interestingly, macrophages had a tendency to form network-like structures surrounding cancer cells, primarily at 1dpi and 4dpi (**Figure 3.9**). This kind of structures have also been described in a previous study of anaplastic thyroid cancer. In this study, authors proposed that these structures permit "cross talk" between macrophages and cancer cells, through overexpression of CX43 protein - required for gap junction-mediated intercellular communication - and that this "symbiotic" feature may be associated with the aggressiveness of the disease[120].

Macrophages are also known to display a high degree of plasticity in response to changes in their surrounding microenvironment[106]. Depending on the activation signals, macrophages can acquire distinct polarization states/phenotypes[106]. In PC, TAMs primarily resemble an M2-like phenotype, important for tumor progression[121]. However, recent evidences show that TAMs also exhibit pro-inflammatory properties (M1-like phenotype) that may function during the initiation of the tumor, and then switch to an M2-like phenotype when the tumor begins to invade and metastasize[121, 107].

Our results showed the presence of two distinct populations of macrophages over-time, which may reflect distinct polarization states: at 6hpi ~62% were M2-like macrophages; at 1dpi ~62% were M1 -like macrophages; and at 4dpi a switch

occurred and M2-like macrophages dominated, again, the Panc-1 TME (**Figure 3.10**). We could speculate that at 1dpi, Panc-1 tumors with high M1-like macrophages are the ones that will be cleared, and the ones with high M2-like macrophages will be the ones maintained until the end of the experiment (4dpi), i.e that escape selection or survive. To explore the role of macrophages in the engraftment process of Panc-1 cells, zebrafish panther mutant was used, in which tissue-resident macrophages are significantly reduced. Our results showed a significant decrease in the tumor size, suggesting that macrophages are important for the maintenance and survival of Panc-1 tumors (**Figure 3.11**). These results are supported by mouse studies, where Panc-1 cells were subcutaneously injected with or without M2 macrophages, and tumors co-injected with M2 macrophages grew more rapidly than tumors alone[121].

Since the innate immune system plays a role in the size of Panc-1 tumors, we wondered whether we could improve the very low engraftment rates of MIA PaCa-2. We started by using zebrafish panther mutants, but our preliminary data showed no significant differences in the engraftment rate of MIA PaCa-2 cells, suggesting that macrophages do not play a major role in the clearance of MIA PaCa-2 tumors (**Figure 3.12**). To validate these results, chemical methods should also be used, such as L-Clodronate. Additionally, experiments in zebrafish runx mutants should also be performed to explore the role of neutrophils in the engraftment potential of MIA PaCa-2 tumors.

5. Summary

In summary, this project highlights the potential of zebrafish larvae xenograft model as an *in vivo* screening platform for PC therapy. The next fundamental step is to validate the predictive power of this model using human biopsies/ samples from PC patients, so that it can be implemented in the clinical setting.

In addition, the interactions between the innate immune compartment and PC cells was also possible. Our results demonstrated that PC microenvironment is richer in macrophages than neutrophils, and they primarily reassemble a M2 polarization state. These results highlight that macrophages in PC should not be neglected, as they may help find new disease indications or treatment combinations.

6. Future Work

In order to enrich and complement the work developed in this project, the following experiments should be performed in the future:

1. **Explore the role of neutrophil populations in the engraftment potential of MIA PaCa-2 tumors**

In this project, the role of macrophages in the engraftment potential of MIA PaCa-2 tumors was explored. The next important step is to evaluate whether neutrophils are important for the maintenance or clearance of MIA PaCa-2 tumors, by using the zebrafish runx mutant line, in which neutrophil populations are reduced.

2. **Characterization of PC zebrafish xenografts with other established PC cell lines**

Panc-1 cell line was the only cell line capable to generate zebrafish xenografts. We would like to use other PC cell lines and challenged them to the same therapeutic regimens tested on this project, in order to make the zebrafish xenograft model even more reliable as a screening platform for PC therapies. There are, at least, more nine established PC cell lines (AspC-1, BsPC-3, Capan-1, Capan-2 , CFPAC-1, HPAC, HPAF-II, Hs 776T, Su.86.86)[101] with phenotypic and genotypic differences that could be used to generate zebrafish xenografts, and also investigate the impact of these molecular differences in terms of engraftment, angiogenic and metastatic potential, as well as tumor responses to PC therapeutic regimens.

3. **Transcriptome analysis to unravel the players behind the severe edema that PC zebrafish xenografts display.**

At 1dpi, more than half of PC zebrafish xenografts displayed severe cardiac edema. In order to investigate the players/mechanisms behind the severe edema, transcriptome profiling of PC zebrafish xenografts with edema should be performed and compared with the transcriptome of PC zebrafish xenografts without edema.

4. **Characterization of the effects of FOLFIRINOX, GnP, nivo and nivo+GnP on innate immune cells in the Panc-1 TME.**

Since the innate compartment of PC zebrafish xenografts was characterized in this project, as a next step, we would like to characterize the changes in neutrophil and macrophage populations upon treatment with FOLFIRINOX, GnP, nivo and nivo+GnP. Additionally, using the zebrafish mutant lines runx (low neutrophils) and panther (low macrophages), we could also assess whether the effects of the therapeutic approaches are dependent or independent on the innate immune cell populations.

5. **Time-lapse movies of PC-innate immune cells interactions.**

Time-lapse movies, using for example light sheet fluorescence microscopy, would be of great value to deeply understand the dynamic interactions between the innate

immune system and PC cells. Different parameters could be observed and analyzed, such as PC clearance overtime, and migration and velocity of innate immune cells.

6. Study the role of fibroblasts in PC progression.

In this research project, the generation of a fibrotic environment in PC zebrafish xenografts was not achievable, and therefore the role of fibroblasts in PC progression was not possible to study. Since PC is primarily known by his dense stroma, that constitutes a large fraction of the tumor volume, we would like to keep the effort of generating PC zebrafish xenografts with desmoplastic tumors. The following experiments should be performed in the near future:

→ Instead of the fibroblasts cell line HS-5 used in this project, co-injection of PC cell lines with PSCs cell lines. There are, at least, three immortalized human PSCs commercially available: HPaSteC derived from normal human pancreas, RLT-PSC isolated from human pancreas with chronic pancreatitis and hPSC21-S/T derived from pancreas tissue of a patient with pancreatic cancer.

→ Pancreatic CAFs were shown to induce a tumor-promoting TAM phenotype when co-culture with human monocytes[122]. If we were able to generate PC zebrafish xenografts with a fibrotic component, it would be interesting to study the immune cross-talk in an *in vivo* setting, and compare with the results of PC zebrafish xenografts without fibroblasts.

→ Injection of PC cells into the zebrafish transgenic line, *Tg(-2vim:EGFP)*[115], to evaluated if PC cells are able to recruit zebrafish fibroblasts and study how drugs impact on their recruitment.

→ Tumor-stroma-targeting strategies are being studied and assessed in human clinical trials, to break down the fibrotic microenvironment and allowing the chemotherapy to reach the cancer. Treatment with hyaluronidase PEGPH20 showed promising results in selected patients with hyaluronan (HA) high tumors, highlighting again the importance of personalize treatment for PC patients[123]. Currently, there is also a clinical trial ongoing, testing the efficacy and safety of the All Trans Retinoic Acid (ATRA), a derivative of vitamin A, in combination with GnP[124]. PSCs when in their quiescent state, store vitamin A lipid droplets in their cytoplasm, that contribute to the normal status of the pancreas[125]. However, the activation of PSCs during PC, is associated with the loss of these vitamin A droplets[125]. Research has shown that giving ATRA is able to diminish the fibrotic stroma by restoring the original phenotype of PSCs[124,125].

After the successful generation of PC zebrafish xenografts with desmoplastic tumors, we would like to challenge them to drugs that target the tumor stroma and in combination with chemotherapy.

7. Generate zebrafish patient-derived xenografts of PC, and challenge them to the major therapeutic options – FOLFIRINOX and GnP.

After establishing PC zebrafish xenografts with established human commercial PC cell lines to validate the ESMO treatment guidelines for advanced PC, our ultimate goal is to generate zPDXs or zAvatars. For the generation of zAvatars, human biopsies/ samples from PC patients will be collected and injected into the PVS of zebrafish larvae. Afterwards, zPDXs will be treated with the same treatment regimens of patients. Patients and their matching zPDXs responses will be compared to evaluate the predictive value of our assay.

However not all therapeutic options can be tested in zPDX, because of the restricted amount of patient material, sometimes with limited tumor cells or low-quality tumor content. To overcome this, we will start to establish patient-derived organoids (PDOs), derived from PC patients biopsies[126]. In this way, we expect to have more biological material to inject into zebrafish larvae, and therefore we will have more zPDXs to test PC therapeutic regimens.

7. References

1. Fior, R. & Zilhão, R. *Molecular and Cell Biology of Cancer*. (Springer, 2019). doi:10.2307/3760417

2. Alberts B, Johnson A, Lewis J, Raff M, Roberts K, W. P. *Molecular Biology of The Cell*. (Garland Science, 2009). doi:10.1017/CBO9781107415324.004

3. Hanahan, D. & Weinberg, R. A. Hallmarks of cancer: The next generation. *Cell* **144**, 646–674 (2011).

4. Martincorena, I. & Campbell, P. J. Somatic mutation in cancer and normal cells. *Science (80-.).* **349**, 1483–1489 (2015).

5. Nowell, P. C. The clonal evolution of tumor cell populations. *Science (80-.).* **194**, 23–28 (1976).

6. Dagogo-Jack, I. & Shaw, A. T. Tumour heterogeneity and resistance to cancer therapies. *Nat. Rev. Clin. Oncol.* **15**, 81–94 (2018).

7. Hinohara, K. & Polyak, K. Intratumoral Heterogeneity: More Than Just Mutations. *Trends Cell Biol.* **29**, 569–579 (2019).

8. Fedele, C., Tothill, R. W. & McArthur, G. A. Navigating the challenge of tumor heterogeneity in cancer therapy. *Cancer Discov.* **4**, 146–148 (2014).

9. Oberstein, P. E. & Olive, K. P. Pancreatic cancer: Why is it so hard to treat? *Therap. Adv. Gastroenterol.* **6**, 321–337 (2013).

10. Rawla, P., Sunkara, T. & Gaduputi, V. Epidemiology of Pancreatic Cancer: Global Trends, Etiology and Risk Factors. *World J. Oncol.* **10**, 10–27 (2019).

11. Bray, F. *et al.* Global cancer statistics 2018: GLOBOCAN estimates of incidence and mortality worldwide for 36 cancers in 185 countries. *CA. Cancer J. Clin.* **68**, 394–424 (2018).

12. Hasan, S., Jacob, R., Manne, U. & Paluri, R. Advances in pancreatic cancer biomarkers. *Oncol. Rev.* **13**, 69–76 (2019).

13. Bardeesy, N. & DePinho, R. A. Pancreatic cancer biology and genetics. *Nat. Rev. Cancer* **2**, 897–909 (2002).

14. Ren, B. *et al.* Tumor microenvironment participates in metastasis of pancreatic cancer. *Mol. Cancer* **17**, 1–15 (2018).

15. Capasso, M. *et al.* Epidemiology and risk factors of pancreatic cancer. *Acta Biomed.* **89**, 141–146 (2018).

16. Huggett, M. T. & Pereira, S. P. Diagnosing and managing pancreatic cancer. *Practitioner* **255**, 21–25 (2011).

17. https://www.mayoclinic.org/diseases-conditions/pancreatic-cancer/symptoms-causes/syc-20355421 (Accessed on October 22nd, 2020).

18. https://columbiasurgery.org/pancreas/pancreas-and-its-functions (Accessed on October 19th, 2020).

19. Birnbaum, D. J., Bertucci, F., Finetti, P., Birnbaum, D. & Mamessier, E. Head and body/tail pancreatic carcinomas are not the same tumors. *Cancers (Basel).* **11**, (2019).

20. Saclarides, T. J., Millikan, K. W. & Godellas, C. V. *Surgical Oncology: An Algorithmic Approach*. (Springer, 2003).

21.   Murtaugh, L. C. Pancreas and beta-cell development: From the actual to the possible. *Development* **134**, 427–438 (2007).

22.   Bertolini, G. *The exocrine pancreas. Body MDCT in Small Animals: Basic Principles, Technology, and Clinical Applications* (2017). doi:10.1007/978-3-319-46904-1_8

23.   Henderson, J. R. Why are the islets of Langerhans? *Lancet* **294**, 469–470 (1969).

24.   Röder, P. V., Wu, B., Liu, Y. & Han, W. Pancreatic regulation of glucose homeostasis. *Exp. Mol. Med.* **48**, e219 (2016).

25.   https://openstax.org/books/anatomy-and-physiology/pages/17-9-the-endocrine-pancreas (Accessed on October 19th, 2020).

26.   Rutter, G. A. Regulating glucagon secretion: Somatostatin in the spotlight. *Diabetes* **58**, 299–301 (2009).

27.   Asakawa, A. *et al.* Characterization of the effects of pancreatic polypeptide in the regulation of energy balance. *Gastroenterology* **124**, 1325–1336 (2003).

28.   Napolitano, T. *et al.* Role of ghrelin in pancreatic development and function. *Diabetes, Obes. Metab.* **20**, 3–10 (2018).

29.   Steiner, D. J., Kim, A., Miller, K. & Hara, M. Pancreatic islet plasticity: Interspecies comparison of islet architecture and composition. *Islets* **2**, 135–145 (2010).

30.   Linnemann, A. K., Baan, M. & Davis, D. B. Pancreatic β-cell proliferation in obesity. *Adv. Nutr.* **5**, 278–288 (2014).

31.   Hanafusa, T. *et al.* Examination of islets in the pancreas biopsy specimens from newly diagnosed Type 1 (insulin-dependent) diabetic patients. *Diabetologia* **33**, 105–111 (1990).

32.   Leptin, M. Gastrulation movements: The logic and the nuts and bolts. *Dev. Cell* **8**, 305–320 (2005).

33.   Solnica-Krezel, L. & Sepich, D. S. Gastrulation: Making and shaping germ layers. *Annu. Rev. Cell Dev. Biol.* **28**, 687–717 (2012).

34.   Pan, F. C. & Wright, C. Pancreas organogenesis: From bud to plexus to gland. *Dev. Dyn.* **240**, 530–565 (2011).

35.   Bastidas-Ponce, A., Scheibner, K., Lickert, H. & Bakhti, M. Cellular and molecular mechanisms coordinating pancreas development. *Dev.* **144**, 2873–2888 (2017).

36.   Shih, H. P., Wang, A. & Sander, M. Pancreas organogenesis: From lineage determination to morphogenesis. *Annu. Rev. Cell Dev. Biol.* **29**, 81–105 (2013).

37.   Murtaugh, L. C., Cleaver, O. & MacDonald, R. J. *Developmental molecular biology of the pancreas. Pancreatic Cancer* (2018). doi:10.1007/978-1-4939-7193-0_4

38.   Orth, M. *et al.* Pancreatic ductal adenocarcinoma: Biological hallmarks, current status, and future perspectives of combined modality treatment approaches. *Radiat. Oncol.* **14**, 1–20 (2019).

39.   Wang, L., Xie, D. & Wei, D. Pancreatic acinar-to-ductal metaplasia and pancreatic cancer. *Methods Mol. Biol.* **1882**, 299–308 (2019).

40.   Recavarren, C. *et al.* Histologic characteristics of pancreatic intraepithelial neoplasia associated with different pancreatic lesions. *Hum. Pathol.* **42**, 18–24 (2011).

41.   Iacobuzio-Donahue, C. A. Genetic evolution of pancreatic cancer: Lessons learnt from the pancreatic cancer genome sequencing project. *Gut* **61**, 1085–1094 (2012).

42.   Cornish, T. C. & Hruban, R. H. Pancreatic Intraepithelial Neoplasia. *Surg. Pathol.*

Clin. **4**, 523–535 (2011).

43. Brosens, L. A. A., Hackeng, W. M., Offerhaus, J., Hruban, R. H. & Wood, L. D. Pancreatic adenocarcinoma pathology: Changing 'landscape'. *J. Gastrointest. Oncol.* **6**, 358–374 (2015).

44. Neureiter, D., Jäger, T., Ocker, M. & Kiesslich, T. Epigenetics and pancreatic cancer: Pathophysiology and novel treatment aspects. *World J. Gastroenterol.* **20**, 7830–7848 (2014).

45. Olson, S. H. & Kurtz, R. C. Epidemiology of Pancreatic Cancer and the Role of Family History. *J. Surg. Oncol.* doi:10.1002/jso.23149.Epidemiology

46. Solomon, S., Das, S., Brand, R. & Whitcomb, D. C. Inherited pancreatic cancer syndromes. *Cancer J. (United States)* **18**, 485–491 (2012).

47. Balkwill, F. R., Capasso, M. & Hagemann, T. The tumor microenvironment at a glance. *J. Cell Sci.* **125**, 5591–5596 (2012).

48. Witz, I. P. The tumour microenvironment in pancreatic cancer - clinical challenges and opportunities. *Semin. Cancer Biol.* **12**, 87–88 (2002).

49. Thomas, D. & Radhakrishnan, P. Tumor-stromal crosstalk in pancreatic cancer and tissue fibrosis. *Mol. Cancer* **18**, 1–15 (2019).

50. Phoebe, P. Pancreatic stellate cells and fibrosis. in *Pancreatic Cancer and Tumor Microenvironment* (Transworld Research Network, 2012).

51. Martinez-Bosch, N., Vinaixa, J. & Navarro, P. Immune evasion in pancreatic cancer: From mechanisms to therapy. *Cancers (Basel).* **10**, 1–16 (2018).

52. Melstrom, L. G., Salazar, M. D. & Diamond, D. J. The pancreatic cancer microenvironment: A true double agent. *J. Surg. Oncol.* **116**, 7–15 (2017).

53. Roshani, R., McCarthy, F. & Hagemann, T. Inflammatory cytokines in human pancreatic cancer. *Cancer Lett.* **345**, 157–163 (2014).

54. Nagaraju, G. P. & Reddy, A. B. M. *Exploring pancreatic metabolism and malignancy. Exploring Pancreatic Metabolism and Malignancy* (2019). doi:10.1007/978-981-32-9393-9

55. Padoan, A., Plebani, M. & Basso, D. Inflammation and pancreatic cancer: Focus on metabolism, cytokines, and immunity. *Int. J. Mol. Sci.* **20**, (2019).

56. Schmiegel, W., Roeder, C., Schmielau, J., Rodeck, U. & Kalthoff, H. Tumor necrosis factor α induces the expression of transforming growth factor α and the epidermal growth factor receptor in human pancreatic cancer cells. *Proc. Natl. Acad. Sci. U. S. A.* **90**, 863–867 (1993).

57. Bellone, G. *et al.* Cytokine expression profile in human pancreatic carcinoma cells and in surgical specimens: Implications for survival. *Cancer Immunol. Immunother.* **55**, 684–698 (2006).

58. Strobel, O., Neoptolemos, J., Jäger, D. & Büchler, M. W. Optimizing the outcomes of pancreatic cancer surgery. *Nat. Rev. Clin. Oncol.* **16**, 11–26 (2019).

59. Ducreux, M. *et al.* Cancer of the pancreas: ESMO Clinical Practice Guidelines for diagnosis, treatment and follow-up. *Ann. Oncol.* **26**, v56–v68 (2015).

60. Neoptolemos, J. P. *et al.* Therapeutic developments in pancreatic cancer: Current and future perspectives. *Nat. Rev. Gastroenterol. Hepatol.* **15**, 333–348 (2018).

61. Lopez, N. E., Prendergast, C. & Lowy, A. M. Borderline resectable pancreatic

cancer: Definitions and management. *World J. Gastroenterol.* **20**, 10740–10751 (2014).

62. van Veldhuisen, E. *et al.* Locally advanced pancreatic cancer: Work-up, staging, and local intervention strategies. *Cancers (Basel).* **11**, 1–17 (2019).

63. Vaccaro, V., Sperduti, I. & Milella, M. FOLFIRINOX versus gemcitabine for metastatic pancreatic cancer. *N. Engl. J. Med.* **365**, 768–769 (2011).

64. Waldman, A. D., Fritz, J. M. & Lenardo, M. J. A guide to cancer immunotherapy: from T cell basic science to clinical practice. *Nat. Rev. Immunol.* (2020). doi:10.1038/s41577-020-0306-5

65. Karamitopoulou, E. Tumour microenvironment of pancreatic cancer: immune landscape is dictated by molecular and histopathological features. *Br. J. Cancer* **121**, 5–14 (2019).

66. Johansson, H. *et al.* Immune checkpoint therapy for pancreatic cancer. *World J. Gastroenterol.* **22**, 9457–9476 (2016).

67. Madden, K. & Kasler, M. K. Immune Checkpoint Inhibitors in Lung Cancer and Melanoma. *Semin. Oncol. Nurs.* **35**, 150932 (2019).

68. Jiang, J. *et al.* Immunotherapy in pancreatic cancer: New hope or mission impossible? *Cancer Lett.* **445**, 57–64 (2019).

69. Gao, M. *et al.* Direct therapeutic targeting of immune checkpoint PD-1 in pancreatic cancer. *Br. J. Cancer* **120**, 88–96 (2019).

70. Sahin, I. H., Askan, G., I. Hu, Z. & O'Reilly, E. M. Immunotherapy in pancreatic ductal adenocarcinoma: An emerging entity? *Ann. Oncol.* **28**, 2950–2961 (2017).

71. Wainberg, Z. A. *et al.* Open-label, Phase I Study of Nivolumab Combined with nab-Paclitaxel Plus Gemcitabine in Advanced Pancreatic Cancer . *Clin. Cancer Res.* **26**, 4814–4822 (2020).

72. Rosenberg, A. & Mahalingam, D. Immunotherapy in pancreatic adenocarcinoma - Overcoming barriers to response. *J. Gastrointest. Oncol.* **9**, 143–159 (2018).

73. Li, K.-Y. *et al.* Pancreatic ductal adenocarcinoma immune microenvironment and immunotherapy prospects. *Chronic Dis. Transl. Med.* **6**, 6–17 (2020).

74. Haas, A. R. *et al.* Phase I Study of Lentiviral-Transduced Chimeric Antigen Receptor-Modified T Cells Recognizing Mesothelin in Advanced Solid Cancers. *Mol. Ther.* **27**, 1919–1929 (2019).

75. Guo, C. *et al. Therapeutic cancer vaccines. Past, present, and future. Advances in Cancer Research* **119**, (2013).

76. Wu, A. A. *et al.* A Phase II Study of Allogeneic GM-CSF–Transfected Pancreatic Tumor Vaccine (GVAX) with Ipilimumab as Maintenance Treatment for Metastatic Pancreatic Cancer. *Clin. Cancer Res.* **01**, (2020).

77. Dell'aquila, E. *et al.* Prognostic and predictive factors in pancreatic cancer. *Oncotarget* **11**, 924–941 (2020).

78. Kim, S. *et al.* Carbohydrate antigen 19-9 elevation without evidence of malignant or pancreatobiliary diseases. *Sci. Rep.* **10**, 1–9 (2020).

79. Herreros-Villanueva, M. & Bujanda, L. Non-invasive biomarkers in pancreatic cancer diagnosis: What we need versus what we have. *Ann. Transl. Med.* **4**, 1–8 (2016).

80. Daoud, A. Z., Mulholland, E. J., Cole, G. & McCarthy, H. O. MicroRNAs in Pancreatic

Cancer: Biomarkers, prognostic, and therapeutic modulators. *BMC Cancer* **19**, 1–13 (2019).

81. Zhang, X. *et al.* Circulating biomarkers for early diagnosis of pancreatic cancer: facts and hopes. *Am. J. Cancer Res.* **8**, 332–353 (2018).

82. Chen, X., Alstead, M., Ballinger, A. & Farthing, J. G. Cancer Study of K-ras Mutations in the Plasma of Pancreatic. **4**, 271–276 (1998).

83. Maire, F. *et al.* Differential diagnosis between chronic pancreatitis and pancreatic cancer: Value of the detection of KRAS2 mutations in circulating DNA. *Br. J. Cancer* **87**, 551–554 (2002).

84. Błogowski, W. *et al.* Selected cytokines in patients with pancreatic cancer: A preliminary report. *PLoS One* **9**, 1–7 (2014).

85. Wang, W. Q. *et al.* Intratumoral infiltrating immune cells and gene mutations in pancreatic ductal adenocarcinoma. *Br. J. Surg.* (2016). doi:10.1002/bjs.10187

86. Costa, B., Estrada, M. F., Mendes, R. V. & Fior, R. Zebrafish Avatars towards Personalized Medicine—A Comparative Review between Avatar Models. *Cells* **9**, 293 (2020).

87. Fior, R. *et al.* Single-cell functional and chemosensitive profiling of combinatorial colorectal therapy in zebrafish xenografts. *Proc. Natl. Acad. Sci. U. S. A.* **114**, E8234–E8243 (2017).

88. Granat, L. M. *et al.* The promises and challenges of patient-derived tumor organoids in drug development and precision oncology. *Anim. Model. Exp. Med.* **2**, 150–161 (2019).

89. Stoletov, K. & Klemke, R. Catch of the day: Zebrafish as a human cancer model. *Oncogene* **27**, 4509–4520 (2008).

90. Xiao, J., Glasgow, E. & Agarwal, S. Zebrafish Xenografts for Drug Discovery and Personalized Medicine. *Trends in Cancer* **6**, 569–579 (2020).

91. Costa, B. *et al.* Developments in zebrafish avatars as radiotherapy sensitivity reporters — towards personalized medicine. *EBioMedicine* **51**, 1–12 (2020).

92. Rebelo de Almeida, C. *et al.* Zebrafish xenografts as a fast screening platform for bevacizumab cancer therapy. *Commun. Biol.* **3**, (2020).

93. Strober, W. Trypan Blue Exclusion Test of Cell Viability. *Curr. Protoc. Immunol.* 2–3 (2001). doi:10.1002/0471142735.ima03bs21

94. Martins, S. *et al.* Toward an Integrated Zebrafish Health Management Program Supporting Cancer and Neuroscience Research. *Zebrafish* **13**, S47–S55 (2016).

95. Lawson, N. D. & Weinstein, B. M. In vivo imaging of embryonic vascular development using transgenic zebrafish. *Dev. Biol.* **248**, 307–318 (2002).

96. Renshaw, S. A. *et al.* A transgenic zebrafish model of neutrophilic inflammation. *Blood* **108**, 3976–3978 (2006).

97. Nguyen-Chi, M. *et al.* Identification of polarized macrophage subsets in zebrafish. *Elife* **4**, 1–14 (2015).

98. White, R. M. *et al.* Transparent Adult Zebrafish as a Tool for In Vivo Transplantation Analysis. *Cell Stem Cell* **2**, 183–189 (2008).

99. Herbomel, P., Thisse, B. & Thisse, C. Zebrafish early macrophages colonize cephalic mesenchyme and developing brain, retina, and epidermis through a M-CSF

receptor-dependent invasive process. *Dev. Biol.* **238**, 274–288 (2001).

100. Sood, R. *et al.* Development of multilineage adult hematopoiesis in the zebrafish with a runx1 truncation mutation. *Blood* **115**, 2806–2809 (2010).

101. Deer, E. L. *et al.* Phenotype and genotype of pancreatic cancer cell lines. *Pancreas* **39**, 425–435 (2010).

102. Sarantis, P., Papadimitropoulou, A., Papadimitropoulou, A. & Papavassiliou, A. G. Cancer and Cachexia — Metabolic Pancreatic Cancer and Cachexia — Metabolic. (2020).

103. Lam, S. H., Chua, H. L., Gong, Z., Lam, T. J. & Sin, Y. M. Development and maturation of the immune system in zebrafish, Danio rerio: A gene expression profiling, in situ hybridization and immunological study. *Dev. Comp. Immunol.* **28**, 9–28 (2004).

104. Flynn, J. L., Chan, J. & Lin, P. L. Macrophages and control of granulomatous inflammation in tuberculosis. *Mucosal Immunol.* **4**, 271–278 (2011).

105. Rosowski, E. E. Determining macrophage versus neutrophil contributions to innate immunity using larval zebrafish. *DMM Dis. Model. Mech.* **13**, (2020).

106. Aras, S. & Raza Zaidi, M. TAMeless traitors: Macrophages in cancer progression and metastasis. *Br. J. Cancer* **117**, 1583–1591 (2017).

107. Cui, R. *et al.* Targeting tumor-associated macrophages to combat pancreatic cancer. *Oncotarget* **7**, 50735–50754 (2016).

108. Miller, Mj., Laird, B. J. A. & Skipworth, R. J. E. The immunological regulation of cancer cachexia and its therapeutic implications. *J. Cancer Metastasis Treat.* **2019**, 1–11 (2019).

109. Guo, M. *et al.* U0126 inhibits pancreatic cancer progression via the KRAS signaling pathway in a zebrafish xenotransplantation model. *Oncol. Rep.* **34**, 699–706 (2015).

110. Masamune, A. *et al.* The angiotensin II type i receptor blocker olmesartan inhibits the growth of pancreatic cancer by targeting stellate cell activities in mice. *Scand. J. Gastroenterol.* **48**, 602–609 (2013).

111. Vonlaufen, A. *et al.* Pancreatic stellate cells: Partners in crime with pancreatic cancer cells. *Cancer Res.* **68**, 2085–2093 (2008).

112. Suklabaidya, S. *et al.* Experimental models of pancreatic cancer desmoplasia. *Lab. Investig.* **98**, 27–40 (2018).

113. Löhr, M. *et al.* Transforming growth factor-β1 induces desmoplasia in an experimental model of human pancreatic carcinoma. *Cancer Res.* **61**, 550–555 (2001).

114. Bailey, J. M. *et al.* Sonic hedgehog promotes desmoplasia in pancreatic cancer. *Clin. Cancer Res.* **14**, 5995–6004 (2008).

115. LeBert, D. *et al.* Damage-induced reactive oxygen species regulate vimentin and dynamic collagen- based projections to mediate wound repair. *Elife* **7**, 1–26 (2018).

116. Di Franco G, Usai A, Funel N, Palmeri M, Montesanti IER, Bianchini M, Gianardi D, Furbetta N, Guadagni S, Vasile E, Falcone A, Pollina LE, Raffa V, M. L. Use of zebrafish embryos as avatar of patients with pancreatic cancer: A new xenotransplantation model towards personalized medicine. *World J Gastroenterol* (2020). doi:10.3748/wjg.v26.i21.2792

117. Guo, L., Zhang, H. & Chen, B. Nivolumab as Programmed Death-1 (PD-1) Inhibitor

for Targeted Immunotherapy in Tumor. *J. Cancer* **8**, 410–416 (2017).

118. Gordon, S. R. *et al.* PD-1 expression by tumour-associated macrophages inhibits phagocytosis and tumour immunity. *Nature* **545**, 495–499 (2017).

119. Lianyuan, T. *et al.* Tumor associated neutrophils promote the metastasis of pancreatic ductal adenocarcinoma. *Cancer Biol. Ther.* (2020). doi:10.1080/15384047.2020.1807250

120. Caillou, B. *et al.* Tumor-Associated macrophages (TAMs) form an interconnected cellular supportive network in anaplastic thyroid carcinoma. *PLoS One* **6**, (2011).

121. Kuwada, K. *et al.* The epithelial-to-mesenchymal transition induced by tumor-associated macrophages confers chemoresistance in peritoneally disseminated pancreatic cancer. *J. Exp. Clin. Cancer Res.* **37**, 1–10 (2018).

122. Zhang, A. *et al.* Cancer-associated fibroblasts promote M2 polarization of macrophages in pancreatic ductal adenocarcinoma. *Cancer Med.* **6**, 463–470 (2017).

123. Hingorani, S. R. *et al.* HALO 202: Randomized phase II Study of PEGPH20 Plus Nab-Paclitaxel/Gemcitabine Versus Nab-Paclitaxel/Gemcitabine in Patients With Untreated, Metastatic Pancreatic Ductal Adenocarcinoma. *J. Clin. Oncol.* **36**, 359–366 (2018).

124. https://clinicaltrials.gov/ct2/show/NCT03307148 (Accessed on November 10th, 2020).

125. Chronopoulos, A. *et al.* ATRA mechanically reprograms pancreatic stellate cells to suppress matrix remodelling and inhibit cancer cell invasion. *Nat. Commun.* **7**, (2016).

126. Driehuis, E. *et al.* Pancreatic cancer organoids recapitulate disease and allow personalized drug screening. *Proc. Natl. Acad. Sci. U. S. A.* **116**, 26580–26590 (2019).

8. Appendix

Table 8. 1 – Composition of stock solutions, and respective working solutions, prepared by the Champalimaud Fish Facility for zebrafish larvae care and handling.

Solution	Preparation
E3 medium 50x (stock)	For 10mL of sterile milli-Q water: 146.9g NaCl 6.3g KCl 24.3g $CaCl_2.2H_2O$ 40.7g $MgSO4.7H_2O$
E3 medium 1X (ready to use)	For 10mL of sterile milli-Q water: 400mL E3 medium 50x 60mL 0.01% Methylene Blue Solution Fill up to 20 liters of system water
Tricaine 25x (stock and euthanasia)	2g tricaine powder 500mL reverse osmosis water 10mL 1M Tris (pH 9) Adjust to pH 7
Pronase 100x – stock (60mg/mL)	1g pronase (Roche) 16.7 mL milli-Q water
Pronase 1x (0.6mg/mL)	100µL pronase 100x 9.9 mL E3 medium 1x

Table 8. 2 – Composition of the blocking solution, PBDX_GS, and the fixative agent, PIPES.

Solution	Preparation
PBDX_GS	For 50mL: 50mL PBS 1x 0.5g BSA 0.5mL DMSO 250µL Triton 10% 750µL Goat Serum (Stock: 15µL/mL)
PIPES 1.5%	For 1mL: 801.3µL distilled water 93.7µL 16% PFA 4µL 0.5M EGTA 1µL 1M $MgSO_4$ 100µL 1M PIPES (Thermo Fisher Scientific)

Table 8. 3 – Stock and working concentrations of the antineoplastic drugs used in this project.

Drug	Stock concentration	Working concentration
5-FU	50mg/mL	426.2µM
Oxaliplatin	5mg/mL	8.1µM
Irinotecan	20mg/mL	8µM
Folinic Acid	10mg/mL	18.5µM
Gemcitabine	40mg/mL	160µM
Paclitaxel	6mg/mL	365ng/mL
Nivolumab	10mg/mL	475µg/mL

Table 8. 4 – Number and respective percentage of zebrafish Panc-1 xenografts with severe edema at 1dpi. Panc-1 cells were resuspended in PBS EDTA 2mM prior to injection.

	Injection Dates	Nº of injected larvae (48hpf)	Nº xenografts w/edema (1dpi)	% Xenografts w/ edema (1dpi)
PBS EDTA (2mM)	4/02/2020	~455	321	70
	10/02/2020	~420	356	85
	13/02/2020	~480	373	78
	18/02/2020	~560	478	85
	2/07/2020	~840	562	67
	8/07/2020	~840	548	65